CYP102A P450 Monooxygenases: Comparative Analysis and Construction of Cytochrome P450 Chimera

Von der Fakultät der Geo-und Biowissenschaften der Universität Stuttgart
zur Erlangung der Würde eines Doktors der Naturwissenschaften
(Dr. rer. nat.)
genehmigte Abhandlung

Vorgelegt von:
Sabine Eiben
geb. in Bonn

Hauptberichter: Prof. Dr. Rolf D. Schmid
Mitberichter: Prof. Dr. Holger Jeske

Tag der mündliche Prüfung: 03.Mai 2007

Institut für Technische Biochemie der Universität Stuttgart
2007

Eidesstattliche Erklärung

Hiermit versichere ich, daß ich die vorliegende Arbeit selbständig und nur unter Verwendung der angegebenen Hilfsmittel und Literatur angefertigt habe.

Stuttgart, den 18. Dezember 2006

Sabine Eiben

Danksagung

Mein besonderer Dank gilt Prof. Dr. Rolf D. Schmid für die Überlassung und Betreuung des interessanten Themas, für seine Unterstützung und für sein Interesse am Fortgang der Arbeit.

Ebenso herzlich danken möchte ich Dr. Vlada Urlacher, der Leiterin der Biokatalysegruppe am ITB, für ihre Freundschaft, ihren unermüdlichen Einsatz, sowie für ihre endlose Geduld und wertvollen Ratschläge.

Ganz besonders möchte ich Dr. Steffen Maurer für die ständige Gesprächsbereitschaft und die hilfreichen Anregungen danken.

Mein Dank gilt den ehemaligen und derzeitigen Kollegen der Biokatalysegruppe für das großartige Arbeitsklima und für die freundliche Zusammenarbeit. Ganz besonders danke ich Michael Budde und Matthias Dietrich für die interessanten Diskussionen über das Thema meiner Arbeit.

Heike Bartelmäs danke ich für die gemeinsame Zeit bei den nächtelangen Messungen der Temperaturstabilitäten und ihren Einsatz während der Studienarbeit

Darüber hinaus danke ich

Prof. Dr. Andrew Munro (Manchester Interdisciplinary Biocentre) für die Einladung in seinem Labor zu Arbeiten und die damit verbundene Betreuung

Dr. Hazel Girvan (Manchester Interdisciplinary Biocentre) für die Einführung zur Messung von Stopped-flow Kinetiken und CD-Spektren

Besonders zum Gelingen dieser Arbeit hat meine Familie beigetragen. Meinem Mann Frank danke ich für die Geduld und Unterstützung, die er mir in den letzten vier Jahren gewährte. Ich danke meinen Kindern dafür, dass sie mir immer wieder zeigen

was wichtig ist im Leben. Meinen Schwiegereltern und insbesondere meinen Eltern danke ich für die Unterstützung und Ermutigung, die sie mir zukommen ließen.

I. Table of Contents

Tables

Figures

II. Abbreviations

12-*p*NCA	*para*-nitrophenoxydodecanoic acid
% (v/v)	volume percent
% (w/v)	weight percent
°C	degree Celsius
A	absorbance
Å	Ångström (=10^{-10} m)
A1A3	chimeric enzyme between CYP102A1 momnooxygenase and CYP102A3 reductase
A1GR	chimeric enzyme between CYP102A1 momnooxygenase and a-subunit of a sulfite reductase
AA	arachindonic acid
AbrB	repressor that controls the expression of genes involved in starvation-induced processes in *B. subtilis*
Amp^R	ampicillin resistance
APS	ammonium persulfate
ATCC	American Type Culture Collection
Bp	base pairs
BCA	bicinchonic acid
BSA	bovine serum albumin
C12-C18	C-atoms of saturated fatty acids
CD	circular dichroism
CPR	Cytochrome P450 reductase
CYP	Cytochrome P450
CYP102A	Subfamily of P450s comprised of a monooxygenase and a reductase domain in one protein
DHA	docosahexaenoic acid
DMSO	dimethylsulfoxide
DNA	deoxyribonucleic acid
dNTP	deoxynucleoside-5'-triphosphate
DSMZ	German Resource Centre for Biological Material
DTT	dithiothreitol
EC	enzyme class
EDTA	ethylendiaminetetraacetic acid
EPA	eicosapentaenoic acid
ESR	electron spin resonance
FAD/FADH/FADH2	flavin adenine dinucleotide at different redox states
FMN/$FMNH^{\cdot}$/FMNH2	riboflavin monophosphate at different redox states
GC	gas chromatography
MS	mass spectrometry
Gstredu	α-subunit of the sulfite reductase from *G. stearothermophilus*
Heme	protoporphyrin IX
HPLC	high performance liquid chromatography
IEX	ion exchange chromatography
IPTG	isopropyl-b-D-thiogalactoside
kb	kilobases

k_{cat}	catalytic constant
K_D	binding constant
K_M	Michaelis constant
lac	lac promoter sequence
LB	Luria-Bertani
LMW	low molecular weight
NADH/NAD^+	b-nicotinamidadenindinucleotide
NADPH/$NADP^+$	b-nicotinamidadenindinucleotidephosphate
NMR	nuclear magnetic resonance
NOS	nitric oxide synthase
OD	optical density
ORF	open reading frame
ori	origin of replication
P450	cytochrome P450 monooxygenase
PAGE	polyacrylamide electrophorese
PCR	polymerase chain reaction
PD10 column	desalting column
PDA	photo diode array
*pel*B	leader sequence that directs a protein to the periplasmic membrane of *E. coli*
PMSF	Phenylmethylsulphonylfluoride
QCPCR™	site directed mutagenesis method
rpm	rotations per minute
RT	retention time
SBS	substrate binding site
SDS	sodium dodecyl sulfate
SiR	α-subunit of sulfite reductases
Spo0A	*B. subtilis* transcription factor
Spo0F	*B. subtilis* transcription factor
SRS	substrate regognition site
TAE	Tris/acetate/EDTA buffer
TB	terrific broth
TE	Tris/EDTA buffer
TEMED	N,N,N',N'-tetramethyl-ethylendiamine
TIC	total ion count
TLC	thin layer chromatography
Tm	melting temperature
Tris	Tris-(hydroxymethyl)-aminomethane
USDA	US Department of Agriculture
UV	ultraviolet
VIS	visible
v_{max}	maximal velocity

III. Zusammenfassung

Die Ziele dieser Arbeit waren die Charakterisierung verschiedener P450 Monooxygenasen der CYP102 Familie, insbesondere der Substrat- und Produktspezifität sowie der Thermostabilität. Weiterhin wurden die gewonnenen Erkenntnisse dazu genutzt Fusionsproteine mit erhöhter Thermostabilität herzustellen.

Cytochrom P450 Monooxygenasen (CYPs) stellen eine der größten Gen-Superfamilien dar. Die neueste Zählung ergab mehr als 6000 Mitglieder. P450 Enzyme enthalten als reaktives Zentrum ein Häm-System in welchem das zentrale Eisen an ein Cysteinat gebunden ist. Dieser Ligand sorgt dafür, dass diese Enzyme im reduzierten Kohlenstoffmonoxid gebundenen Zustand eine maximale Absorption bei 450 nm zeigen, wodurch sie ihren Namen erhalten haben. CYPs katalysieren die Aktivierung von molekularem Sauerstoff, wobei ein Sauerstoffatom zu Wasser reduziert wird während das andere Sauerstoffatom in das organische Substrat eingeführt wird. Viele dieser Reaktionen sind streng regio- und stereoselektiv. P450 Monooxygenasen spielen eine der Hauptrollen im Abbau von Xenobiotika in der Leber und der Aktivierung von pharmazeutischen Substanzen. Neben diesen eher unspezifischen Mikrosomalen Monooxygenasen gibt es aber auch eine große Zahl an spezifischen CYPs, die zum Beispiel an der Steroidbiosynthese, der Synthese von Pflanzen- und Insektenhormonen sowie an der Ausbildung von Farbe und Geruch in Pflanzen beteiligt sind. P450 Enzyme sind interessante Kandidaten für die Anwendung in industriellen Prozessen. Hier haben speziell bakterielle Enzyme Vorteile, da sie löslich vorkommen und häufig eine höhere Stabilität und Aktivität vorweisen als eukaryotische P450 Enzyme. Nichtsdestotrotz gibt es zurzeit nur wenige Beispiele für die industrielle Nutzung von CYPs wobei es sich ausschließlich um Ganzzellbiokatalyse-Prozesse handelt. Die Verwendung isolierter CYPs in der organischen Synthese hingegen wurde bisher als nicht praktikabel erachtet. Ein Grund dafür ist die geringe Stabilität der Enzyme, ein weiterer, dass für die enzymatische Aktivität in den meisten Fällen mehrere Elektronentransportproteine sowie der teure Kofaktor Nicotinamidadenin-dinucleotid(phosphat) (NAD(P)H) benötigt werden.

Bei Verwendung von P450 Monooxygenasen der CYP102A Unterfamilie kann das Problem der zusätzlich benötigten Elektronentransportsysteme umgangen werden, da es sich um NADPH-abhängige, natürliche Fusionsproteine handelt. Sie bestehen aus einer P450-Monooxygenasedomäne, die über eine Verbindungsregion mit einer FAD und FMN enthaltenden Reduktasedomäne fusioniert sind. Gegen ihre natürlichen Substrate, mittel- und langkettige Fettsäuren, zeigen diese Enzyme eine der höchsten je für ein CYP gemessenen Umsatzraten (>5000 min^{-1}).

Die Unterfamilie CYP102A beinhaltet zurzeit acht Enzyme von denen jedoch nur vier kloniert und charakterisiert sind. Bereits in den 80igern wurde CYP102A1 aus *Bacillus megaterium* (P450 BM-3) zum ersten Mal beschrieben (Miura and Fulco 1975; Narhi and Fulco 1982). Da es bezüglich seiner Aminosäuresequenz und dem Elektronentransfersystem weit mehr Ähnlichkeiten zu mikrosomalen als zu bakteriellen CYPs aufwies, wurde es lange als Modellenzym für die Wirkungsweise von mikrosomalen P450 Monooxygenasen benutzt. Erst 2004 erschienen mehrere Publikationen, die unabhängig voneinander von der Klonierung und Charakterisierung zweier weiterer Mitglieder dieser Unterfamilie berichteten, CYP102A2 und CYP102A3 aus *Bacillus subtilis*. Im Zuge einer Diplomarbeit (Asta Chimene 2005) konnten wir ein weiteres Protein heterolog exprimieren und charakterisieren. Nach Rücksprache mit Prof. Nelson erhielt diese Monooxygenase aus *Bacillus licheniformis* die Bezeichnung CYP102A7. Alle weiteren Mitglieder dieser Unterfamilie wurden bisher nur anhand ihrer Proteinsequenz im Zusammenhang mit Genomprojekten identifiziert.

Obwohl alle betrachteten Enzyme zur selben Unterfamilie gehören kann man sie zusätzlich anhand ihrer Ähnlichkeit in vier Gruppen einteilen. Diese Einteilung ergibt sich sowohl bei der Betrachtung der Monooxygenasedomäne alleine, als auch bei Untersuchung der gesamten Aminosäuresequenz. Gruppe 1 beinhaltet als einziges Enzym CYP102A1, während CYP102A6 aus *Bradyrhizobium japonicum* noch das alleinige Mitglied aus Gruppe 2 darstellt. Gruppe 3 besteht aus 2 Vertretern, CYP102A3 und CYP102A7. Gruppe 4 ist mit bisher 4 Vertretern die größte Gruppe; sie besteht aus CYP102A4 (*Bacillus anthracis*), CYP102A5 (*Bacillus cereus*) und YP037304 (*Bacillus thuringienis*). Diese drei Enzyme stammen aus drei eng verwandten *Bacillus* species und weisen Homologien von über 90 % auf. Die vierte

Monooxygenase in dieser Gruppe zeigt nur noch 80 % Ähnlichkeit zu den anderen Enzymen, es handelt sich hierbei um CYP102A2.

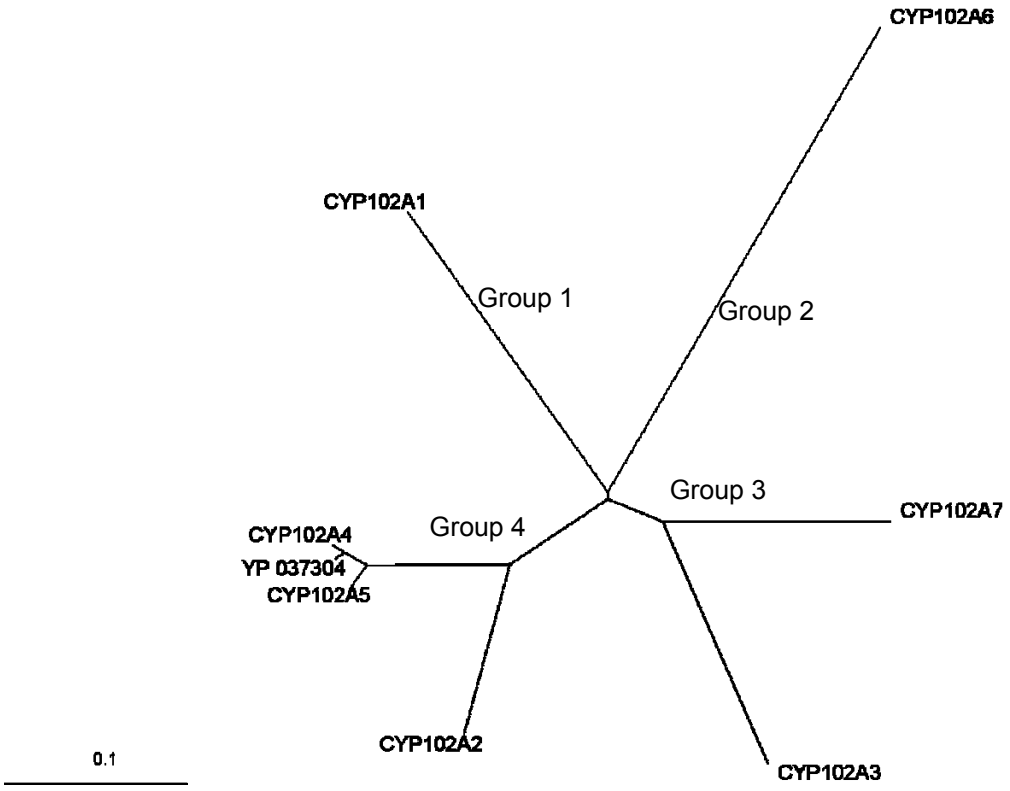

Phylogenetischer Baum der CYP102A Monooxygenasen

Da es erhebliche Unterschiede in der Zielsetzung, Methodik und auch Analytik der bisherigen Untersuchungen zu den P450 Monooxygenasen der CYP102A Unterfamilie gab, wurde im Rahmen dieser Arbeit die Aktivität und Stabilität der vier klonierten Enzyme unter identischen Bedingungen betrachtet. Alle vier P450 Monooxygenasen zeigten hohe Aktivität gegen gesättigte Fettsäuren der Kettenlänge C12 bis C17, wobei das Optimum jeweils bei C14 oder C15 lag und mit sinkender, bzw. steigender Kettenlänge abnahm. Geradzahligkeit bzw. Ungeradzahligkeit der C-Atome hatte keinen Einfluss auf die Aktivtät. Außer bei der Umsetzung von Dodekansäure konnten nicht mehr als 10 % unproduktiver Zyklen (Entkopplung, NADPH Verbrauch ohne Bildung eines oxidierten Produkts) beobachtet werden. Obwohl es sich hier nicht um Geschwindigkeiten unter v_{max} Bedingungen handelt (Substrat nicht in der Sättigung und NADPH im Unterschuss) konnten doch

Aktivitäten gegen Tetradekansäure zwischen 470 min^{-1} (CYP102A3) und 2650 min^{-1} (CYP102A7) gemessen werden.

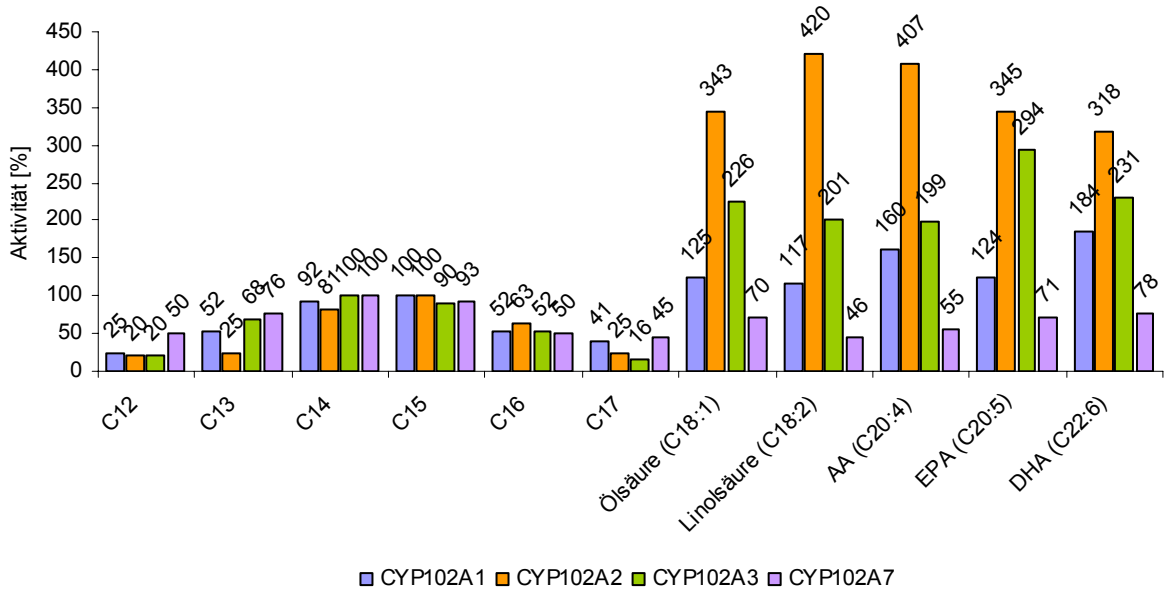

Aktivität gegenüber gesättigten und ungesättigten Fettsäuren in % vom Maximalwert gegenüber der besten gesättigten Fettsäure. C12-C17, Kettenlänge der gesättigten Fettsäuren; AA, Arachidonsäure; EPA, Eicosapentaensäure; DHA, Docosahexaensäure

Die Analytik erfolgte über Messung der NADPH Verbrauchsrate mit Anschließender Isolierung des Substrat/Produkt Gemisches, welches über GC/MS Anhand der Peakflächen bestimmt wurde. Zusätzlich zu den gesättigten Fettsäuren wurden auch mehrere, teils mehrfach ungesättigte Fettsäuren als Substrate untersucht. Hierbei zeigten fast alle P450 Monooxygenasen eine erhebliche Steigerung ihrer Aktivitäten. Nur CYP102A7 erfuhr keine Steigerung seiner Aktivität mit ungesättigten Fettsäuren. Ein besonders starker Aktivierungseffekt wurde bei der Umsetzung von Linolsäure mit CYP102A2 beobachtet. Mit einer Geschwindigkeit von über 4700 min^{-1} ergibt sich eine Steigerung um mehr als das vierfache der Aktivität gegenüber Tetradekansäure.

Anhand der Analyse mittels GC/MS konnten neben den Substrat/Produktverhältnissen auch die Regioselektivität der Reaktionen bestimmt werden. Hierbei wurden zwei interessante Effekte beobachtet. Zum einen zeigte CYP102A3 eine Abweichung zum bisher beobachteten und als allgemeingültig für

diese Enzymunterfamilie geltenden Verhalten. Bisher wurde immer nur von Hydroxylierungen der gesättigten Fettsäuren an Position ω-1, ω-2 und ω-3 berichtet. CYP102A3 hydroxyliert gesättigte Fettsäuren jedoch auch an weiter entfernten Positionen. Bei der Umsetzung von Hexadekansäure erhält man zu 25 % ω-7-Hydroxyhexadekansäure. Des Weiteren fällt auf, dass das Hydroxylierungsmuster von CYP102A2 nicht von der Kettenlänge abhängig zu sein scheint. Während die anderen Enzyme je nach Fettsäure unterschiedliche Positionspräferenzen aufweisen, hydroxyliert CYP102A2 immer bevorzugt an Position ω-2, gefolgt von ω-1 und ω-3. Diese beiden festgestellten Phänomene lassen folgende Schlussfolgerungen zu: zum einen scheint die Substratbindungstasche von CYP102A3 erheblich größer zu sein als die der anderen Enzyme, so dass ein wesentlich längerer Kettenabschnitt der Fettsäuren Platz findet. Zum anderen sieht es so aus, als ob speziell CYP102A2 einen eher eingeschränkten Zugangskanal zum aktiven Zentrum hat, in dem das ω-Ende der Fettsäuren immer in einer fest definierten Konformation vorliegt.

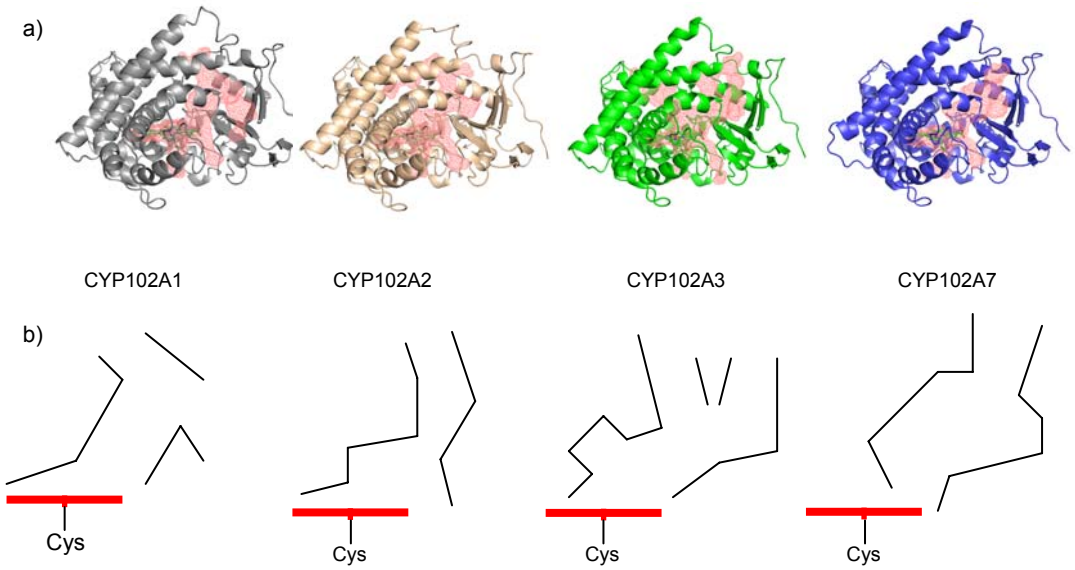

a) Die modellierten Substratbindungstaschen (SBS) von CYP102A1-3 und CYP102A7 zur Verfügung gestellt von Tuan A. Do; b) Schema der SBS, in rot die Häm-Ebene

Betrachtet man die Substratbindungsstellen der untersuchten P450 Enzyme, die anhand der bekannten Kristallstruktur von CYP102A1 modelliert wurden (laufende Doktorarbeit von Tuan Do, Bioinformatik-Gruppe), so erkennt man, dass CYP102A2 tatsächlich den vom Volumen her engsten Zugang zum Häm hat. Weiterhin weist die Substratbindungsstelle von CYP102A3 einen zusätzlichen Hohlraum auf. Interessanterweise zeigt auch eine Mutante von CYP102A1 (A74G, F87V, L188Q) diesen zusätzlichen Hohlraum und es konnte nachgewiesen werden, dass diese Mutante längerkettige gesättigte Fettsäuren wie zum Beispiel Tetradekan- oder Hexadekansäure auch an den Positionen von ω-1 bis ω-7 hydroxyliert.

Neben den "natürlichen" Substraten der CYP102A Unterfamilie wurden auch weitere eher ungewöhnliche Substrate wie zum Beispiel 12-*para*-Nitrophenoxycarbonsäure (12-*p*NCA) oder 7-Ethoxycumarin untersucht. *p*NCA ist eine Substanz, die bevorzugt zum Durchmustern von P450 Mutantenbibliotheken verwendet wird, da das Produkt der Hydroxylierung an der ω-Position, ein Halbacetal, zu einer spontanen Spaltung in die Oxo-carbonsäure und das photometrisch bei 410 nm detektierbare *para*-Nitrophenolat führt. Bei der Untersuchung der Aktivität gegenüber 12-*p*NCA wurden beispielhaft die Produkte der Umsetzung mit CYP102A1 und CYP102A3 extrahiert und mittels GC/MS Analyse weiter untersucht. Die Auswertung der Umsetzung mit CYP102A1 zeigte, dass neben dem erwarteten Produkt Oxo-Dodekansäure als Hauptprodukt die doppelt hydroxylierte 1,12-Dodekandisäure enstand. Bei der Umsetzung mit CYP102A3 konnte keine Dicarbonsäure identifiziert werden. Diese Ergebnisse spiegeln die Präferenzen der beiden Enzyme gegenüber Fettsäuren wieder: CYP102A1 hydroxyliert Dodekansäure vornehmlich an Position ω-1, während die Präferenz von CYP102A3 auf der Position ω-3 liegt.

Eine weitere, eher ungewöhnliche Eigenschaft ist die Fähigkeit von CYP102A7 7-Ethoxycumarin zu deethylieren, da diese Substanz normalerweise von den wesentlich flexibleren, mikrosomalen P450 Enzymen umgesetzt wird. 7-Ethoxycumarin hat als Grundgerüst ein planares Doppelringsystem und somit keine strukturellen Ähnlichkeiten zu den Fettsäuren. Weder CYP102A1, CYP102A2 noch CYP102A3 zeigten als Wildtyp-Enzyme meßbare Aktivitäten gegenüber diesem Substrat. Die Geschwindigkeit der Deethylierung durch CYP102A7 war jedoch mit 2 min^{-1} durchaus im Bereich der Aktivitäten der mikrosomalen Enzyme.

Zusätzlich zur Produkt und Substratspezifität wurde auch die Temperaturstabilität der verschiedenen CYP102A Monooxygenasen untersucht. Hierbei stellte sich heraus, dass es gravierende Unterschiede in der Stabilität der einzelnen Domänen innerhalb eines Enzyms gab. Zum Beispiel wurden 50 % der Monooxygenasedomäne von CYP102A1 erst bei einer Inkubationstemperatur von 56°C inaktiviert, wohingegen die Reduktase schon bei 49°C zur Hälfte inaktiviert war. Diese Eigenschaften waren bei CYP102A2 und A3 vertauscht, hier war die Reduktasedomäne jeweils stabiler als die Monooxygenasedomäne. Besonders auffällig war dies bei CYP102A3, bei dem die Temperatur für 50 % Inaktivierung der Monooxygenasedomäne bei 49°C lag und die der Reduktasedomäne bei 59°C. Basierend auf diesen Ergebnissen wurde eine Chimäre aus der Monooxygenasedomäne von CYP102A1 und der Reduktasedomäne aus CYP102A3 konstruiert. Spektroskopische Untersuchungen zeigten, dass die Chimäre A1A3 funktionell exprimiert werden konnte. Dies wurde im Folgenden durch Bestimmung der Aktivität gegenüber dem Surrogatsubstrat 12-*para*-Nitrophenoxydodekansäure (12-*p*NCA) bestätigt. Mit nur 50 % der Aktivität von CYP102A1 war diese zwar niedriger, aber ausreichend für die folgende Bestimmung der Temperaturstabilität. Es zeigte sich, dass die Temperaturstabilität der einzelnen Domänen in A1A3 der Stabilität der jeweiligen Domäne im Ausgangsenzym entsprach.

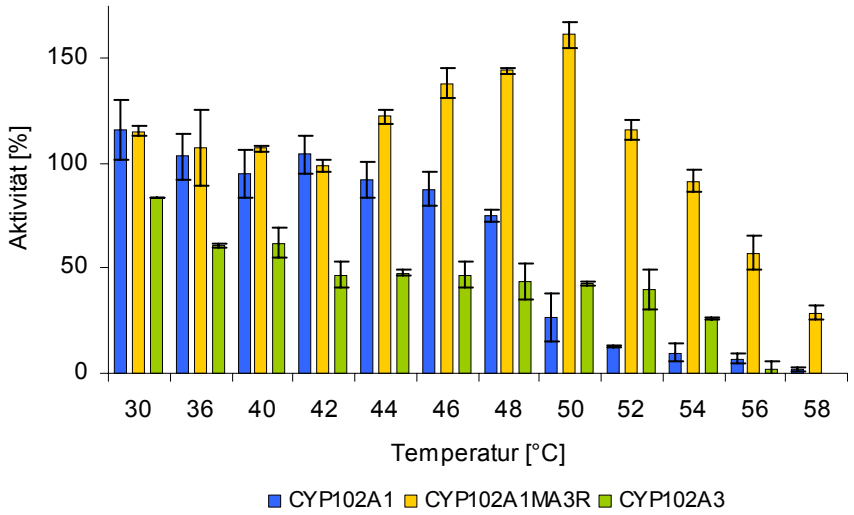

Aktivität von CYP102A1 und A3 sowie der Chimäre A1A3 gegenüber 12-*p*NCA nach Inkubation bei verschiedenen Temperaturen

Interessant war jedoch die Auswirkung der Fusion auf die Aktivität nach Inkubation bei verschieden Temperaturen, gemessen über die Hydroxylierung von 12-*p*NCA. Die Chimäre A1A3 zeigte nicht nur eine erhöhte Stabilität gegenüber CYP102A1 und A3, sondern einen erheblichen Aktivitätsanstieg nach Inkubation bei 48-54°C. Dieser Effekt kann eventuell auf eine bessere Orientierung der Monooxygenase- und Reduktasedomäne zueinander zurückgeführt werden, oder auf die Auflösung von höheren Aggregationsformen des Enzyms zu funktionellen Dimeren, ausgelöst durch höhere Temperaturen.

Aufgrund der hohen Aktivität von A1A3 bei 50°C wurde auch die Inaktivierungsrate bei dieser Temperatur durch den *p*NCA-Assay bestimmt und mit der Inaktivierungsrate von CYP102A1 verglichen. CYP102A3 konnte nicht zu einem Vergleich herangezogen werden, da hier die Stabilität bei 50°C zu gering war. Mit einer Halbwertszeit von 100 min war A1A3 mehr als 10-mal stabiler als CYP102A1 (8 min). Weiterhin wurden Untersuchungen zur Bestimmung der Prozessstabilität durchgeführt. Auch hierbei ergab sich für A1A3 eine erhöhte Stabilität: während CYP102A1 nach 6 Stunden keine Produktbildung mehr aufwies (trotz Substratüberschuss), war die Produktbildung für A1A3 auch nach 12 Stunden noch messbar.

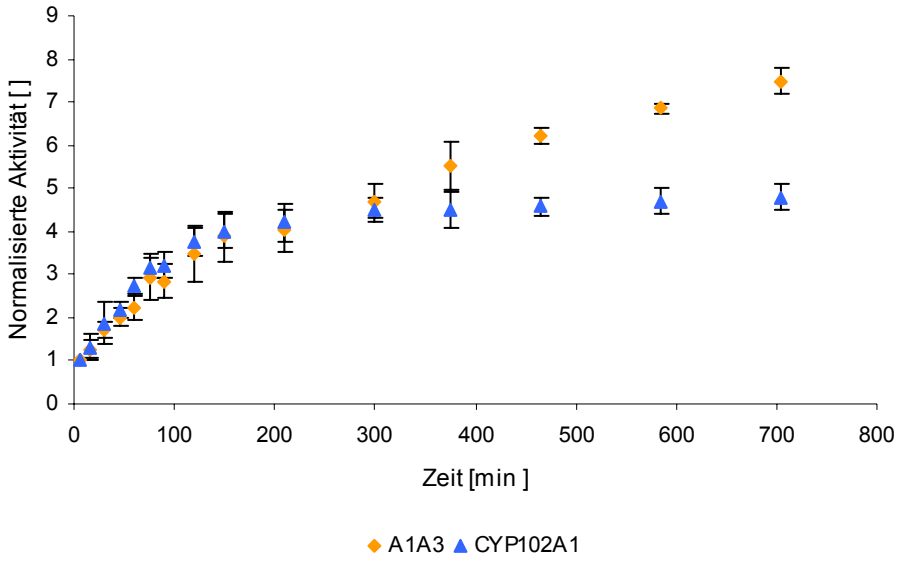

Prozessstabilität von CYP102A1 und A1A3

Neben der Chimäre aus zwei Mitgliedern der CYP102A Unterfamilie wurde im Rahmen dieser Arbeit auch eine Chimäre aus der Monooxygenasedomäne von CYP102A1 und der α-Untereinheit einer Sulfit Reduktase kloniert und exprimiert. Die α-Untereinheit der Sulfit Reduktase aus dem thermophilen Stamm *Geobacillus stearothermophilus* gehört auch zu den Diflavin Reduktasen wie die Cytochrom P450 Reduktase. Zu dieser Gruppe gehört außerdem die Stickoxid-Synthase (NOS). Frühere Untersuchungen hatten gezeigt, dass die Elektronenübertragung zwischen Chimären aus CYP102A1 und humaner NOS möglich ist (Fuziwara et al. 2002). Dies sollte nun auch für eine Chimäre aus der Monooxygenasedomäne von CYP102A1 und der α-Untereinheit einer Sulfit Reduktase (Gstredu) gezeigt werden. Die Gstredu wurde aus genomischer DNA über PCR amplifiziert und in den Expressionsvektor pET22b+ einkloniert. Die funktionelle Expression der Gstredu in *E.coli* konnte durch den Cytochrom C Assay nachgewiesen werden. Cytochrom C ist ein künstlicher Elektronenakzeptor, dessen Reduktion zum Nachweis der Übertragung von einzelnen Elektronen, wie das bei FMN enthaltenden Reduktasen der Fall ist, verwendet wird. Das Temperaturoptimum wurde mit 60°C bestimmt. Anschließend wurde die Gstredu hinter die Monooxygenasedomäne von CYP102A1 im pET22b+ Vektor eingefügt und in *E. coli* exprimiert. Das erhaltene Fusionsprotein (A1GR) wurde über Anionenaustauschchromatographie aufgereinigt und zeigte ein typisches P450 Monooxygenase Spektrum. Zunächst konnte bewiesen werden, dass die Gstredu, auch nach Inkubation bei Temperaturen höher als 42°C, in der Lage ist, Elektronen von NADPH auf die Monooxygenasedomäne von CYP102A1 effektiv zu übertragen. Dies erfolgte unter anaeroben Bedingungen in Anwesenheit von Substrat (Tetradekansäure). Die erfolgreiche Reduktion des Häm-Eisens wurde über die Bindung von Kohlenmonoxid photometrisch nachgewiesen. A1GR zeigte keine Aktivität gegenüber 12-*p*NCA jedoch gegenüber den natürlichen Substraten Tetradekansäure und Hexadekansäure.

Während die Aktivität von CYP102A1 gegenüber Fettsäuren nach 30 minütiger Inkubation bei 49°C auf 5 % der Ausgangsaktivität sank, wurde die Aktivität der A1GR durch Inkubation bei dieser Temperatur nur unwesentlich beeinflußt.

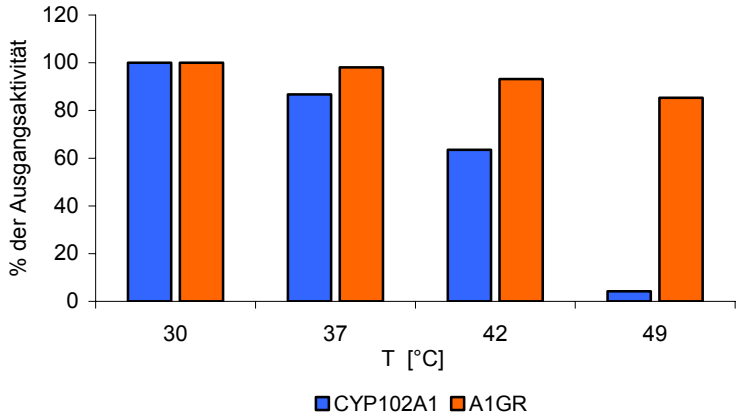

Relative Aktivität von CYP102A1 und A1GR gegenüber Hexadekansäure nach Inkubation bei verschiedenen Temperaturen

Obwohl die Aktivität von A1GR wesentlich niedriger als die Aktivität von CYP102A1 war (0,5 min^{-1} gegenüber ~2000 min^{-1}) und auch die Kopplungseffizienz bei weniger als 10 % lag, so konnte doch gezeigt werden, dass die Gstredu in der Lage ist Elektronen an die Monooxygenasedomäne von CYP102A1 zu liefern und auch eine höhere Stabilität aufweist.

Bisher gibt es keine Kristallstruktur des kompletten CYP102A1 Fusionsenzyms und daher auch keine genauen Informationen wie die Reduktasedomäne mit der Monooxygenasedomäne interagiert und welche Aminosäuren am Elektronentransport beteiligt sind. Ein tieferer Einblick in diese Interaktion in künftigen Untersuchungen wäre eine große Hilfe in der Konstruktion von aktiveren, stabilen Chimären.

IV. Summary

The members of the CYP102A subfamily are in several ways unique. They are natural fusion enzymes of approximately 117-119 kDa comprised of the N-terminal monooxygenase domain and a FAD and FMN containing diflavin reductase domain. The natural substrates of the CYP102A members are fatty acids. Due to their structural organisation the CYP102A members exhibit extraordinary activities in comparison to other P450 monooxygenases of 3000-10000 min^{-1}. These exceptional activities of the members of the CYP102A subfamily make them promising candidates for the use in industrial applications. Up to now cloning and characterisation of only three members of this subfamily have been published. CYP102A1 from *Bacillus megaterium* and CYP102A2 and CYP102A3 from *Bacillus subtilis* strain 168. We have currently cloned and characterised another member of this family, CYP102A7, and there are at least eight more genes for CYP102A P450s which have been identified in several genome sequencing projects. Alignment of all amino acid sequences revealed that the homology between different members is between 50 and 90 % according to which these enzymes can be divided into four Groups. The four cloned enzymes belonging to three different Groups but with 65 to 70 % homology were used for further investigation. Despite their appearance to be similar they often exhibit different properties. For example, the new isolated P450, CYP102A7, catalyses the deethylation of 7-ethoxycoumarin which is not accepted as substrate by CYP102A1-3. The hydroxylation patterns produced by these four monooxygenases are also different. Additionally we investigated solvent and thermal stability of these enzymes. For example, the monooxygenase domain of CYP102A1 is much more stable than those of CYP102A2/A3. On the other hand, its reductase domain is less stable than the corresponding ones of CYP102A2 and A3. Therefore we exchanged the natural more unstable reductase domain of CYP102A1 with the more stable reductase domain of CYP102A3, using the natural linker region of CYP102A1. Stability of the chimerical fusion protein A1A3 was determined using spectral analysis as well as by measuring FAD/FMN fluorescence and the hydroxylation activity towards 12-*para*-nitrophenoxydodecanoic acid and fatty acids after incubation at elevated temperatures. The new chimera was able to hydroxylate

substrates within a wider temperature range compared to the parental enzymes and has a half-life at 50°C more than ten times longer than CYP102A1.

Additionally we substituted the reductase domain of CYP102A1 by a thermostable analogue. In the genome of the thermophilic *Geobacillus stearothermophilus* a gene was found exhibiting 50 % protein similarity to the reductase domain of CYP102A1. The gene encodes a hypothetical α-subunit of sulfite reductases. Nevertheless the organisation of this protein into a flavodoxin-like FMN domain and an FAD containing domain is the same as in CYP102A1. This reductase was cloned downstream of the monooxygenase domain of CYP102A1. Activity of the foreign reductase within the chimera A1GR was confirmed by cytochrome c reduction. Next to the ability to transfer electrons to the heme iron, oxidation of C14-C18 fatty acids was proven. While the hydroxylation activity of CYP102A1 towards myristic and palmitic acid decreased to about 5 % of the initial rate after incubation at 49°C, the chimera exhibited no loss of activity under the same conditions.

V. Thesis

1 Introduction

1.1 P450 Monooxygenases

P450 monooxygenases belong to the class of oxidoreductases EC 1.14.X.Y. They are heme containing enzymes abundant in all kingdoms of life.

1.1.1 History of Cytochrome P450's

In 1958 Garfinkel and Klingenberg discovered independently a carbon monoxide binding pigment in pig and rat livers with an absorption maximum at 450 nm (Garfinkel 1958; Klingenberg 1958). Nearly 10 years later Omura and Sato could prove that this pigment was in fact a hemoprotein of the b-type cytochrome class (Omura and Sato 1964). In the late 1960's many Groups contributed evidence to the existence of either an NADH or NADPH-dependant flavoprotein involved in electron transfer to the P450 monooxygenases of microsomal, mitochondrial and bacterial origin (Mason et al. 1965; Strittmatter 1965). The reduction of the flavoprotein was found to be a two electron step, while the transfers to the monooxygenase are two one electron steps (Estabrook 1968). Mitochondrial and bacterial P450s seemed to be dependant of an additional electron transfer protein an iron-sulfur cluster containing ferredoxin (e.g. adrenodoxin, putidaredoxin (Sih 1969; Gunsalus et al. 1971)). The discovering of a thiol residue as the axial heme ligand produced an explanation of the unusual Soret peak position of 450 nm in the carbon monoxide bound form (Bayer et al. 1969; Hill et al. 1969; Hill et al. 1970). 1985 the first crystal structure of a P450 monooxygenase, P450cam (CYP101) from *Pseudomonas putida* was solved by Poulos et al. and the thiol residue identified as a cysteinate (Poulos et al. 1985). Up to now more than twenty crystal structures of P450 monooxygenases from different origin and several mutants with and without substrate have been solved (see http://www.rcsb.org/pdb/).

1.1.2 Nomenclature of P450 Monooxygenases

The first nomenclature of P450 enzymes was proposed in 1987 the 65 P450 genes that were known at that time including one plant and one bacterial gene were classified on the basis of amino acid identity, phylogenetic criteria and gene organisation. They were annotated by Roman numerals and upper case letters e.g. P450cam was designated as P450CI (Nebert et al. 1987). This first nomenclature was then revised in 1993 (Nelson et al. 1993; Nelson et al. 1996). According to the recommendation of a nomenclature committee P450 superfamily genes are now labelled as CYPs (CYP, CYtochrome P450). The characteristic for enzymes belonging to the same family is a sequence similarity of more than 40 % while P450s exhibiting more than 55 % form a subfamily. For example CYP102A1 belongs to the CYP102 family, CYP102A subfamily and is identified as CYP102A1. Except of the CYP51 family which is the only family with members from all five kingdoms of life all bacterial P450s belong to CYP families with a family name >100. The number of P450 genes is constantly rising and reached more than 6000 in July 2006. They are organised in 711 families including 177 of bacterial origin (see http://drnelson.utmem.edu/CytochromeP450.html).

1.1.3 Structure of Cytochrome P450 Monooxygenases

P450 monooxygenases got their name from their absorption maximum at 450 nm in the reduced CO-bound form (Pigment 450). The reason why cytochrome P450 absorbs in this range is the unusual ligand of the heme iron, a cysteinate. The heme iron can bind six ligands, four are nitrogens provided by the porphyrin ring which built a plane. The fifth and sixth ligand can bind above (distal) and below (proximal) this plane. In cytochrome P450s, the fifth ligand is a thiolate anion, sulphur with a negative charge which is provided by a conserved cysteine. The sixth ligand in the resting state is a water molecule (Denisov et al. 2005).

1.1.3.1 Primary and Secondary Structure

Sequence identity among P450 proteins is often less than 20 %. The regions with highest homology comprise: a) the heme binding loop, containing the most

characteristic P450 consensus sequence (Phe-Gly/Ser-X-Gly-X-His/Arg-X-**Cys**-X-Gly-X-Ile/Leu/Phe-X) with the absolutely conserved cysteine that serves as fifth ligand to the heme iron; b) the conserved **Glu**-X-X-**Arg** motif probably needed to stabilise the core structure through a salt bridge; and c) the consensus sequence considered as P450 signature (Ala/Gly-Gly-X-Asp/Glu-**Thr**), which is thought to play a role in oxygen activation through proton transfer (Graham-Lorence and Peterson 1996).

The typical secondary structure arrangement of P450's is shown in Figure 1-1. P450 monooxygenases have a high helical content and the helices are numbered from A to L while the β-sheets are numbered from 1-1 to 5-2. The four highly conserved residues are displayed in colour and bold script. Next to the organised secondary elements two further regions can be found in these enzymes an unstructured region called meander and the cysteine pocket (Mestres 2005).

```
                                          αA          β1-1        β1-2     αB
  1  TIKEMPQPKT FGELKNLPLL NTDKPVQALM KIADELGEIF KFEAPGRVTR YLSSQRLIKE

          β1-5        αB'                    αC
 61  ACDESRFDKN LSQALKFVRD FAGDGLFTSW THEKNWKKAH NILLPSFSQQ AMKGYHAMMV

     αD                  β3-1       αE                                  αF
121  DIAVQLVQKW ERLNADEHIE VPEDMTRLTL DTIGLCGFNY RFNSFYRDQP HPFITSMVRA

                                     αG                            αH
181  LDEAMNKLQR ANPDDPAYDE NKRQFQEDIK VMNDLVDKII ADRKASGEQS DDLLTHMLNG

    β5-1   β5-2              αI                      „       αJ
241  KDPETGEPLD DENIRYQIIT FLIAGHETTS GLLSFALYFL VKNPHVLQKA AEEAARVLVD

          αJ'          αK              β1-4      β2-1  β2-2    β1-3     αK'
301  PVPSYKQVKQ LKYVGMVLNE ALRLWPTAPA FSLYAKEDTV LGGEYPLEKG DELMVLIPQL

         αK''         Meander            Cys Pocket          αL
361  HRDKTIWGDD VEEFRPERFE NPSAIPQHAF KPFGNGQRAC IGQQFALHEA TLVLGMMLKH

     β3-3          β4-1   β4-2  3-2
421  FDFEDHTNYE LDIKETLTLK PEGFVVKAKS KKIPLGGIPS PSTEQSA
```

Figure 1-1 Organisation of the secondary structural elements in P450 monooxygenases

CYP102A1 monooxygenase sequence (adapted from (Hasemann et al. 1995)), the α-helices are denoted by upper case letters while the β-sheets are labelled with numbers. In the sequence the secondary structure is indicated by bold script for α-helices and italic script for β-sheets. Highly conserved amino acids are marked by colour according to the text.

1.1.3.2 Tertiary Structure

Although sequence similarity is quite low all crystal structures of P450s show the same structural organisation (Graham and Peterson 1999). Highest structural conservation is found in the core of the protein around the heme and reflects a common mechanism of electron and proton transfer and oxygen activation. The conserved core is formed by a four-helix (D, E, I and L) bundle which is surrounded by the helices J and K, two sets of β-sheets as well as in the substrate free form a rather unstructured coil called the meander. The prosthetic protoporphyrin IX (heme) is placed between the distal helix I and the proximal helix L (Figure 1-2). The proximal absolutely conserved cysteinate ligand of the heme iron is situated in the neighboured cysteine pocket.

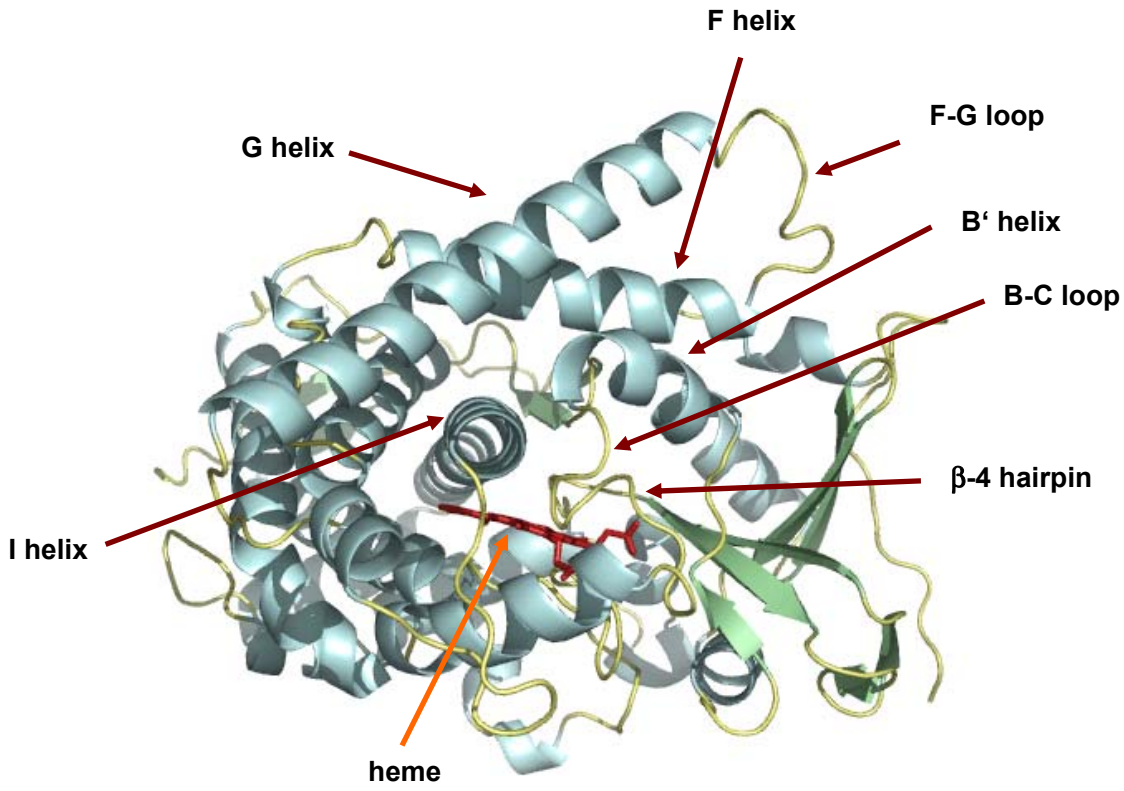

Figure 1-2 The crystal structure of the CYP102A1 monooxygenase domain (adapted from pdb 1ZO9)

Helix I is also part of the defined substrate access channel. This helix also contains a conserved amino acid sequence including the absolutely conserved threonine. Exchange of this side chain with hydrophobic residues results in enzyme variants

forming high amounts of hydrogen peroxide, they are no longer able to cleave the oxygen-oxygen bond.

Next to the highly conserved structural regions there exist however also some extremely variable regions. These constitute the substrate binding site causing the wide acceptance of very different substrates (e.g. ethanol in CYP2E1 and peptide antibiotics in CYP165B1). Belonging to these regions are the B-C and F-G loop which are located along the substrate access channel therefore situated distal of the protoporphyrin system. Substrate recognition and binding are mainly arranged through six substrate recognition sites (SRS), the B' helix (SRS1) parts of helix F (SRS2), G (SRS3) and I (SRS4) the β4-hairpin (SRS5) and the β2-loop (SRS6). Mutations in these regions, marked red in Figure 1-2, have a high impact on substrate specificity. Crystal structures obtained from x-ray analysis of P450s with bound substrate indicate that the substrate binding region is very flexible and often susceptible to structural reorganisation upon substrate binding encouraging an induced fit model (Li and Poulos 2004). This accounts for the broad substrate spectra of many P450 monooxygenases especially the microsomal ones.

1.1.4 Reactions and Mechanism

1.1.4.1 Mechanism

Based on crystal structures with and without substrate, ESR and NMR studies and other physicochemical methods a reaction mechanism for P450 monooxygenases was proposed. The actual reaction cycle shown in Figure 1-3 is nowadays commonly accepted (Denisov, Makris et al. 2005).

(**1**) In the substrate free, inactive state the ferric heme iron (Fe^{III}) is six times coordinated and in the low-spin state. The equatorial positions of the contorted octahedral iron complex are coordinated with the nitrogens of protoporphyrin IX, while the cysteinate and a water molecule bind the axial positions.

(**2**)The water at the distal site of the heme is displaced upon substrate binding. The substrate is not taking the place of the water but binds mostly by hydrophobic interaction in the vicinity of the heme. This results in the transition to the high-spin Fe

(III) complex, where the iron is only five times coordinated and in a pronounced “out of plane” structure. While some amino acid side chains show distinctive conformational changes, substrate binding induces only marginal rearrangement of the protein backbone (Haines et al. 2001). More important than structural differences is the increase of the redox potential from around -300 to -170 mV. This is an important regulation mechanism, as after substrate binding the electron transfer guided by the potential gradient from NAD(P)H through the electron transfer chain to the heme iron is possible. The one electron transfer results in a high spin ferrous iron (Fe II) (**3**).

(**4**) Due to its four unpaired electrons and it’s out of plane structure this complex is predestined to bind triplet oxygen with very high affinity, resulting in “in plane” coordination. This is the last stable (at low temperature) intermediate of this cycle.

(**5**) The next step is again a one electron reduction to a very unstable postulated peroxo-iron (III) complex.

(**6**) Due to their high reactivity the following intermediates can not be spectroscopically characterised but it can be assumed that after incorporation of one proton a hydroperoxo-ferric intermediate is formed while through incorporation of the second proton the oxygen-oxygen bond is cleaved under release of water.

(**7**) The emerging reactive complex is often in literature termed “compound I” which most likely switches back to the initial state through a rebound mechanism (Figure 1-4).

(**8**) The reaction of this iron-oxo complex with the substrate is in general formulated as a radical reaction. However carbocations as intermediates or direct addition of the substrate to (**7**) under insertion of oxygen into a C-H bond are also discussed. During the rebound mechanism the carbon centred intermediate should oscillate through the binding plane under loss of the sterical information. Due to the often high enantioselectivity of the P450 catalysed oxidation the recombination of this radical state has to be extremely fast. The resulting alcohol in (Figure 1-4) is probably shortly bound to the oxygen of the Fe (III) - porphyrin system before its dissociation. Next to the rebound mechanism heterolysis or addition of R-H as reaction mechanism can not be completely excluded.

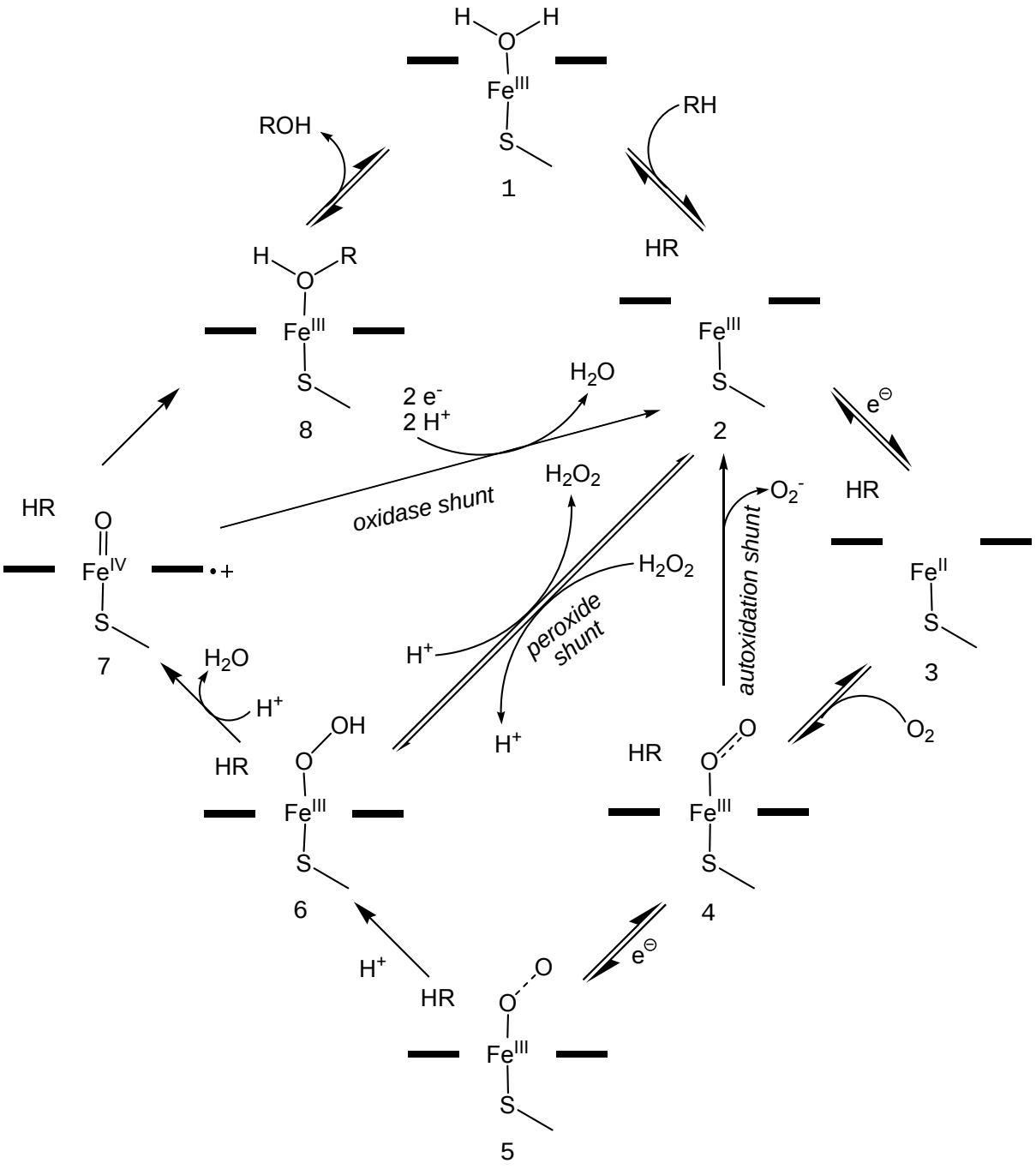

Figure 1-3 Catalytic cycle of P450 monooxygenases

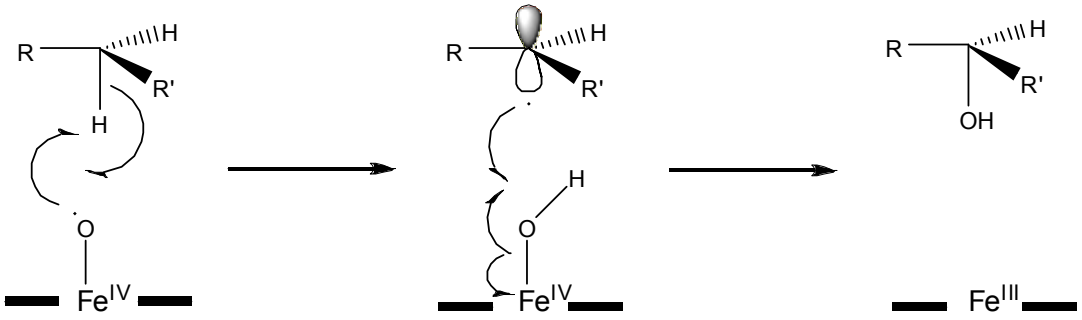

Figure 1-4 Rebound mechanism of the P450 catalysed hydroxylation

At least three more ways for dissociation of the activated oxygen from the heme iron apart from the already discussed one exist. These reactions are called *shunt pathways*. The most thoroughly investigated reaction is the *peroxide shunt*. In the presence of powerful oxidants like periodates, organic peroxides and hydrogen peroxide the peroxocomplex (**6**) can directly be formed from the substrate bound high spin complex (**2**). This reaction is interesting for synthetic processes because it enables product formation without the use of NAD(P)H. The *auto-oxidation shunt* complex (**2**) is formed by dissociation of the superoxide from complex (**4**). On the other hand complex (**2**) can be formed through the *oxidase shunt* where oxygen is reduced under consumption of two molecules of NAD(P)H to water. These two reactions as well as the reverse *peroxide shunt* are often consolidated as the uncoupling reactions because they are unproductive concerning substrate oxidation but nevertheless consume NAD(P)H.

1.1.4.2 Natural Role of P450 Monooxygenases

Cytochrome P450 proteins as mentioned before are ubiquitous in the whole living nature. As diverse as their sources are their roles in the metabolism of different species. Next to the more or less selective oxidation of hydrophobic organic compounds (e.g. in the liver) a huge amount of highly selective reactions for synthesis of hormones, signal transducers and other important secondary metabolites is described. They are involved in for example ergosterol synthesis, biosynthesis of insect- and phyto-hormones, development of fruit ripening as well as fragrance, flavour and colour development in plants (Berg et al. 1988; Feyereisen

1999; Morant et al. 2003; Schuler and Werck-Reichhart 2003). Furthermore they are drug metabolising enzymes and enzymes that are used to make cholesterol, steroids and other important lipids such as prostaglandines and thromboxanes (Payne and Hales 2004). These last two are metabolites of arachidonic acid (Nicosia and Patrono 1989; Ulrich et al. 2005). Their role in xenobiotic metabolism in mammals/humans is pivotal, especially for activation/clearance of lipophilic drugs. The metabolism of these compounds takes place in two phases. Phase I is chemical modification to add a functional group that can be used to attach a conjugate. The conjugate makes the modified compound more water soluble and easily excreted in the urine. Many P450s add a hydroxyl group in a Phase I step of drug metabolism (Meyer 1996). The hydroxyl group then serves as the site for further modifications in Phase 2 drug metabolism (Goldstein and Faletto 1993; Ioannides and Lewis 2004).

Mutations in cytochrome P450 genes, expression levels or deficiencies of the enzymes are related with several human diseases (Liu et al. 2004; Villeneuve and Pichette 2004). Induction of some P450s is a risk factor in several cancers since these enzymes can convert procarcinogens to carcinogens (Agundez 2004; Tsigelny et al. 2004).

1.1.4.3 Possible Role for Industrial Use

From industrial point of view P450 enzymes are interesting targets for the production of macrolide- and peptide- antibiotics as well as fine chemicals (Hezari and Croteau 1997; Betlach et al. 1998; Zerbe et al. 2004). For the pharmaceutical industry it is necessary to know how a putative drug will be processed in the human liver to prevent health risks during the longsome and expensive trial phase or to avoid recourse expanses. Despite this interest there exist only few processes in industry for the use of P450 monooxygenases and all of them are whole cell processes. One of the commercial applications of P450 monooxygenases is the use of *Curvularia* sp. for the 11ß-hydroxylation of Reichstein S to hydrocortisone, run by the Schering AG at a scale of approximately 100 tons per year (Petzoldt 1982; van Beilen et al. 2003). This process has no abiotic equivalent and allows skipping half of the steps of the chemical synthesis of hydrocortisone. In another process established by Pharmacia (former Upjohn) in the 1950s *Rhizopus* sp. is applied for the conversion of

progesterone to cortisone (Peterson et al. 1952; Hogg 1992). A drug reducing the cholesterol level, pravastatin is produced by microbial oxidation of compactin at Sankyo Pharma and Bristol-Myers Squibb Company. The annual market value reaches US$ $3{,}6 \times 10^{9}$ (van Beilen, Duetz et al. 2003). Recently it was reported that the *Streptomyces* sp. strain Y-110 produces up to 1000 mg pravastatin per litre, at 15 mg L^{-1} h^{-1} space-time yield upon optimised feeding of the substrate compactin (Park et al. 2003).

1.1.4.4 Electron Transfer Systems

These enzymes are called mixed function oxidases or monooxygenases, because they incorporate one atom of molecular Oxygen into the substrate and one atom is reduced to water.

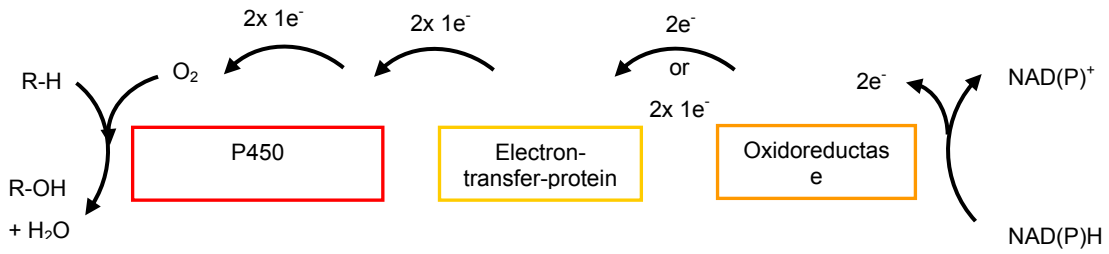

Figure 1-5 Standard electron transfer scheme for P450s

To perform this reaction the P450 monooxygenase needs electron equivalents (Figure 1-5). In the past the electron donor and/or the electron transfer system were used to divide P450 systems into four classes. According to the old classification to the first class belong the bacterial and mitochondrial P450s which receive their electrons from a NADH dependant FAD oxidoreductase and an iron sulphur cluster containing ferredoxin. The second class contained the microsomal P450s which use a NADPH depending diflavinreductase as electron transfer protein. The third class was represented by the P450s which are independent of electron transfer proteins hydroxylating peroxidised substrates as well as the fourth class where the sole member CYP55A1 ($P450_{nor}$) accepts NADH directly (Werck-Reichhart and Feyereisen 2000). Due to the high number of newly found and characterised P450 monooxygenases the number of electron transfer systems also increased. Table 1-1

gives an overview over the identified electron transfer systems and their structural organisation, e.g. the CYP102A family where the FAD oxidoreductase is fused to a flavodoxin type domain which is then fused to the heme domain. Even more diverse than the electron transfer partners are the reactions catalysed by P450 monooxygenases.

Table 1-1 P450s and their electron transfer systems (adapted from (McLean et al. 2005))

Typical P450s[a]	**Fused**[b]	**Fe/S; FMN**[c]	**Fused**[b]	**Reductase**[d]	**Other**[e]
Microsomal P450s	-	FMN	+	FAD, CPR[f]	CytB5
CYP102	+	FMN	+	FAD, CPR-type	-
CYP176A1, CYP107H1	-	FMN	-	FAD, AdR[g]-type	-
R. rhodochrous[h] P450	+	FMN	-	FAD, AdR-type	-
Mitochondrial P450s	-	2Fe–2S	-	FAD, AdR-type	-
CYP101, CYP106, CYP116A	-	2Fe–2S	-	FAD, GR[i]-type	-
CYP116B	+	2Fe–2S	+	FMN, PdR[j]-like	-
CYP105, CYP107	-	3Fe–4S	-	FAD, GR-type	-
CYP51 FX	+	3Fe–4S	-	NI[k]	-
CYP74A	-	-	-	-	peroxydised substrates
CYP152A1	-	-	-	-	H_2O_2
CYP55A1	-	-	-	-	directly NADH
CYP119[l]	-	Fe–S	-	2-oxoacid–ferredoxin oxidoreductase	pyruvate

[a] representative CYPs for this electron transfer system; [b] + the indicated domains (FAD: flavin–adenine-dinucleotide; FMN: flavin-mononucleotide; Fe/S: iron–sulphur proteins) are expressed in one polypeptide chain; [c] electron transfer protein containing the indicated co-factor; [d] reductase type with indicated co-factor; [e] other enzymes or mediators involved in electron transfer and/or supply for P450s; [f] cytochrome P450 reductase; [g] adrenodoxin reductase; [h] *Rhodococcus rhodochrous*; [i] glutathione reductase; [j] phtalate dioxygenase reductase; [k] not identified; [l] artificial electron transport chain

1.1.4.5 Reactions

The reactions carried out by P450 monooxygenases in the presence of oxygen, the co-factor NAD(P)H, and corresponding electron transfer systems are very diverse (Cryle et al. 2003; McLean, Sabri et al. 2005). Next to hydroxylation, epoxidation and special reactions like sulfoxidation the introduction of oxygen can lead to instable intermediates (e.g. semi-acetals or vicinal halogen hydrins) which then dissociate. This is the reason why N-and O-demethylation or oxidative dehalogenation are also catalysed by P450s.

One of the “standard” reactions of P450 monooxygenases is the hydroxylation of sp^3 hybridised C-atoms (Figure 1-6).The in the first step built alcohols can by some monooxygenases even be further oxidised to ketones (secondary alcohols) or aldehydes or even carbon acids.

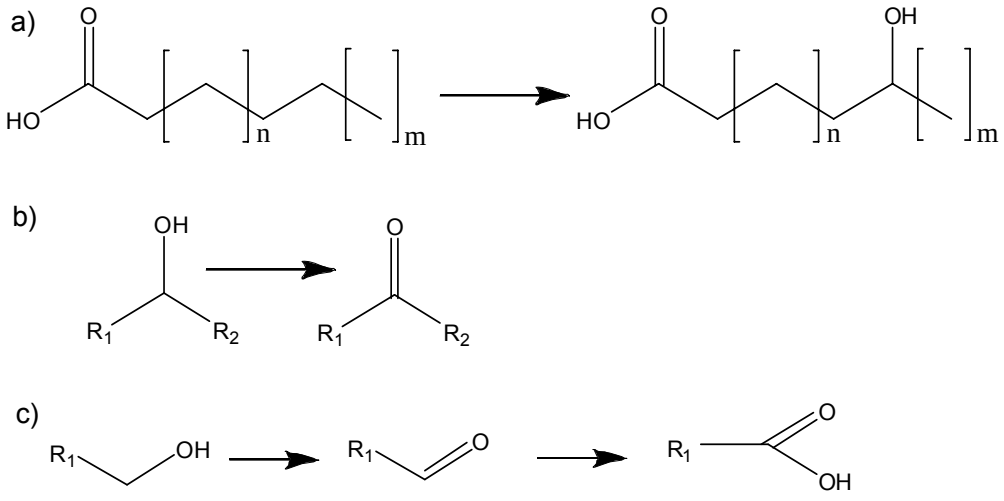

Figure 1-6 Activation of sp3 hybridised C-atoms

a) Hydroxylation of fatty acids to hydroxy-fatty acids, n = 1-16, m = 0-7; b) Oxidation of secondary alcohols to ketones; c) Oxidation of primary alcohols to aldehydes and carboxylic acids; R_1, R_2 alkyl groups

Other reactions with hydrocarbons are epoxidation of C=C double bonds (Figure 1-7a), and aromatic hydroxylation (Figure 1-7b) (Cryle, Stok et al. 2003).

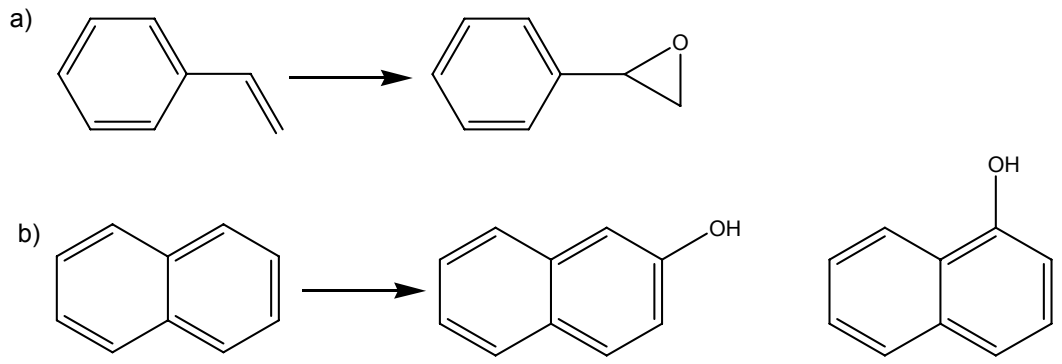

Figure 1-7 P450 catalysed a) epoxidation of styrene to styrene epoxide and b) hydroxylation of the aromatic compound naphthalene to 2-naphtol and/or 1-naphtol

P450 enzymes also catalyse dealkylation reactions that are often used for high-throughput screening of mutant libraries of microsomal P450s or for toxicity assays by use of fluorescence substrates like alkyl-coumarins or alkyl-resorufins (Figure 1-8) (Crespi et al. 2002; Stresser et al. 2002).

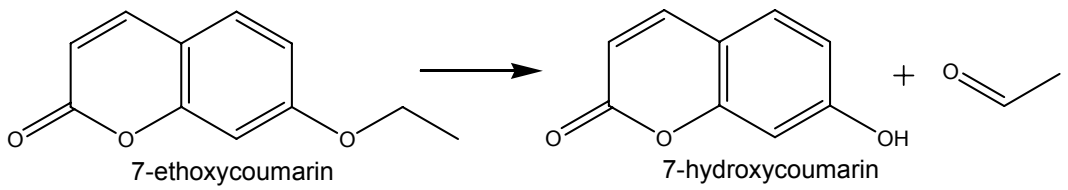

Figure 1-8 Dealkylation of 7-ethoxycoumarin

Deethylation of 7-ethoxycoumarin resulting in 7-hydroxycoumarin and acetaldehyde;

P450 monooxygenases are also able to catalyse the cleavage of carbon-carbon bonds via multiple substrate oxidations, for example, demethylation of lanosterol to 4,4-dimethyl-5α-cholesta-8,14,24-diene-3β-ol by a lanosterol 14α-demethylase (CYP51) (Shyadehi et al. 1996) (Figure 1-9).

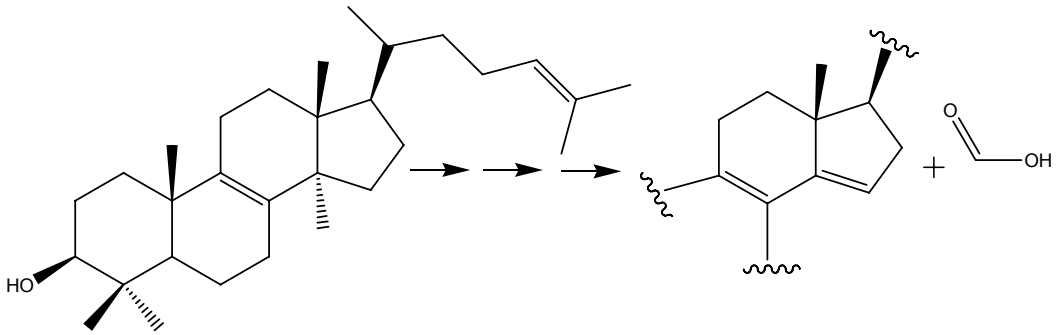

Figure 1-9 Demethylation of lanosterol

Cleavage of an acyl-carbon bond in the demethylation of lanosterol to 4,4-dimethyl.5α-cholesta-8,14,24-diene-3β-ol by a lanosterol 14α-demethylase (CYP51). The demethylation involves three consecutive oxidations resulting in the alcohol, the aldehyde and after homolytic C-C cleavage, in the released formic acid.

Remarkable is the ability of P450 enzymes to catalyse oxidative phenol coupling, a reaction usually carried out by peroxidases (Sato and Guengerich 2000). Three independent P450 monooxygenases with such activity have been proven to be involved in the synthesis of vancomycin-type antibiotics in *Amycolatopsis balhimycina* (Figure 1-10) (Bischoff et al. 2005).

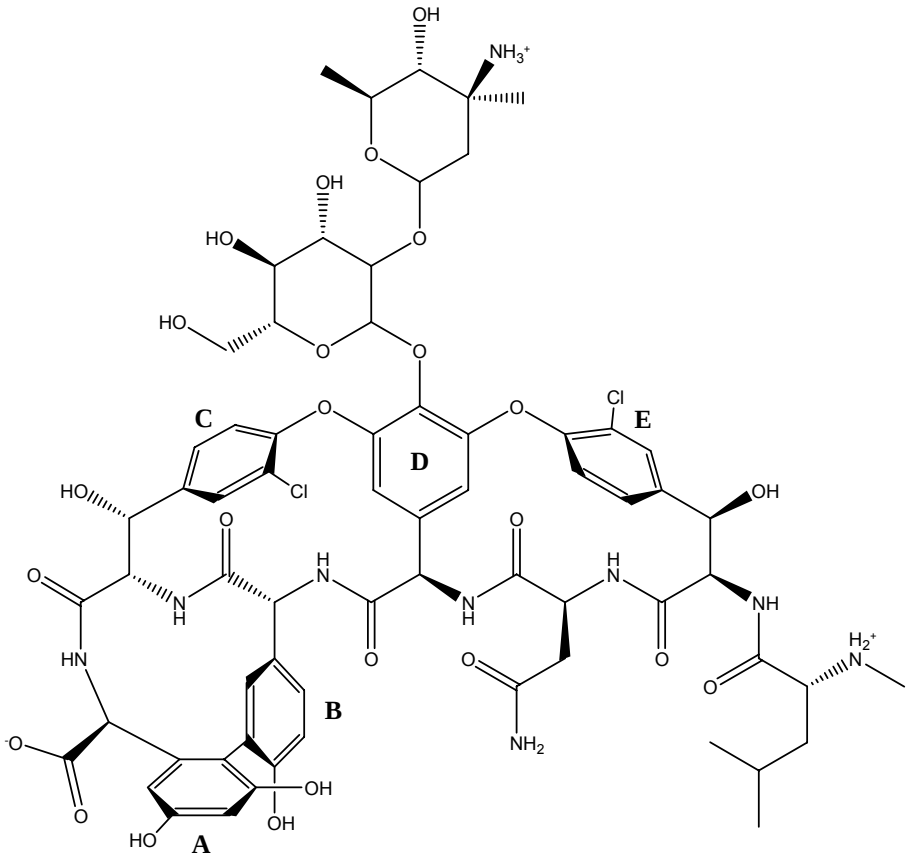

Figure 1-10 Phenol coupling during synthesis of vancomycin mediated through the P450 monooxygenases OxyA, OxyB, OxyC

Three different ring couplings are required in the order CD ring (OxyB), DE ring (OxyA) and AB ring (OxyC)

1.2 The CYP102A Subfamily

1.2.1 The Family Members and their Origin

The CYP102A subfamily is in several ways unique. In this subfamily the complete electron transfer chain and the P450 monooxygenase are expressed as one polypeptide of approximately 117-119 kDa. The electron transfer system is composed of an FMN containing flavodoxin type domain and an FAD containing oxidoreductase domain (Narhi and Fulco 1987). This and the higher homology to microsomal P450s than to other bacterial ones made these P450s an interesting target for investigation (Li et al. 1991). The natural substrates of the CYP102A members are fatty acids. Because of their structural organisation the CYP102A members exhibit extraordinary activities in comparison to other P450 monooxygenases of 3000-10000 min^{-1}. Up to now cloning and characterisation of only three members of this subfamily have been published. CYP102A1 from *Bacillus megaterium* and CYP102A2 and CYP102A3 from *Bacillus subtilis* strain 168 (Li, Darwish et al. 1991; Black et al. 1994; Budde et al. 2004; Gustafsson et al. 2004; Lentz et al. 2004). In this work we present some characteristics of a new member of this family, CYP102A7 from *Bacillus licheniformis* DSMZ 13 and also discuss some properties of those members which have not been characterised so far. These are CYP102A4 from *Bacillus anthracis* strain *ames*, CYP102A5 from *Bacillus cereus* ATCC 14579, CYP102A6 from *Bradyrhizobium japonicum* USDA 110 and the protein YP 037304 from *Bacillus thuringiensis* serovar konkukian 97-27 (Kaneko et al. 2002; Ivanova et al. 2003; Read et al. 2003; Rey et al. 2004; Han et al. 2006).

It is interesting to note that seven of the members of this subfamily have been found in the genus Bacillus.

Bacillus subtilis was one of the first bacteria studied and is used as a model organism for gram positive bacteria as is *E. coli* for gram negative bacteria. This organism is a soil-dwelling endospore-forming microbe similar to other *Bacilli*. At times of nutritional stress the *Bacilli* can divide asymmetrically producing a heat, salt and acid resistant endospore. Before the endospore is formed the bacteria might become motile and also through the competence system might take up environmental DNA. In *Bacilli* the production of antimicrobial and antifungal proteins

as well as insecticides is often associated with spore-forming (Katz and Demain 1977).

Bacillus licheniformis is a close relative of *B.subtilis* and is used to make the polypeptide antibiotic Bacitracin (Konz et al. 1997).

Two bacteria of the genus *Bacillus* are of significant medical importance, ***Bacillus anthracis*** the causative agent of anthrax, and ***Bacillus cereus***, which causes food poisoning.

Bacillus thuringiensis producing an intracellular parasporal crystal during spore formation is lethal to lepidoptera and other insects and therefore used as a biological insecticide (Du et al. 1999). Although not a human pathogen *Bacillus thuringiensis* is closely related to *B. cereus* and is therefore considered to belong to the *B. cereus B. anthracis B. thuringiensis* group.

Bacillus megaterium is the biggest aerobic spore forming bacterium. It is commonly found in soil.

The only member not originating from *Bacilli* is CYP102A6 from ***Bradyrhizobium japonicum*** an organism completely different from *Bacilli. Bradyrhizobium* belongs to the family of *Rhizobiaceae* which are gram negative, rod-shaped, nitrogen-fixing bacteria which live in symbiosis with plants, in the case of *B. japonicum* with the soybean *Glycine max* (Delgado et al. 1998).

1.2.1.1 CYP102A1 from *Bacillus megaterium*

First evidence of a soluble ω-1, ω-2 and ω-3 specific fatty acid hydroxylase in the soil bacterium *Bacillus megaterium* ATCC14581 was reported by Miura and Fulco (Miura and Fulco 1974; Miura and Fulco 1975). About ten years later Narhi and co-workers were able to isolate the respective P450 enzyme (Narhi and Fulco 1986). It was the third P450 enzyme isolated from *Bacillus megaterium* and was therefore called P450 BM-3. In the following years it was possible not only to express the holoenzyme in *E. coli* but also the discrete domains (Wen and Fulco 1987; Li, Darwish et al. 1991). CYP102A1 exhibits considerable homology to microsomal P450s but lacking the membrane anchor it can be produced and purified at much higher amounts and was therefore much easier to study. This enzyme, as well as CYP101A1 (P450 cam),

which represents a “standard” bacterial P450, were for a long time used as model enzymes to investigate the properties and reaction mechanism of cytochrome P450s. When in 1993 the crystal structure of the monooxygenase domain of CYP102A1 was solved it was used as a template to model many microsomal P450s which could not as easily be crystallised because they were not soluble (Ravichandran et al. 1993; Lewis et al. 1996; Lewis et al. 1999; Lewis et al. 1999) In the following years wild type enzyme and several mutants of CYP102A1 were crystallised with and without substrate (Haines, Tomchick et al. 2001; Ost et al. 2001; Joyce et al. 2004; Li and Poulos 2004). It was a big step forward in understanding the electron transfer system in CYP102A1 when in 1999 Sevrioukova et al. were able to analyse the crystal structure of the monooxygenase domain complexed with the FMN-domain although the linker was missing (Sevrioukova et al. 1999). The last piece in the jigsaw of CYP102A1, the FAD domain was crystallised in 2005, however up to now the complete enzyme could not be crystallised (Warman et al. 2005).

In 1997 the redox potentials for the electron transfer chain in CYP102A1 were determined (Munro et al. 1997). Figure 1-11 gives an overview of the midpoint potentials while Figure 1-12 presents the detailed electron transfer. In comparison to other measured potentials in similar electron transfer chains (CPR, NOS etc. see 1.3.1) the hydroquinone form of FMN (FMNH2) has a more positive potential than the semiquinone ($FMNH\cdot^{-}$). Additionally the semiquinone is the negatively charged red semiquinone in contrast to the neutral blue semiquinone in the other enzymes. But it has been shown later that the hydroquinone form of FMN is a cul-de-sac and electron transfer to the heme is mediated through $FMNH\cdot^{-}$ (Murataliev et al. 1997). The diagram shows clearly the increase in redox potential of the heme upon substrate binding. The difference between substrate free and substrate bound heme depends on the substrate e.g. the increase of the mid-point-potential after addition of hexadecanoic acid is only +103 mV while arachidonic acid induces a change of +129 mV. Still the potential of the heme is more negative then for $FMNH\cdot^{-}$ but it has to be taken in account that the measured potentials are only midpoint potentials and that even with arachidonic acid at saturation concentrations there exists a mixed population of high and low spin heme iron. Therefore it can be assumed that part of this population has a redox potential equal or even higher than $FMNH\cdot^{-}$.

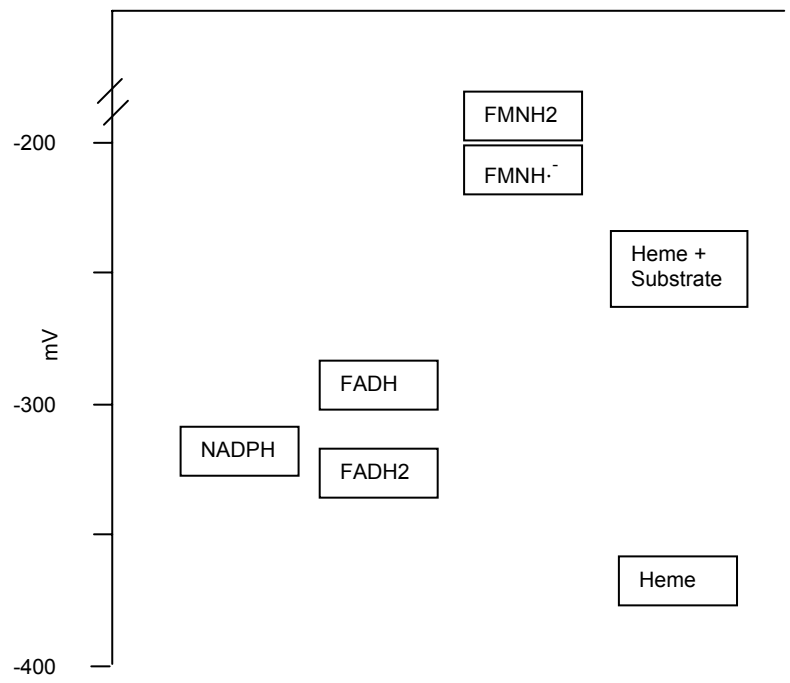

Figure 1-11 Potentials of the electron transfer chain in CYP102A1

The electron transfer proceeds in three steps. In the first step FAD is reduced to FADH2 while a substrate displaces the water in the vicinity of the heme resulting in a more positive redox potential. In the next step one reduction equivalent is transferred to FMN so that both flavins are now in their semiquinone form. This electron is directly passed to the heme iron which is now able to bind triplet oxygen. In the last phase the second reduction equivalent reduces again FMN to $FMNH^{\cdot -}$ with subsequent transfer to the heme; one oxygen atom is used to form water while the other one is introduced into the substrate.

When CYP102A1 was first discovered it was assumed to exist and be functional in a monomeric form. However S. D. Black and S. T. Martin could show by sedimentation velocity experiments and size exclusion HPLC that CYP102A1 exists in the presence of DTT solely as a dimer (sedimentation equilibrium analysis) and as a mixture of tetramer, trimer, dimer and monomer in the absence of DTT (Black and Martin 1994). It was supposed that not the monooxygenase domain but the reductase domain is responsible for the aggregation.

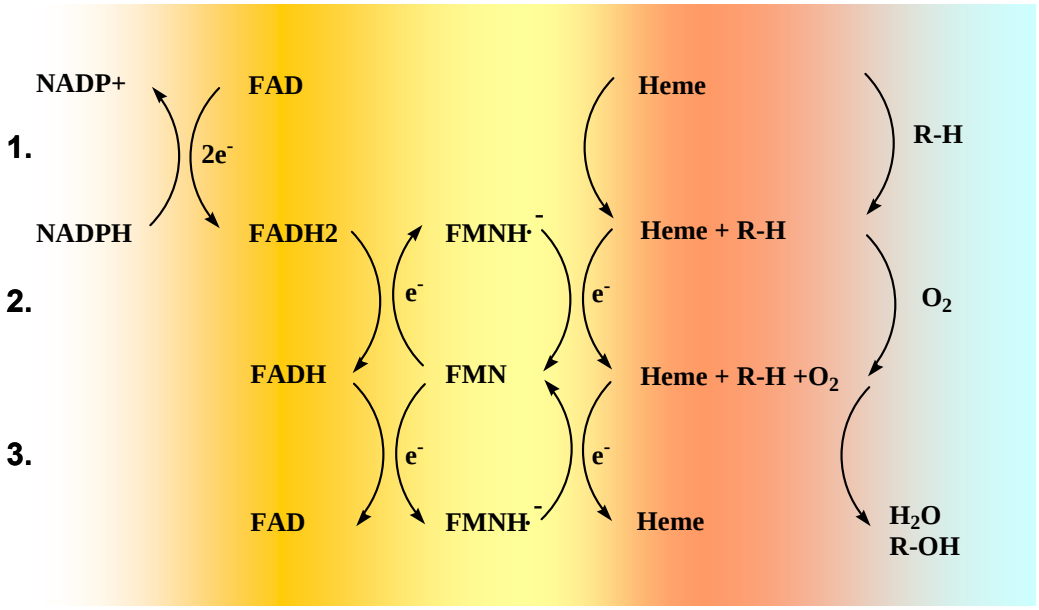

Figure 1-12 Electron transfer in CYP102A1

The functional structure of CYP102A1 was then reinvestigated in 2005 (Neeli et al. 2005). Dilution experiments were used to identify the critical concentration for separation of the active dimer into inactive monomers. Additionally a CYP102A1 with mutation in the monooxygenase (A264H) was mixed with a CYP102A1 with mutation in the reductase domain (G570D) resulting in mixed dimers. While none of the mutants were functional on their own the hetero dimer could hydroxylate dodecanoic acid at activities up to 20 % of wild type enzyme depending on incubation time and DTT concentration. These experiments have proven that electron transfer can occur crosswise.

1.2.1.2 CYP102A2 and CYP102A3 from *Bacillus subtilis*

Sequencing of *Bacillus subtilis strain 168* revealed two genes *yfnJ* (*yetO*)and *yrhJ* which exhibited high homology to CYP102A1 and the gene products were therefore annotated as CYP102A2 and CYP102A3 (Sorokin et al. 1997; Yamamoto et al. 1997). CYP102A3 was first cloned by Lentz et al. in 2000 while cloning and characterisation of CYP102A2 were nearly simultaneously published by Gustafsson et al. and Budde et al (Budde, Maurer et al. 2004; Gustafsson, Roitel et al. 2004; Lentz, Urlacher et al. 2004). Especially CYP102A2 showed some interesting features

in comparison to CYP102A1. For example, activities towards saturated fatty acids were considerably lower than those for CYP102A1. In contrast hydroxylation of unsaturated and branched fatty acids by CYP102A2 was much faster (Budde et al. 2006).

1.2.1.3 CYP102A7 from *Bacillus licheniformis*

A genome sequencing project of *Bacillus licheniformis* strain 13 also revealed a CYP102 type gene. This organism is interesting because of the production of antibiotics. The gene was cloned and expressed in *E. coli* followed by preliminary characterisation in a course of a Diploma thesis (Asta Chimene). The enzyme was special in its ability to accept 7-ethoxycoumarin as a substrate

1.2.2 Expression Control and Physiological Role

Expression of CYP102A1 in *Bacillus megaterium* is inducible by Phenobarbital, although further investigations showed that Phenobarbital is not a substrate of CYP102A1 (Narhi et al. 1983). During investigation of the method of induction two regulative regions could be found. One is a palindromic sequence about 620 bp upstream of the *CYP102A1* gene. This region is in the open reading frame of *bm3R1*. The resulting protein Bm3R1 binds to this palindromic sequence and negatively regulates its own expression and CYP102A1 expression (Shaw and Fulco 1992; Shaw and Fulco 1993). It could be shown by the gel mobility shift assay that substances that were able to induce CYP102A1 expression *in vivo* like barbiturates, peroxisome proliferators and also unsaturated fatty acids were able to dissociate the Bm3R1-DNA complex *in vitro* (English et al. 1994). Later another regulatory region, the so-called Barbie Box which was also negatively controlled by Bm3R1, was found 277 bp upstream of the *CYP102A1* gene (Liang et al. 1995). When the genome of *Bacillus subtilis* was sequenced the same regulatory palindromic sequence (bscR operon) as in *Bacillus megaterium* was found in the vicinity of the *CYP102A3* gene (*yrhJ*) (Gustafsson et al. 2001). There is some evidence that unsaturated fatty acids are the natural inducers of CYP102A1 and CYP102A3, because induction of these P450s by, for example, linoleic acid results in a higher resistance of *B. subtilis* and *B.*

megaterium to these unsaturated fatty acids (Palmer et al. 1997; Palmer et al. 1998). Using phytanic acid (3,7,11,15-tetramethylhexanoic acid) as inducer of CYP102A1 expression it could be shown that phytanic acid is a good substrate for CYP102A1 and the hydroxylation product, hydroxyphytanic acid is a considerably less effective inducer of CYP102A1 (English et al. 1997). This shows that expression of these P450s is down regulated after clearance of deleterious fatty acids. Interestingly CYP102A2 expression is not under control of the bscR/Bm3R1 operator/repressor and although a similar operator can be found in the genome of the other *Bacillus* species containing CYP102A genes these genes seem not to be under its control. Because of the high activity of CYP102A2 towards branched fatty acids there are some speculations that this enzyme plays a role in the maintenance of membrane fluidity. The fact that branched chain fatty acids represent 95 % of membrane composition of *Bacillus subtilis* has also contributed to this speculation (Kaneda 1991).

Then there is also the possibility that the CYP102A members play a role in spore forming. It could be shown that unsaturated fatty acids inhibit autophosphorylation of kinA, the first member of a signal cascade leading to sporogenesis. When kinA is not autophosphorylated the following factors Spo0F as well as Spo0A can also not be phosphorylated, and AbrB transcription is therefore not repressed (Strauch et al. 1992). AbrB repression is necessary for the following steps in sporogenesis. Although the direct involvement of CYP102A monooxygenases has not been proven it was reported that a certain pheromone necessary for full expression of the *CYP102A3* operon is negatively regulated by AbrB (Palmer et al. 1999).

1.2.3 The Power of Enzyme Engineering

The members of the CYP102A subfamily are fatty acid hydroxylases which hydroxylate carboxylic acids, alcohols and amides of a chain length from ~C12 to C22 at subterminal positions. Their regiospecificity and activity depends on chain length of the fatty acid.

The published crystal structures of CYP102A1 and the resulting extractable information about important amino acids in the substrate binding site provide the

opportunity for rational protein design as well as for building homology models of the related enzymes CYP102A2, CYP102A3 and CYP102A7. Based on this information, mutants of CYP102A1 and CYP102A3 have been engineered to meet the following needs: new substrate specificities, higher thermal stability and altered co-factor specificity.

Comparatively fewer publications are dedicated to protein engineering of these monooxygenases than to bio-chemical and -physical characterisation. Nevertheless good results have been obtained, for example, by construction of CYP102A1 mutants using polycyclic aromatic hydrocarbons as substrates (Carmichael and Wong 2001; Li et al. 2001) or by engineering CYP102A1 to accept ever smaller alkanes resulting in a mutant, which oxidises ethane to ethanol (Glieder et al. 2002; Peters et al. 2003; Meinhold et al. 2005).

Using a combination of site-directed mutagenesis, directed evolution and high throughput screening the substrate specificity of CYP102A1 and CYP102A3 could be altered to substrates with little or no structural similarity to the natural substrate (Li et al. 2000; Appel et al. 2001; Lentz et al. 2006). During mutagenesis of enzymes towards non-natural substrates, activity usually drops, indicating a more unfavourable geometry of the substrate binding site and often leading to unproductive NADPH consumption. Directed evolution of CYP102A1, however, may lead to recovery of activity even towards non-natural substrates. Thus, a triple mutant of CYP102A1 hydroxylates β-ionone in a regioselective manner, while exhibiting a turnover 80-fold higher than the wild type enzyme (Urlacher et al. 2006). The activities of CYP102A1 and CYP102A3 mutants towards many other substrates exceed those of the wild type enzyme by a factor of 40-100. Such a broad substrate spectrum comes close to the wide substrate specificities of eukaryotic microsomal monooxygenases.

CYP102A1 as well as CYP102A3 show only limited regioselectivity, producing a mixture of hydroxylated fatty acids. Also in reaction with unnatural substrates these enzymes and their variants often demonstrate low regioselectivity, producing, for instance, a mixture of secondary alcohols upon hydroxylation of *n*-octane (Appel, Lutz-Wahl et al. 2001; Lentz, Urlacher et al. 2004). The regioselectivity of CYP102A3 was changed by methods of directed evolution and protein design to hydroxylate substrates not only in different subterminal positions but to a high extent at the

terminal carbon. A double mutant of CYP102A3 was thus obtained that produces almost 50 % 1-octanol as the main product of reaction (Lentz, Feenstra et al. 2006).

Besides engineering of regioselectivity and activity, enantioselectivity of CYP102A1 was also engineered. Starting with CYP102A1 variant F87G, which was reported by Li et al. to produce (*R*)-chlorostyrene oxide with 94.6 % enantiomeric excess (*ee*), CYP102A1 mutants were obtained which oxidised styrene to both types of enantiomeric styrene oxides (Li et al. 2001; Eiben et al. 2006). The enantiomeric excess of the reaction product ranged from 58 % *ee* of (*S*)-styrene oxide (CYP102A1 A74E/F87V/P386S) to 92 % *ee* of (*R*)-styrene oxide when the epoxidation was catalysed by CYP102A1 variant F87G.

1.3 Other Enzymes

1.3.1 Diflavinreductases

As mentioned above all CYP102A enzymes are fusion proteins between a P450 monooxygenase domain and a diflavin reductase domain. Diflavinreductases in term are fusion proteins between an FMN containing flavodoxin type protein and an FAD reductase. This family of electron transfer complexes includes besides the diflavinreductase from the CYP102A subfamily the microsomal cytochrome P450 reductases (CPR), the α-subunit of the sulfite reductases (SiR), a putative methionine synthase and also the reductase domain of the nitric oxide synthases (NOS) (Murataliev et al. 2004). The mammalian CPR is a membrane bound enzyme expressed in the liver microsomes, there is only one CPR delivering reduction equivalents to all the different microsomal P450s. In plants in the contrary exist several isoforms of the CPR with different redox properties (Ohta and Mizutani 2004). In NOS the diflavinreductase is fused to a P450 type heme containing protein as in the CYP102A subfamily. This enzyme is only functional as a homodimer and has as an additional regulating domain a calmodulin binding site. The reaction cycle includes the oxidation of three mol of NADPH under consumption of two mol of arginine to form two mol nitric oxide by two heme domains. Sulfite reductases show the most complex organisation. They are heterodimers consisting of eight α-subunits (diflavinreductases) and four β-subunits which contain a siro-heme domain and an iron-sulfur cluster (Fe_4/S_4). In the reaction 12 mol of NADPH are used to reduce four mol sulfite to four mol sulfide.

The general structure of the diflavinreductases can be divided into three domains, the FMN and the FAD containing domains and an interdomain. The FMN binding domain is built by a α-β-structure with a centre of five parallel β-sheets surrounded by four α-helices the so called *Rossman*-fold. The FMN is sandwiched between two aromatic amino acids while the isoalloxazine ring of the FMN is facing the isoalloxazine ring of FAD. This is embedded in a β-β-sandwich of eight anti parallel β-sheets. As shown for FMN, the FAD is stabilised through two aromatic residues. The NADPH binding site on the surface of the protein in the diflavinreductases is also a *Rossman*-fold like binding motif. Recently there have been two publications about chimeric enzymes

between CYP102A1 and NOS proving that it is possible to switch the reductase domains of these two proteins. However, activities of the chimera, especially where the NOS reductase domain is fused to the CYP102A1 monooxygenase, were quite low probably due to the distance of the redox partners in the chimera (Fuziwara, Sagami et al. 2002).

1.3.1.1 Sulfite Reductase from *Geobacilllus stearothermophilus*

Geobacillus stearothermophilus (DSMZ strain 13240) is recently being sequenced at the Advanced Centre of Genome Technology at the University of Oklahoma. This organism was isolated from hot springs in the Yellowstone National Park exhibiting a growth optimum at 65°C.

1.3.2 The Formate Dehydrogenase from *Pseudomonas sp*.

Up to now industrial processes using P450 monooxygenases are restricted to whole cell processes (van Beilen, Duetz et al. 2003). One of the reasons is the consumption of equimolar amounts of the very expensive co-factors NADPH and NADH for each reaction cycle. Therefore several attempts to supply electrons by different methods have been investigated (Wichmann and Vasic-Racki 2005). The most successful method is the regeneration of the reduced co-factors by dehydrogenases. One very elegant solution is the use of formate dehydrogenases, where the cheap substrate formate is reduced to carbon dioxide and water while NAD^+ is oxidised to NADH. The equilibrium of this reaction is completely on the product side because the gaseous compound carbon dioxide is constantly removed from the system.

In this work we used the formate dehydrogenase from *Pseudomonas spec*. The enzyme is a homodimer, each monomer contains 400 amino acids with a molecular mass of 43 kDa. It was over-expressed in *E. coli* by Tishkov (1991) and crystallised (Tishkov et al. 1991). The crystal structure was used to identify important residues which were mutated to stabilise the enzyme but also to change the co-factor specificity from NAD^+ to $NADP^+$ (Seelbach et al. 1996; Tishkov et al. 1999).

1.4 Aim of the Work

Since 1985 when CYP102A1 was first described several other members of this P450 subfamily were discovered. Due to their high activities, their solubility, and the established methods to change their substrate spectra these enzymes are ideal candidates for the use in industrial applications. However, there are still drawbacks limiting their implementation. One of the main reasons is their insufficient stability in *in vitro* applications and also their dependence on expensive reduction equivalents. These make only the synthesis of high value products economical.

The scope of this work was the characterisation of the CYP102A subfamily of their common features but also their differences in regard of substrate spectra, activity and stability. Understanding of reasons for low stability should be used for construction of active enzymes with higher stability.

2 Results

2.1 Characterisation of Different Members of the CYP102A Family

The CYP102A subfamily represents a unique group of bacterial self-sufficient cytochrome P450 Monooxygenases. These P450s consist of a heme domain fused to a diflavin reductase. Up to now eight members have been identified within the CYP102A subfamily. According to the sequence homology of their monooxygenase domains the enzymes can be divided into four subgroups represented by the phylogenetic tree of the monooxygenase domains (Figure 2-1).

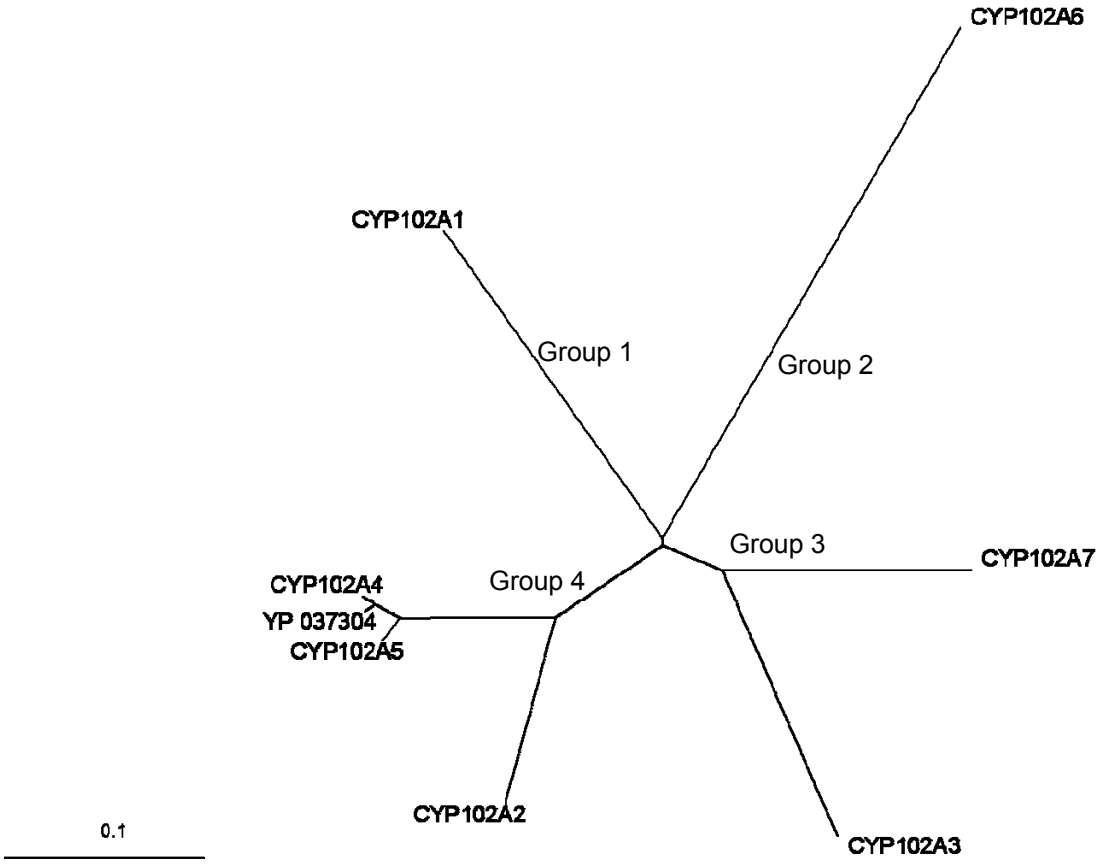

Figure 2-1 Phylogenetic tree of the CYP102A monooxygenase domains

Identities were obtained by alignment using ClustalW and the Blosom matrix, the tree was generated by treev32.

Group 1 and 2 are consisting just of one enzyme, CYP102A1 from *Bacillus megaterium* and CYP102A6 from *Bradyrhizobium japonicum*. Group 3 includes

CYP102A3 from *Bacillus subtilis* and CYP102A7 from *Bacillus licheniformis*. The biggest group 4 contains four enzymes. Three of them CYP102A4 from *Bacillus anthracis*, CYP102A5 from *Bacillus cereus* and YP_037304 from *Bacillus thuringiensis* demonstrating more than 90 % homology have never been characterised. The last member of this group is CYP102A2 from *Bacillus subtilis* exhibiting at least 80 % homology to the former three enzymes (Table 2-1).

Table 2-1 Similarity between the different members of the CYP102A subfamily

CYP102	A1	A2	A3	A4	A5	A6	YP_037304	A7
A1		63	64	64	65	50	64	65
A2	59		65	80	81	53	80	69
A3	58	60		65	65	51	64	73
A4	60	74	59		96	52	98	68
A5	60	75	59	95		52	96	68
A6	47	48	46	47	47		52	53
YP_037304	60	75	59	98	95	47		68
A7	59	64	64	61	61	48	61	

All values are expressed in % similarity (amino acid sequence); values on white background represent homology of the monooxygenase domains while values on grey background represent the whole enzymes.

More interesting than their overall similarity is the composition of the substrate binding site (SBS) (Table 2-2 and Table 2-3).

For some enzyme pairs the homology in the substrate binding site is even lower than the homology of the whole enzymes, as, for example for CYP102A2 versus CYP102A3 (50 % SBS and 65 %) or CYP102A7 (50 % SBS and 69 %). Other enzyme pairs show higher homology in the SBS compared to the whole heme domain, for example CYP102A2 and CYP102A6 (64 % SBS and 53 %) and also CYP102A3 and CYP102A7 (85 % SBS and 73 %).

Table 2-2 Amino acids in the substrate binding site adopted from (Ost et al. 2000; Sowden et al. 2005)

P450	42	47	51	72	74	**75**	**87**	**181**	188	**263**	**264**	**437**
CYP102A1	F	R	Y	S	A	**L**	**F**	**L**	L	**I**	**A**	**L**
CYP102A6	L	S	V	R	A	**L**	**F**	**L**	T	**I**	**A**	**L**
CYP102A3	F	V	F	G	G	**L**	**F**	**L**	S	**I**	**A**	**L**
CYP102A7	F	A	F	G	G	**L**	**F**	**L**	T	**I**	**A**	**L**
CYP102A4	I	D	V	E	A	**L**	**F**	**L**	L	**I**	**A**	**L**
CYP102A5	M	D	V	E	A	**L**	**F**	**L**	L	**I**	**A**	**L**
YP_0307304	I	D	V	E	A	**L**	**F**	**L**	L	**I**	**A**	**L**
CYP102A2	I	G	V	E	A	**L**	**F**	**L**	M	**I**	**A**	**L**

The amino acids are numbered according to CYP102A1; highly conserved amino acids are indicated in blue

Especially CYP102A6 exhibiting the lowest overall similarity to all other CYP102A enzymes shows higher similarities in the substrate binding site. Although some amino acids in the SBS are highly conserved the differences are high enough to expect individual substrate and product spectra.

Table 2-3 Homologies in the substrate binding site

CYP102	A2	A3	A4	A5	A6	A7
A1	57	57	64	64	57	57
A2		50	85	78	64	50
A3			50	50	57	85
A4				92	64	50
A5					64	50
A6						64

All values are expressed in % homology; YP_0307304 has the same SBS composition as CYP102A4

In this work the properties of CYP102A1, CYP102A2, CYP102A3 and CYP102A7 were investigated. The latter P450 enzyme has been identified and cloned first time at our institute within the scope of a diploma thesis (Asta Chimene 2005). An alignment of their heme domains can be seen in Figure 2-2

```
CYP102A7        MNKLDGIPIPKTYGPLGNLPLLDKNRVSQSLWKIADEMGPIFQFKFADAIGVFVSSHELV 60
CYP102A3        MKQASAIPQPKTYGPLKNLPHLEKEQLSQSLWRIADELGPIFRFDFPGVSSVFVSGHNLV 60
CYP102A2        MKETSPIPQPKTFGPLGNLPLIDKDKPTLSLIKLAEEQGPIFQIHTPAGTTIVVSGHELV 60
CYP102A1        -MTIKEMPQPKTFGELKNLPLLNTDKPVQALMKIADELGEIFKFEAPGRVTRYLSSQRLI 59
                     . :* ***:* * *** ::.::   :* ::*:* * **::. .      :*.:.*:

CYP102A7        KEVSEESRFDKNMGKGLLKVREFSGDGLFTSWTEEPNWRKAHNILLPSFSQKAMKGYHPM 120
CYP102A3        AEVCDEKRFDKNLGKGLQKVREFGGDGLFTSWTHEPNWQKAHRILLPSFSQKAMKGYHSM 120
CYP102A2        KEVCDEERFDKSIEGALEKVRAFSGDGLFTSWTHEPNWRKAHNILMPTFSQRAMKDYHEK 120
CYP102A1        KEACDESRFDKNLSQALKFVRDFAGDGLFTSWTHEKNWKKAHNILLPSFSQQAMKGYHAM 119
                 *..:*.****.:  .*  ** *.*********.* **:***.**:*:***:***.**

CYP102A7        MQDIAVQLIQKWSRLNQDESIDVPDDMTRLTLDTIGLCGFNYRFNSFYREGQHPFIESMV 180
CYP102A3        MLDIATQLIQKWSRLNPNEEIDVADDMTRLTLDTIGLCGFNYRFNSFYRDSQHPFITSML 180
CYP102A2        MVDIAVQLIQKWARLNPNEAVDVPGDMTRLTLDTIGLCGFNYRFNSYYRETPHPFINSMV 180
CYP102A1        MVDIAVQLVQKWERLNADEHIEVPEDMTRLTLDTIGLCGFNYRFNSFYRDQPHPFITSMV 179
                * ***.**:*** *** :* ::*. **********************:**:  **** **:

CYP102A7        RGLSEAMRQTKRFPLQDKLMIQTKRRFNSDVESMFSLVDRIIADRKQAESESGNDLLSLM 240
CYP102A3        RALKEAMNQSKRLGLQDKMMVKTKLQFQKDIEVMNSLVDRMIAERKANPDENIKDLLSLM 240
CYP102A2        RALDEAMHQMQRLDVQDKLMVRTKRQFRYDIQTMFSLVDSIIAERRANGDQDEKDLLARM 240
CYP102A1        RALDEAMNKLQRANPDDPAYDENKRQFQEDIKVMNDLVDKIIADRKASGEQS-DDLLTHM 238
                *.*.***.: :*   :*    ..* :*. *:: * .*** :**:*:   .:. .***: *

CYP102A7        LHAKDPETGEKLDDENIRYQIITFLIAGHETTSGLLSFAIYLLLKHPDKLKKAYEEADRV 300
CYP102A3        LYAKDPVTGETLDDENIRYQIITFLIAGHETTSGLLSFAIYCLLTHPEKLKKAQEEADRV 300
CYP102A2        LNVEDPETGEKLDDENIRFQIITFLIAGHETTSGLLSFATYFLLKHPDKLKKAYEEVDRV 300
CYP102A1        LNGKDPETGEPLDDENIRYQIITFLIAGHETTSGLLSFALYFLVKNPHVLQKAAEEAARV 298
                *  :** *** *******:********************* * *:.:*. *:** **. **

CYP102A7        LTDPVPSYKQVQQLKYIRMILNESIRLWPTAPAFSLYAKEETVIGGKYLIPKGQSVTVLI 360
CYP102A3        LTDDTPEYKQIQQLKYIRMVLNETLRLYPTAPAFSLYAKEDTVLGGEYPISKGQPVTVLI 360
CYP102A2        LTDAAPTYKQVLELTYIRMILNESLRLWPTAPAFSLYPKEDTVIGGKFPITTNDRISVLI 360
CYP102A1        LVDPVPSYKQVKQLKYVGMVLNEALRLWPTAPAFSLYAKEDTVLGGEYPLEKGDELMVLI 358
                *.* .* ***: :*.*: *:***::**:*********.**:**:**:: : ..: : ***

CYP102A7        PKLHRDQSVWGEDAEAFRPERFEQMDSIPAHAYKPFGNGQRACIGMQFALHEATLVLGMI 420
CYP102A3        PKLHRDQNAWGPDAEDFRPERFEDPSSIPHHAYKPFGNGQRACIGMQFALQEATMVLGLV 420
CYP102A2        PQLHRDRDAWGKDAEEFRPERFEHQDQVPHHAYKPFGNGQRACIGMQFALHEATLVLGMI 420
CYP102A1        PQLHRDKTIWGDDVEEFRPERFENPSAIPQHAFKPFGNGQRACIGQQFALHEATLVLGMM 418
                *:****:  ** *.* *******. . :* **:************ ****:***:***::

CYP102A7        LQYFDLEDHANYQLKIKESLTLKPDGFTIRVRPRKKEAMTAMPGAQPEENGRQEERPSAP 480
CYP102A3        LKHFELINHTGYELKIKEALTIKPDDFKITVKPRKTAAINVQRKEQADIKAETKPKETKP 480
CYP102A2        LKYFTLIDHENYELDIKQTLTLKPGDFHISVQSRHQEAIHADVQAAEKAAPDEQKEKTEA 480
CYP102A1        LKHFDFEDHTNYELDIKETLTLKPEGFVVKAKSKKIPLGGIPSPSTEQSAKKVRKKAENA 478
                *::* : :* .*:*.**::**:** .* : .::::            .     . .   .
```

Figure 2-2 Amino acid alignment of the monooxygenase domains from CYP102A1-3 and CYP102A7

The best characterised enzyme from this group is CYP102A1 from *B. megaterium* (better known as P450 BM3), but most literature data can not be directly used for comparison with CYP102A2 and CYP102A3 because of the difference in applied methods and goals in the different publications. In this work we wanted to investigate the P450 monooxygenases under identical conditions, therefore the first steps were to find a suitable vector system and to improve the expression conditions.

2.1.1 Cloning

The P450 monooxygenase genes investigated in this work were obtained in different expression plasmids (pET20b+, pET28a+ and pET28b+). The pET20b+ and pET22b+ vector contain a potential N-terminal *pel*B leader sequence allowing the introduced gene product to be transported into the periplasmatic space of *E. coli*. The difference between pET20b+ and pET22b+ is the *lac* operator sequence which can also be found in pET28a+ and allows for a more stringent control of expression. All three plasmids contain facultative His_6-tags which can be added to the carboxy-terminus of the desired protein and the pET28 vectors additionally contain an obligate N-terminal His_6-tag.

2.1.1.1 Choice of Plasmid

First expression experiments with the CYP102 enzymes showed that the yield for CYP102A3 cloned into pET20b+ including the *pel*B leader sequence was about five to ten times lower compared to the enzymes expressed in pET28 vectors (100-150 nmol/L to 400-1000 nmol/L respectively). Additionally the carbon monoxide difference spectra for CYP102A3 always exhibited a shoulder at 420 nm indicating non functional heme. To investigate whether the lower expression rate of this enzyme is due to its instability or the different expression vectors have an influence on expression rate the CYP102A3 gene was cloned into pET28a+. Furthermore it was also cloned into pET22b+ for expression of an enzyme without additional amino acids (tags).

2.1.1.2 Introduction of a *Nhe*I Restriction Site into pET22b+

In contrast to pET28a+ pET22b+ does not contain a *NheI* restriction site. For convenience of cloning the different P450 genes in both vectors the *Nde*I restriction site in pET22b+ was changed by site directed mutagenesis to an *Nhe*I site using the QCPCR primers SEIpET22NheF and SEIpET22NheR (Tm 64°C). A standard QCPCR at 55°C did not yield any PCR products. Therefore a touch down PCR was used starting with 55°C annealing and reducing the temperature by 0.5°C each following cycle for 25 cycles. After digestion with *Dpn*I endonuclease for 3 hours a

band at 5.5 kb could be identified on a 1 % TAE-agarose gel. After transformation of *E. coli* cells and following plasmid isolation the correct insertion of the *Nhe*I restriction site was confirmed by digestion of the new plasmid pET22Hb+ with *Nhe*I and *Pst*I. Agarose gel electrophoresis showed that all investigated transformants could be digested, resulting in a 1.5 kb and 4 kb fragment (Figure 2-3).

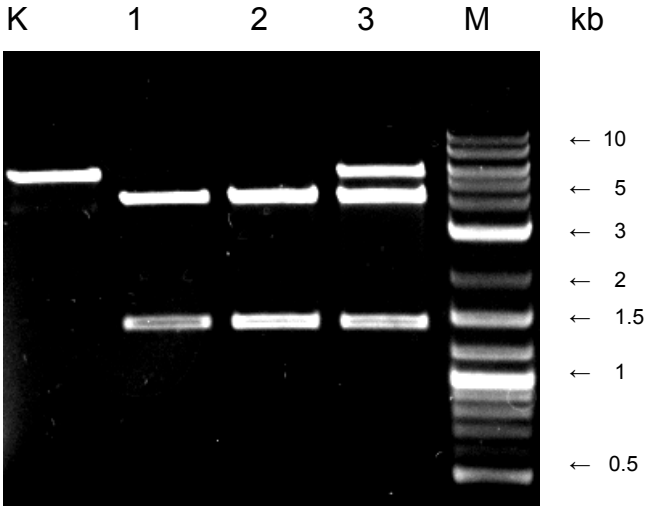

Figure 2-3 Restriction of pET22Hb+ with *Nhe*I and *Pst*I (1-3) Lane K shows the parental Plasmid digested with the same restriction endonucleases, M is the standard marker.

2.1.1.3 Cloning of CYP102A1 and CYP102A3 in pET22Hb+ and pET28a+

The CYP102A1 gene was obtained from the vector pET28CYP102A1 were the gene had been cloned between *Eco*RI and *Bam*HI restriction sites. To introduce the desired restriction sites the gene was amplified using the oligonucleotides SEIMonoLNhe1 and Spf_pET28a_BM_R. CYP102A3 was amplified from pET20bCYP102A3 using the oligonucleotides SeiCypA3Nhe1F and HBACYPA3RecoR1.

The PCR products were digested with *Nhe*I and *Eco*RI and ligated into pET22Hb+ and pET28a+ also digested with these restriction enzymes. After transformation into competent *E. coli* DH5α and plating on agar plates containing the specific antibiotics colonies were cultivated for plasmid isolation. The correct insertion of the P450 genes was determined by control digestion with *Nhe*I and *Eco*RI (Figure 2-4)

followed by sequencing. From each construct one of the verified plasmids was then named pET22HbA1, pET22HbA3, pET28aA1 and pET28aA3.

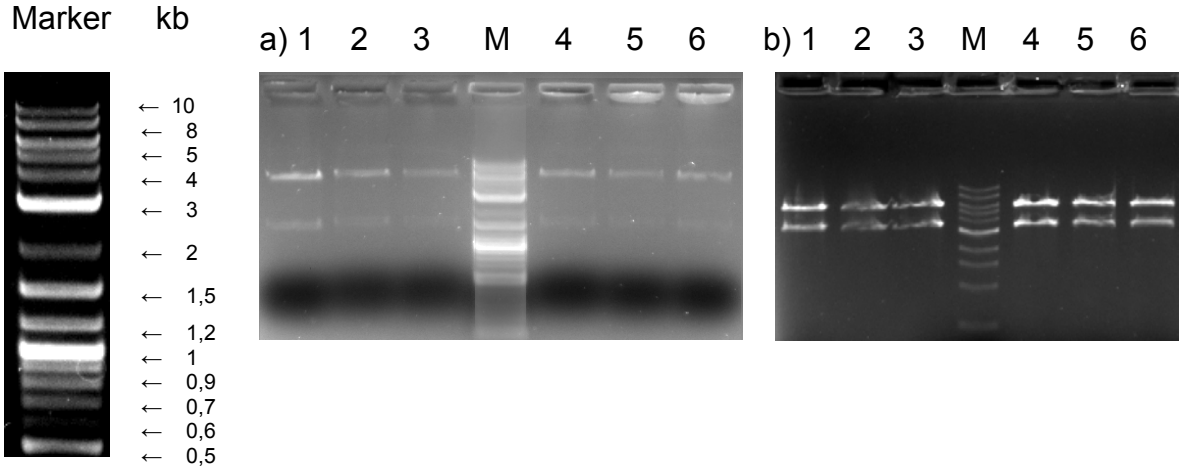

Figure 2-4 Control digestion with *Nhe*I and *Eco*RI of: a) pET22HbA1 and b) pET22HbA3

2.1.2 Optimisation of Recombinant Expression in *E. coli*

The former standard protocol for expression was to inoculate 5 ml LB with 5 µl glycerol stock or from a fresh colony and incubate overnight at 37°C and 180 rpm. On the next morning 400 ml TB medium were inoculated with the complete overnight culture and incubated at 37°C at 180 rpm until the culture reached OD_{600} of 0.8 to1.0. Expression was induced by addition of 0.5 mM IPTG and the cells were harvested after 4 hours incubation at 30°C and 150 rpm (yielding about 200 nmol P450 per 1g cells wet weight, ~1000 nmol/L). Although the expression levels were quite high the amount of host proteins was also very high. By reducing the time for the preculture the *E. coli* cells were still in the exponential phase. By reducing the OD for induction to 0.6 to 0.8 and the expression temperature from 30°C to 25°C we could get the same amount of P450 enzyme but with a lower amount of host proteins (about 250 nmol P450 per 1g cells wet weight, ~1000 nmol/L) facilitating further purification.

2.1.2.1 Expression of CYP102A3 Using Three Different Plasmids

The three plasmids pET20bCYP102A3, pET22HbCYP102A3 and pET28aCYP102A3 were introduced into *E. coli* BL21 (DE3) cells. For each construct a single fresh colony was used to inoculate 5 ml LB precultures. Expression was performed in 400

ml TB medium according to the improved expression protocol. At several time points 1 ml samples were taken and after appropriate dilution the optical density was measured spectrophotometrically. The three *E.coli* BL21 (DE3) cultures exhibited similar growth curves before induction of expression. After pelleting the cells were resuspended in 10 ml buffer A supplemented with PMSF (0.1 mM) and disrupted by sonication (6 bursts of 1.5 minutes with 5 minutes cooling). The following P450 yields show the range of three independent experiments:

CYP102A3 expressed from pET20bA3	100-150 nmol/L
CYP102A3 expressed from pET22HbA3	375-500 nmol/L
CYP102A3 expressed from pET28aA3	425-650 nmol/L

The CO-difference spectra of CYP102A3 still showed a low amount of non functional heme according to the shoulder at 420 nm, but changing the expression vector from pET20bA3 to pET22HbA3 or pET28aA3 led to a five-fold increase in expression of functional CYP102A3.

Influence of the additional *pe*lB leader sequence and N-terminal His_6 tag on enzyme solvent stability and hydroxylation pattern was investigated after purification by anion exchange chromatography.

2.1.2.2 Purification

To investigate enzyme properties the P450 monooxygenases had to be purified. Depending on the expression plasmid two purification strategies were applied.

2.1.2.3 Anion Exchange Chromatography

Those enzymes expressed from pET22Hb+ (CYP102A1 and A3) and pET20b+ (CYP102A3) were purified by a standard anion exchange chromatography protocol using a DEAE 650M or Source Q column on an Äkta explorerer system. The cell lysates were diluted 1:2 in 50 mM potassium phosphate buffer pH 8.1 to decrease ionic strength and increase pH (to pH 7.8) for enhanced binding of the P450 enzymes. After washing of the columns according to the protocol (4.2.3.3.1) the elution of the P450 enzymes during the applied salt gradient could be monitored at 417 nm. To calculate the purity of the enzyme preparations the protein concentration

was determined using the BCA assay kit in microtiter plate scale with at least 6 standards per assay (Figure 2-5). The resulting equation was used to calculate the unknown protein concentrations. The P450 concentration was calculated from the CO-difference spectrum and a molar mass of 119 000 g/mol. The following table shows the protein concentration and P450 concentration in a typical purification of CYP102A1 and A3 (Table 2-4). Both enzymes were expressed from pET22Hb+ and the purification factor was 2.2 for CYP102A1 and 2.5 for CYP102A3.

Table 2-4 P450 purification using a DEAE650M anion exchange column

	cell lysate				eluate				
CYP102	Protein µg/ml	P450 µg/ml	P450 %	P450 nmol	Protein µg/ml	P450 µg/ml	P450 %	P450 nmol	recovery %
A1	21200	3030	14.3	257	4420	1420	32	167	65
A3	19800	1480	7.5	124	4090	760	18.6	76	61

CYP102A2 which was only expressed from pET28b+ was not purified by anion exchange chromatography while CYP102A7 expressed from pET28a+ did not bind to either of the two used columns.

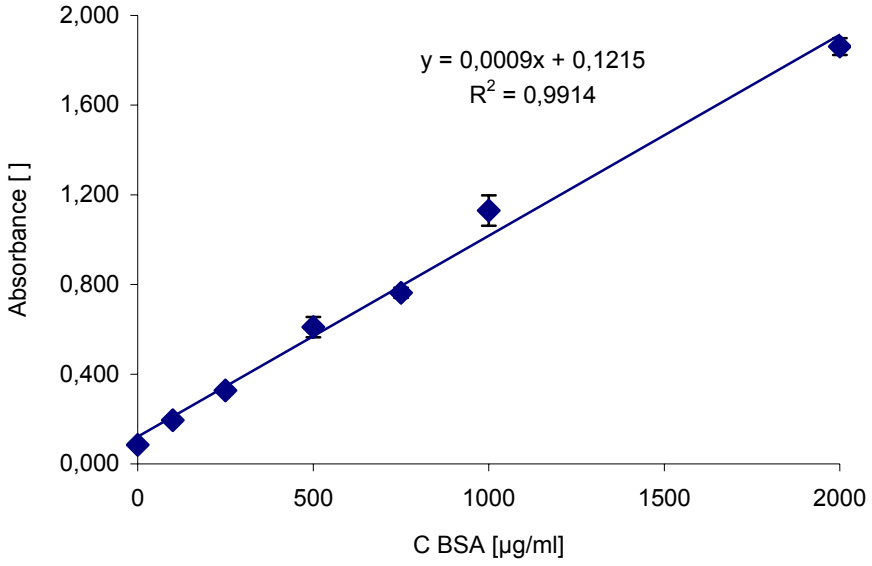

Figure 2-5 Calibration curve for the BCA assay with bovine serum albumin (BSA)

2.1.2.4 Metal Affinity Chromatography

Those enzymes containing the N-terminal His_6-tag (pET28 vector system) were purified by metal affinity chromatography as described in the methods section (4.2.3.3.2). The purity after chromatography varied between 64 and 78 % (Table 2-5).

Table 2-5 P450 purification using Ni-Sepharose

	cell lysate				eluate				
CYP102	Protein µg/ml	P450 µg/ml	P450 %	P450 nmol	Protein µg/ml	P450 µg/ml	P450 %	P450 nmol	recovery %
A1	26016	1778	6.8	327	9269	7218	78	260	80
A2	22314	940	4.2	158	5387	3868	72	130	82
A3	21889	1178	5.4	198	7783	4974	64	167	84

By applying metal affinity chromatography as purification method purity could be increased ~5-fold and the yield could be extended from ~60 to ~80 %. Although imidazole is a standard inhibitor active enzymes could be retained after dialysis in buffer A. The exception was again CYP102A7, although it was expressed with an N-terminal His_6-tag binding to the Ni-sepharose was extremely weak and the enzyme was eluted in a much diluted state already during washing.

2.1.3 Spectral Characterisation of the Purified Enzymes

The spectra of CYP102A1-A3 were measured after purification by IMAC on Ni-sepharose. Enzymes at a final concentration of 1-1.5 µM were measured first only diluted in buffer A, followed by measurement of the sodium dithionite reduced spectrum and then after saturation with carbon monoxide. The following figures (Figure 2-6, Figure 2-7 and Figure 2-8) show the absorption spectra of the oxidised and reduced form and also the CO difference spectra calculated from the CO-bound and reduced state.

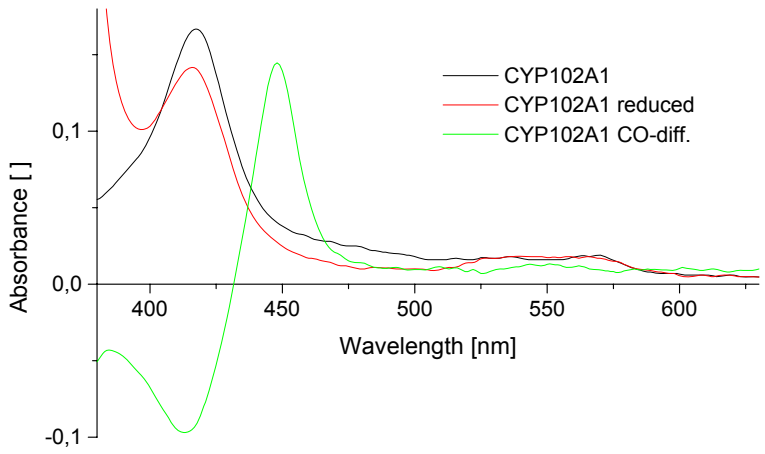

Figure 2-6 Absorption spectra of CYP102A1

Although there was no substrate or reducing agent added, the spectrum of the "oxidised" form of CYP102A1 indicated that some part of the enzyme preparation already existed in the high spin form as shown by the maximum at 417 nm instead of 420 nm. Additionally the shoulder at around 470 nm due to oxidised flavins was not very pronounced. After addition of sodium dithionite the maximum of the heme shifted to 416 nm while the shoulder at 470 nm disappeared completely.

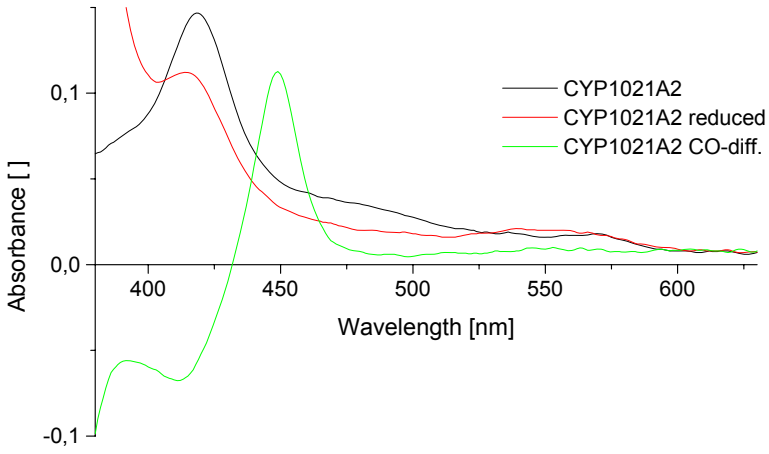

Figure 2-7 Absorption spectra of CYP102A2

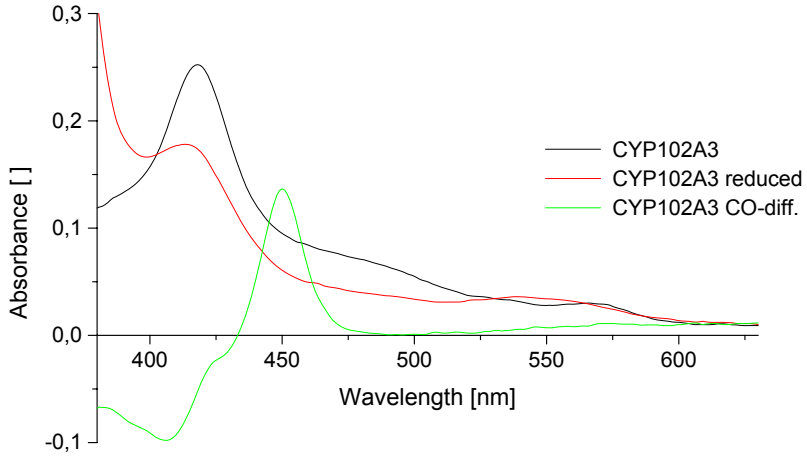

Figure 2-8 Absorption spectra of CYP102A3

Spectra of CYP102A2 and A3 revealed the more definite absorption of the oxidised flavins and both exhibited a maximum in their oxidised forms at 418 nm. After reduction the heme absorption relocates to 414 nm. The maxima for the CO- bound forms were 448 nm for CYP102A1, 449 nm and 450 nm for CYP102A2 and A3 respectively. Additionally CYP102A3 exhibited a shoulder between 422-425 nm indicating a non-functional heme species which is no longer able to bind CO.

2.1.4 Stability in the Presence of Organic Solvents

The stability in the presence of DMSO of CYP102A3 expressed in different vectors (see 2.1.2.1) was measured at enzyme concentrations of 0.24 µM, 0.13 µM or 0.16 µM CYP102A3 (from pET20bA3, pET22HbA3, pET28aA3) and 200 µM 12-pNCA in 2-20 % DMSO. The reactions were started by addition of 200 µM NADPH and the changes in absorbance at 410 nm were used to calculate substrate conversion/enzyme ($\varepsilon_{paranitrophenolat}$ = 13.2 mM^{-1} cm^{-1}). The highest activity 120 min^{-1} was used as reference with 100 % activity (Figure 2-9). This activity could be obtained using the native enzyme while the enzyme with the *pel*B leader (from pET20bA3) exhibited less than 60 % activity and was inactivated by lower DMSO concentrations. More than 50 % decrease in activity was found at DMSO concentrations of 8 % for pET20bA3, 11 % for pET22bA3 and 14 % pET28aA3. All

three CYP102A3 constructs showed extended solvent stability when the crude cell lysate was used for the assay (around 75 % activity at 11 % DMSO).

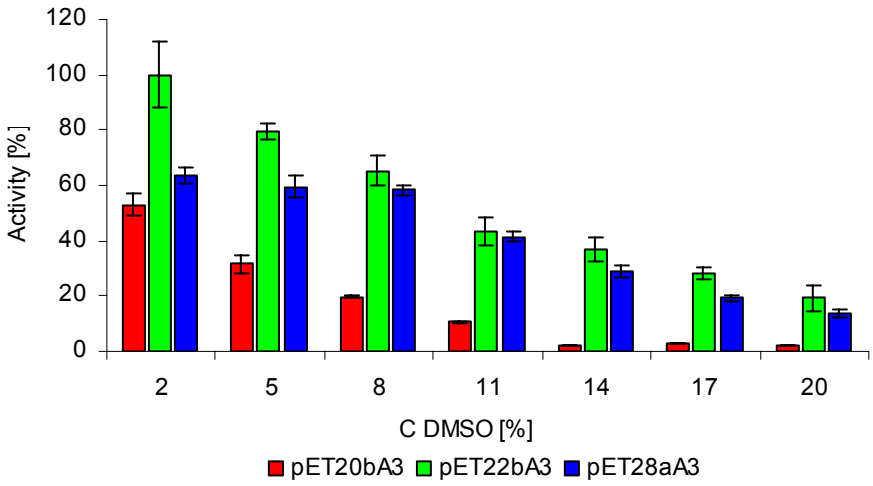

Figure 2-9 Solvent stability of different CYP102A3 constructs measured by the 12-pNCA assay

2.1.5 Activity Towards Saturated and Unsaturated Fatty Acids

2.1.5.1 Activity Profile at Constant Substrate Concentration

Recent investigations at this institute and also several publications concerning members of the CYP102A subfamily have shown that these enzymes exhibit different activities towards several substrates. The problem in comparing these data is that different people use different reaction conditions and in older publications the identification of the resulting products is not complete. In this work always one enzyme preparation was used for all measured substrates at constant substrate concentration (150 µM). Therefore the data do not reflect k_{cat} values but activities at a given substrate concentration. Additionally the NADPH concentration was not in excess but in depletion (100 µM). Thereby it was possible to examine if the NADPH consumption really resulted in product formation. The coupling efficiency was for all reactions higher than 95 % except for CYP102A2 with dodecanoic acid as substrate.

For comparative analysis the highest activity towards a saturated fatty acid was taken as 100 % activity (usually towards tetradecanoic (C14) - or pentadecanoic (C15) acid) (Figure 2-10, Table 2-7). The activity profile in terms of length of saturated fatty

acids was nearly the same for all four tested enzymes. Highest activity was observed towards C14 or C15 with decreasing activity towards shorter and longer chain length (tridecanoic- and dodecanoic acid (C13 and C12) and hexadecanoic- and heptadecanoic acid (C16 and C17)). This was independent from the fatty acids having even or odd numbers of C-atoms. The more interesting behaviour of the enzymes could be observed towards unsaturated and polyunsaturated fatty acids. CYP102A1 exhibited slightly higher activities towards the unsaturated fatty acids (120-180 %) while the activity increases with chain length and decreases with number of double bonds. CYP102A2 showed the highest activation effect with a maximum of 420 % activation with linoleic acid and then decreasing again with chain length. The best substrate for CYP102A3 seemed to be 5,8,11,14,17-eicosapentaenoic acid (EPA) with around three-fold higher activity than towards tetradecanoic acid. The only enzyme exhibiting lower activities towards unsaturated fatty acids was CYP102A7 isolated from *Bacillus licheniformis* with only 50-80 % activity.

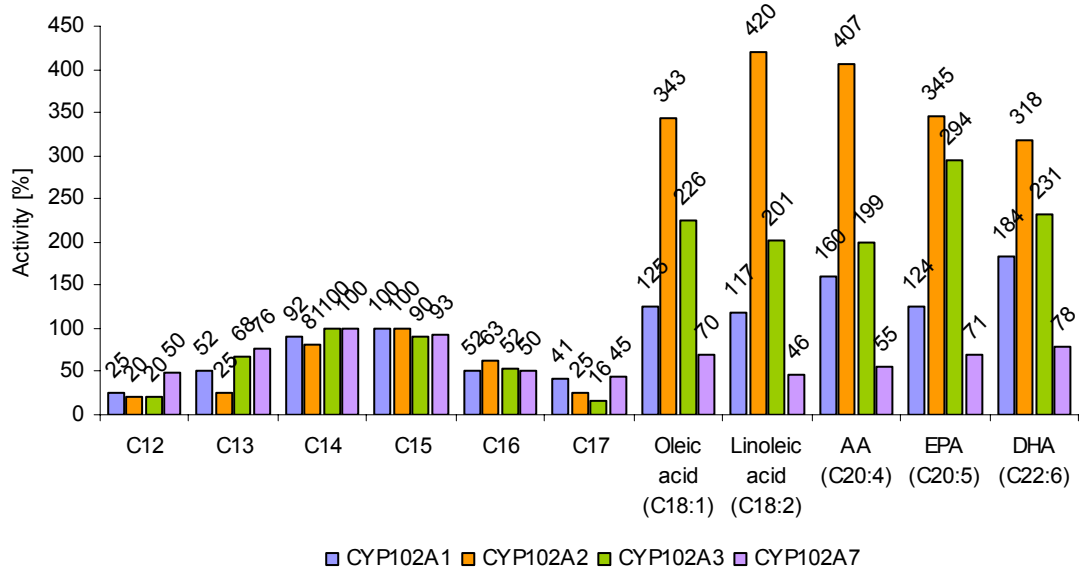

Figure 2-10 Activity profile of CYP102A1-3 and CYP102A7 towards fatty acids

Activities are represented in % of the highest NADPH consumption with a saturated fatty acid.

2.1.5.2 Product Profiling

After measuring activity towards different fatty acids by NADPH consumption the substrate and products were isolated by extraction with acidified diethyl ether. The organic phase was left to evaporate completely at room temperature and the substrate/product mixture resuspended in derivatising reagent. After incubation at 80°C products were determined by GC/MS analysis under the assumption that all components were extracted with the same efficiency. Substrate and products were identified by their characteristic fragmentation patterns. Positions for the fragmentation of the hydroxylated products of tetradecanoic acid are shown in Figure 2-11 while Table 2-6 gives an overview over the characteristic fragments for the products of the investigated saturated fatty acids.

Percentages of the different products were calculated from peak areas. As an example the chromatograms for the hydroxylation of hexadecanoic acid for all four monooxygenases are presented in Figure 2-13. The peak at a retention time (RT) of 9.300 minutes was caused by an impurity from octadecanoic acid which could be found in nearly all preparations. It has to be noted that the GC program for CYP102A3 and hexadecanoic acid differed from the standard protocol in heating velocity to allow for a better separation of the products. Still the peaks for ω-6 to ω-8 overlap, in this case the peak areas were identified by the different mass spectra (Figure 2-13 d).

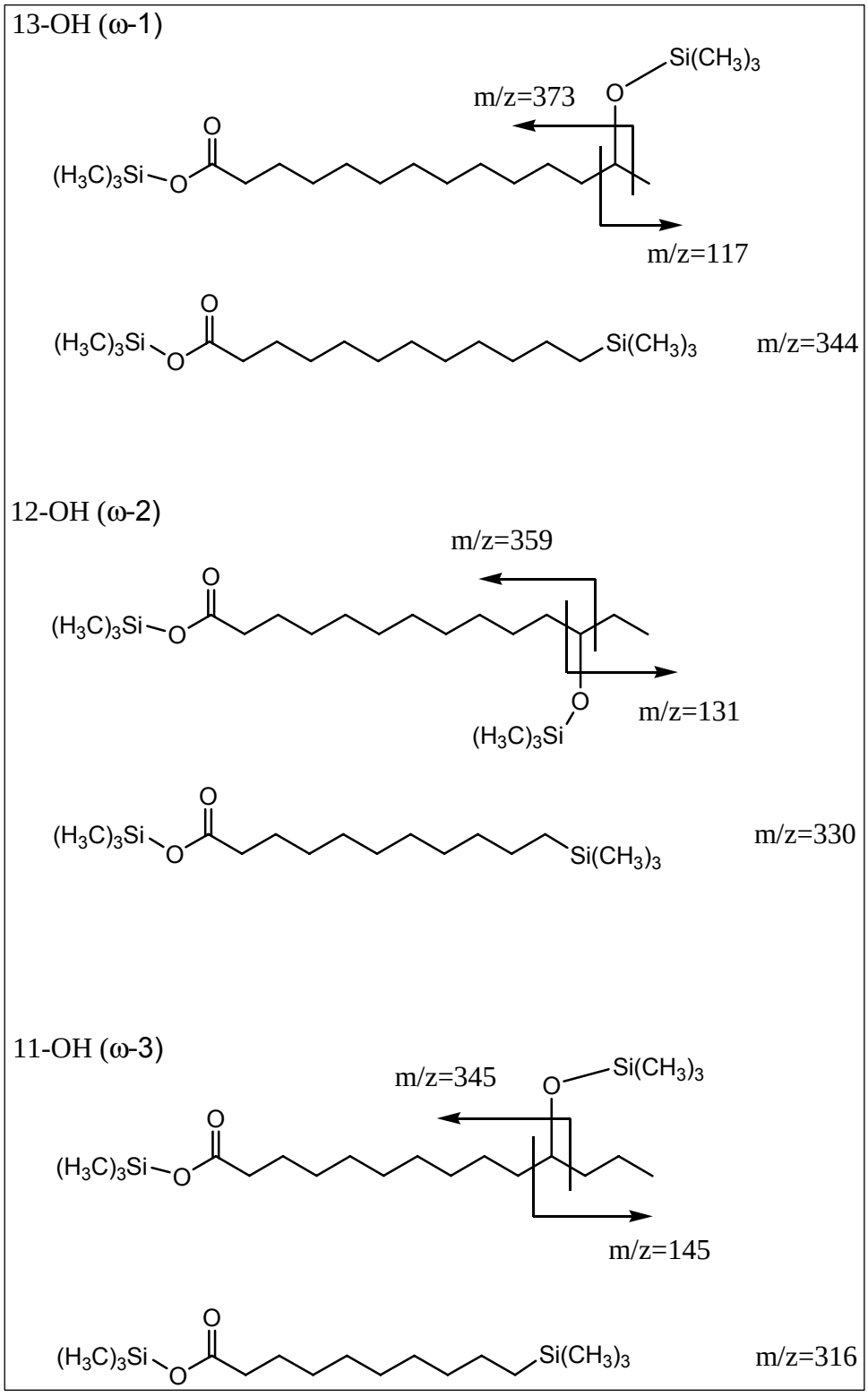

Figure 2-11 Characteristic fragments for the silylated hydroxylation products of tetradecanoic acid

Table 2-6 Characteristic fragment sizes for the silylated hydroxylation products from different fatty acids

Substrate	ω-1[a]	ω-2	ω-3	ω-4	ω-5	ω-6	ω-7	ω-8
C12	117, 316, 345	131, 302, 331	145, 288, 317					
C13	117, 330, 359	131, 316, 345	145, 302, 331	159, 288, 317				
C14	117, 344, 373	131, 330, 359	145, 316, 345	159, 302, 331	173, 288, 317	187, 274, 303	201, 260, 289	
C15	117, 358, 387	131, 344, 373	145, 330, 359	159, 316, 345	173, 302, 331	187, 288, 317	201, 274, 303	215, 260, 289
C16	117, 372, 401	131, 358, 387	145, 344, 373	159, 330, 359	173, 316, 345	187, 302, 331	201, 288, 317	215, 274, 303
C17	117, 386, 415	131, 372, 401	145, 358, 373	159, 344, 373	173, 330, 359	187, 316, 345	201, 302, 331	
C18	117, 400, 429	131, 386, 415	145, 372, 401	159, 358, 387	173, 344, 373	187, 330, 359	201, 316, 345	

[a] Mono-hydroxylated fatty acids counted from the ω-end

The mass spectra for hexadecanoic acid, the ω-1 to ω-4 hydroxylated products and the ω-7 hydroxylated hexadecanoic acids, which was only produced by CYP102A3, are shown in Figure 2-12. Not all of the possible fragments are observable in all products at least two have been used for identification together with the characteristic retention time.

The oxidation products of arachidonic acid (Figure 2-14) could only partially be identified and it was not possible to identify products for the other unsaturated fatty acids.

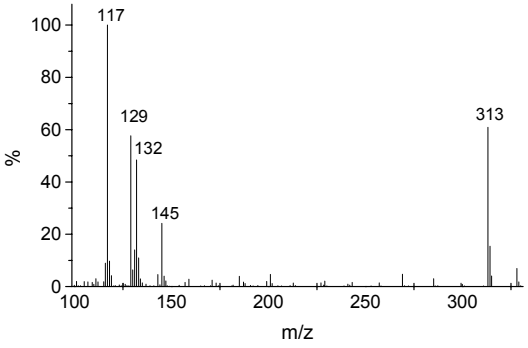

a) Mass spectrum of hexadecanoic acid after derivatisation

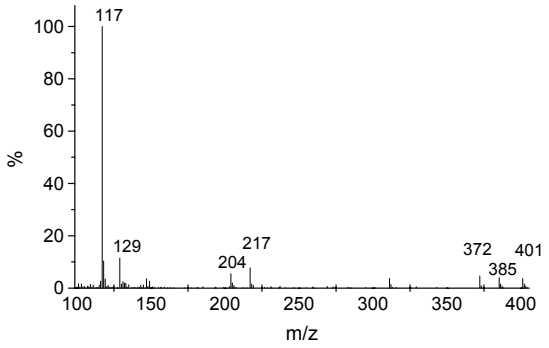

b) Mass spectrum of 15-hydroxy-hexadecanoic acid (ω-1) after derivatisation

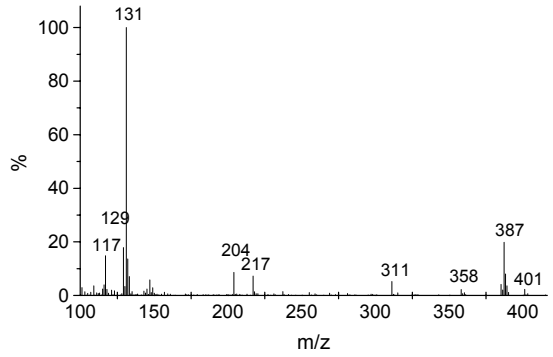

c) Mass spectrum of 14-hydroxy-hexadecanoic acid (ω-2) after derivatisation

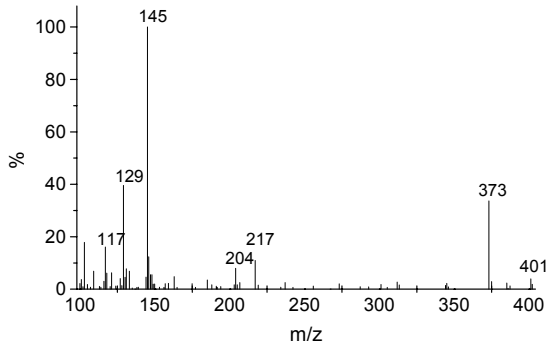

d) Mass spectrum of 13-hydroxy-hexadecanoic acid (ω-3) after derivatisation

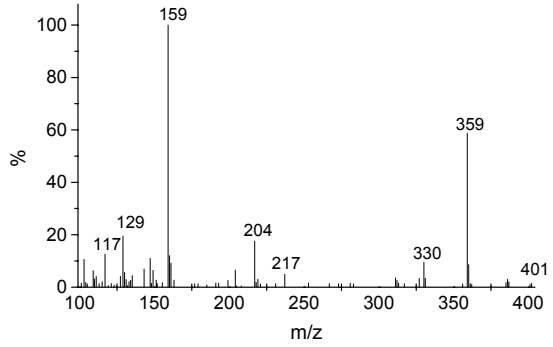

e) Mass spectrum of 12-hydroxy-hexadecanoic acid (ω-4) after derivatisation

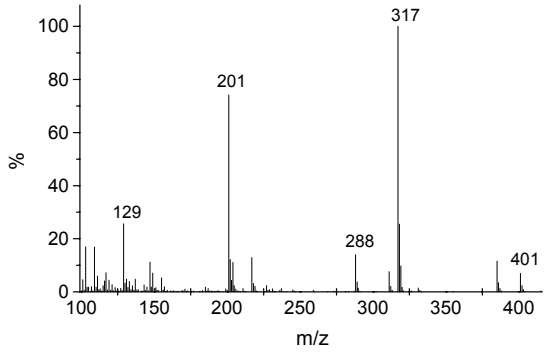

f) Mass spectrum of 9-hydroxy-hexadecanoic acid (ω-7) after derivatisation

Figure 2-12 Mass spectra for hexadecanoic acid and some products

a)

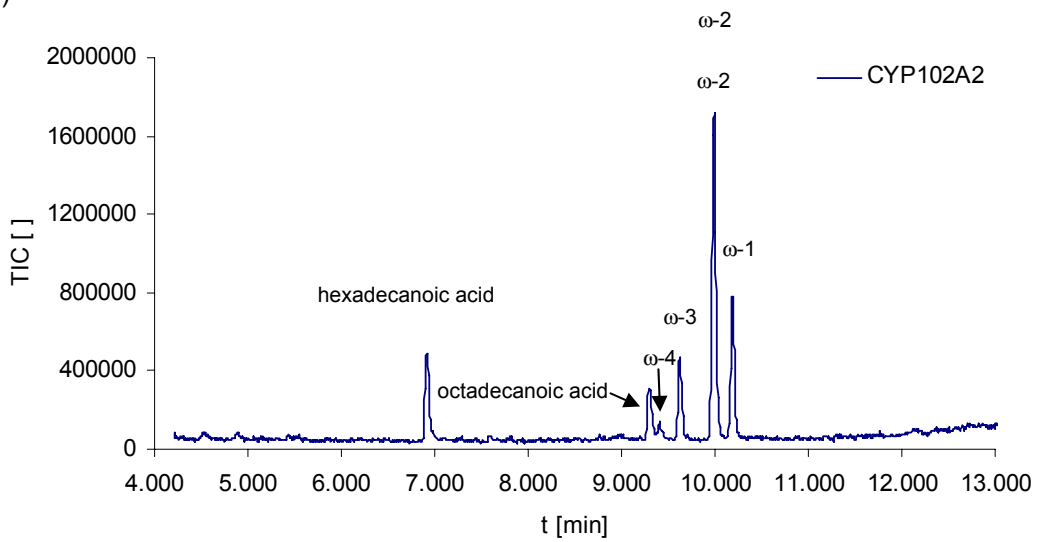

b)

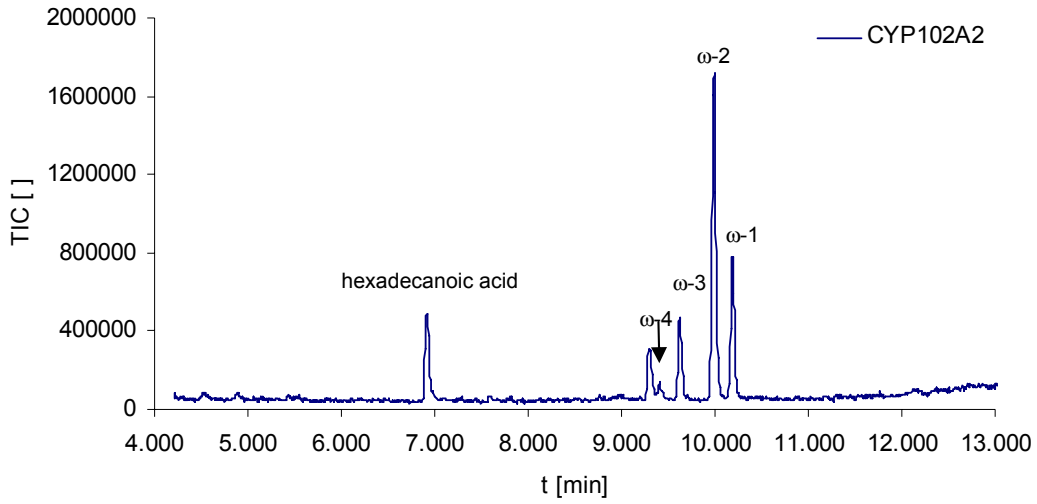
CYP102A2
TIC [ ]
t [min]
hexadecanoic acid
ω-4
ω-3
ω-2
ω-1
2000000
1600000
1200000
800000
400000
0
4.000
5.000
6.000
7.000
8.000
9.000
10.000
11.000
12.000
13.000

c)

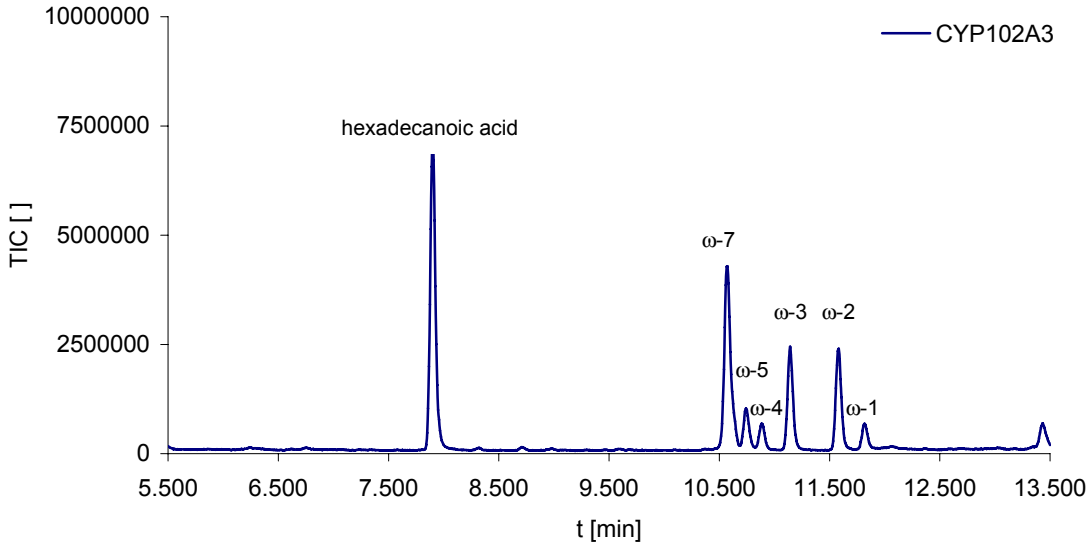
CYP102A3
TIC [ ]
t [min]
hexadecanoic acid
ω-7
ω-3
ω-2
ω-5
ω-4
ω-1
10000000
7500000
5000000
2500000
0
5.500
6.500
7.500
8.500
9.500
10.500
11.500
12.500
13.500

d)

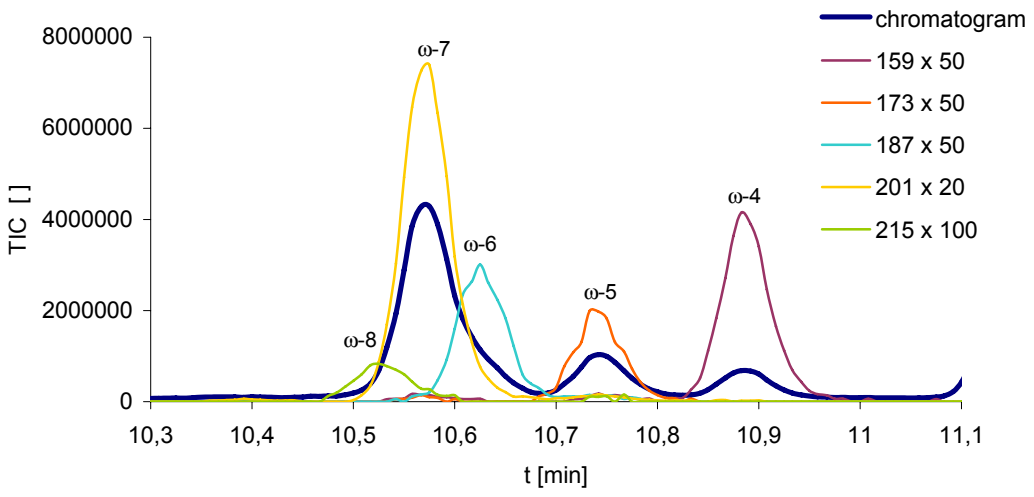
chromatogram
159 x 50
173 x 50
187 x 50
201 x 20
215 x 100
TIC [ ]
t [min]
ω-8
ω-7
ω-6
ω-5
ω-4
8000000
6000000
4000000
2000000
0
10,3
10,4
10,5
10,6
10,7
10,8
10,9
11
11,1

e)

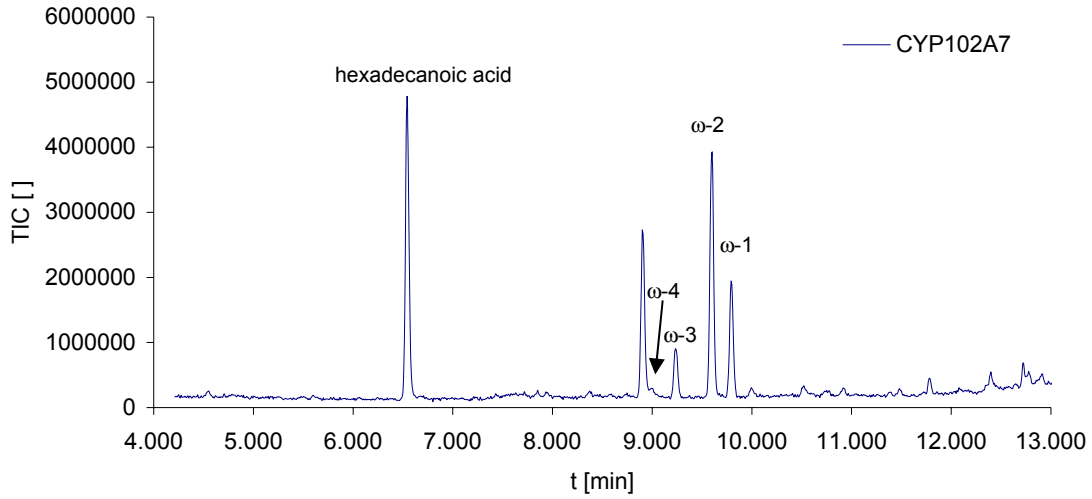

Figure 2-13 GC-chromatograms for the hydroxylation of palmitic acid

a) CYP102A1; b) CYP102A2; c) CYP102A3 complete chromatogram; d) CYP102A3 enlarged section showing the mass peaks specific for the different hydroxylation positions and e) CYP102A7; TIC, Total Ion Count

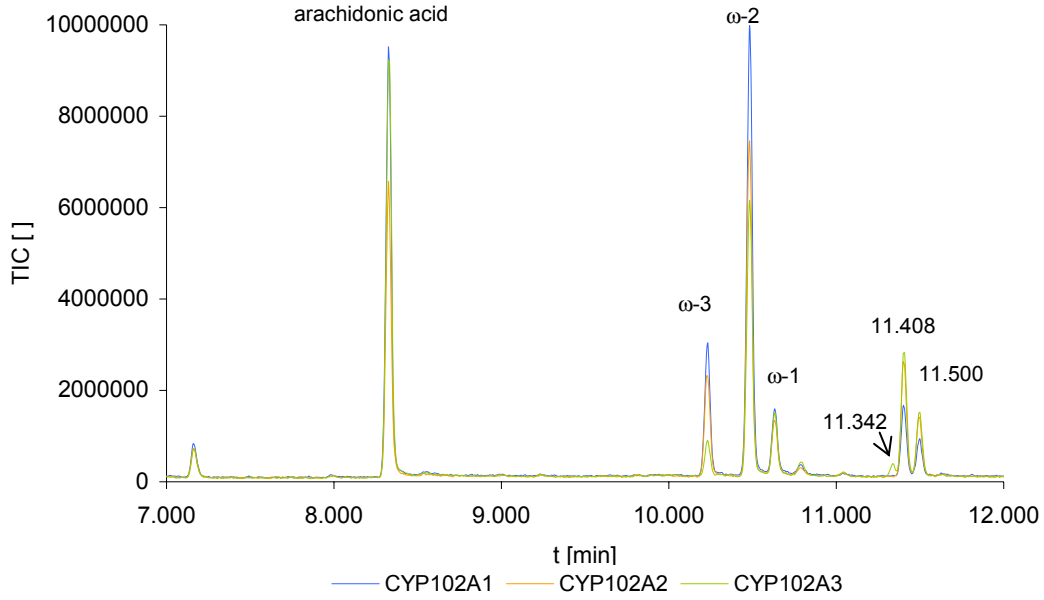

Figure 2-14 GC-chromatograms of the hydroxylation of arachidonic acid by CYP102A1-3

The following table (Table 2-7) shows the ratio of the different products and the activity in nmol product / nmol enzyme / min calculated from NADPH consumption. All measurements were done at least in duplicates with less than 10 % deviation for

activity and less than 5 % deviation for hydroxylation pattern. From the table it can be seen, that not only the activities towards the fatty acids differ but also the hydroxylation pattern. While for CYP102A1, CYP102A2 and CYP102A7 the farthest C-atom for hydroxylation is the ω-4 C-atom, CYP102A3 has the ability to hydroxylate pentadecanoic and hexadecanoic acid even at position ω-8 with ω-7 the main product for hexadecanoic acid. CYP102A3 is also the only enzyme which produces a third unidentified product in the reaction with arachidonic acid.

Table 2-7 Product profile for CYP102A1-A3 and CYP102A7 with different fatty acids

					ω-3	**ω-2**	**ω-1**	**activity**	**C12**
					36	28	36	352	CYP102A1
					20	45	36	200	CYP102A2
					59	35	9	95	CYP102A3
					34	38	28	1322	CYP102A7

				ω-4	**ω-3**	**ω-2**	**ω-1**	**activity**	**C13**
				2	16	65	17	733	CYP102A1
				0	17	51	33	282	CYP102A2
				6	43	36	15	318	CYP102A3
				1	21	54	25	2020	CYP102A7

	ω-7	**ω-6**	**ω-5**	**ω-4**	**ω-3**	**ω-2**	**ω-1**	**activity**	**C14**
	0	0	0	1	26	24	49	1295	CYP102A1
	0	0	0	1	18	53	27	919	CYP102A2
	5	0	5	5	30	45	10	468	CYP102A3
	0	0	0	1	20	50	29	2650	CYP102A7

ω-8	**ω-7**	**ω-6**	**ω-5**	**ω-4**	**ω-3**	**ω-2**	**ω-1**	**activity**	**C15**
	0	0	0	2	19	47	33	1414	CYP102A1
	0	0	0	1	34	33	31	1127	CYP102A2
1	3	5	3	3	52	22	11	420	CYP102A3
0	0	0	0	0	38	27	35	2460	CYP102A7

ω-8	**ω-7**	**ω-6**	**ω-5**	**ω-4**	**ω-3**	**ω-2**	**ω-1**	**activity**	**C16**
	0	0	0	1	19	48	31	736	CYP102A1
	0	0	0	2	14	59	25	705	CYP102A2
1	27	2	6	6	25	26	7	246	CYP102A3
0	0	0	0	0	10	51	38	1330	CYP102A7

	ω-7	ω-6	ω-5	ω-4	ω-3	ω-2	ω-1	activity	C17
	0	0	0	0	19	34	49	576	CYP102A1
	0	0	0	0	19	39	42	281	CYP102A2
	4	1	0	1	7	12	8	75	CYP102A3
	0	0	0	0	19	36	44	1194	CYP102A7

	RT 11,500	RT 11,408	RT 11,342	ω-3	ω-2	ω-1	activity	AA
	5	9	0	18	60	9	2267	CYP102A1
	9	18	0	17	53	7	4588	CYP102A2
	12	22	2	6	49	10	933	CYP102A3
	0	0	0	7	82	11	1598	CYP102A7

Activity is defined as nmol product / nmol enzyme / min; product distribution in % of all products

The summary of the preferred hydroxylation positions (Table 2-8) reveals that the pattern always depends on the chain length of the substrate except for CYP102A2 it exhibits nearly always a preference for position ω-2 over ω-1 and ω-3.

Table 2-8 Summary of the preferred hydroxylation positions

	C12 [a]	C13 [a]	C14 [a]	C15 [a]	C16 [a]
CYP102A1	1=3>2	2>1=3>4	1>3>2>4	2>1>3>4	3>2>1>4
CYP102A2	2>1>3	2>1>3	2>1>3>4	3=2=1>4	2>1>3>4
CYP102A3	3>2>1	3>2>1>4	3>2>1>4=5=7	3>2>1>6>5=4=7>8	7=2=3>1=4=5>6>8
CYP102A7	2>3>1	2>1>3	2>1>3>4	3>1>2	1>2>3>4

[a] chain length of the saturated fatty acid; numbers indicate the position of hydroxylation counted from the ω–position

2.1.6 Other Substrates

2.1.6.1 The Surrogate Substrate 12-pNCA

Para-nitrophenoxy carboxylic acids (*p*NCA) are standard substrates usually used for characterisation of fatty acid hydroxylases like the members of the CYP102A subfamily and their mutants. Hydroxylation of *p*NCA at the ω-C-atom of the carboxylic acid results in formation of an instable semi-acetale which dissociates into the ω-oxo fatty acid and *para*-nitrophenol. At pH>8.1 *para*-nitrophenol exists mainly as *para*-nitrophenolate with an absorption maximum at 410 nm. The prerequisite for comparison of activities using this substrate is hydroxylation at the ω-C-atom. By monitoring the increase of absorbance at 410 nm simultaneously to the decrease of absorbance at 340 nm (NADPH consumption) the coupling efficiency for this reaction could be calculated using the extinction coefficients for *para*-nitrophenolate and NADPH (13200 $M^{-1}cm^{-1}$ and 6220 $M^{-1}cm^{-1}$ respectively) resulting in coupling efficiencies of 5-10 % for all CYP102A members. As the hydroxylation pattern for CYP102A3 differs the most in comparison to CYP102A1 the hydroxylation products for both enzymes with 12-*p*NCA were investigated by GC/MS using the same derivatisation protocol as for fatty acids and the oven program for dodecanoic acid. To get enough products a co-factor recycling system with NADP+ dependant formate dehydrogenase from *Pseudomonas* sp. 101 was used and the reaction was performed over 4 hours. As references ω-hydroxy-dodecanoic acid (substrate reference) and 1,12-dicarboxydodecanoic acid were applied. The resulting products for the hydroxylation of 12-pNCA with CYP102A1 were identified as the expected oxo-dodecanoic acid, although at very low concentration, and as the main product, the further hydroxylated 1,12-dicarboxydodecanoic acid. In contrast CYP102A3 produced no dicarboxylic acid.

2.1.6.2 7-Ethoxycoumarin an Unnatural Substrate

The fluorescent probe 7-ethoxycoumarin is used as a standard to determine the activities of microsomal P450 enzymes. In a whole cell assay system it could be shown that wild type CYP102A1 was not able to convert this substance to 7-hydroxycoumarin. At least one mutation in the substrate binding site is needed

(F87A) to get measurable conversion. In contrast to CYP102A1-A3 CYP102A7 wild type enzyme was able to deethylate 7-ethoxycoumarin with turnover rates of around 2 equivalents per minute. The activity was clearly dependant on the substrate concentration (Figure 2-15) but did not follow a Michaelis-Menten –type kinetic.

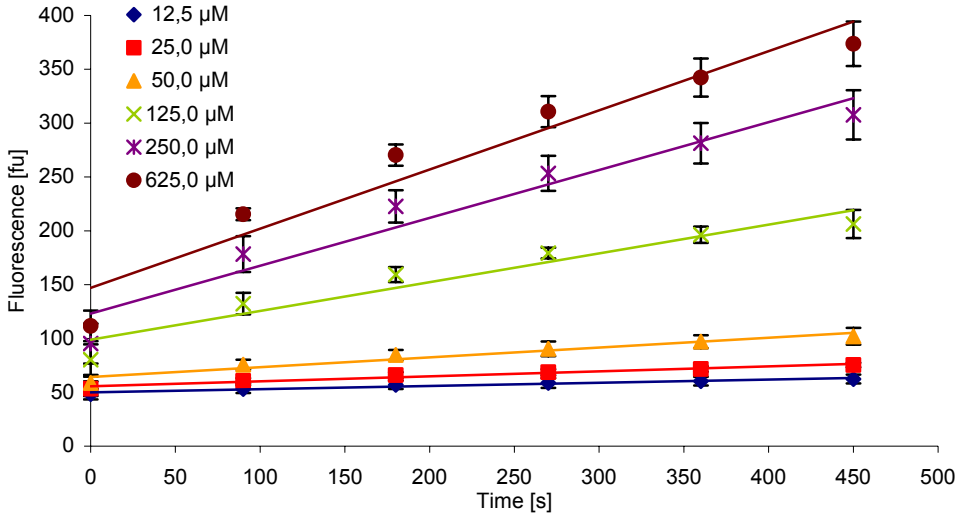

Figure 2-15 Substrate dependant increase in fluorescence for the conversion of 7-ethoxycoumarin with CYP102A7 (substrate concentration in µM)

2.1.7 Substrate Binding

Therefore it was interesting to investigate if the different activities towards saturated and unsaturated fatty acids were due to different binding constants. For the determination of the apparent binding constants pentadecanoic acid and DHA were used. The enzyme concentration was in all cases around 2 µM. The reciprocal absorption difference of 390-422 nm was plotted against the reciprocal substrate concentration. The $-1/K_D$ value was determined from the intersection of the linear smoothing function with the x-axis. All substrate binding spectra exhibited the characteristic change of the absorption maximum from 418 to 390 nm with an isobestic point around 406-409 nm. While it was possible to calculate the K_D values for all enzymes with pentadecanoic acid, the absorption differences of CYP102A2 with DHA did not yield a hyperbolic curve with saturation at higher substrate concentrations and could also not be fitted to the Hill function. The DHA concentration could not be increased to saturating values because of the solubility of

the substrate. The spectral perturbations observed for titration of CYP102A1, A2 and A3 with pentadecanoic acid and DHA are shown in Figure 2-16 Figure 2-18.

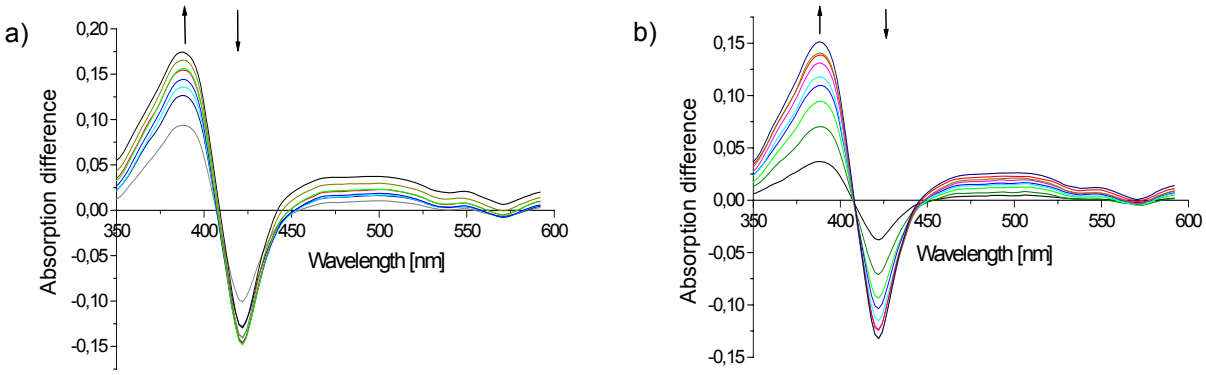

Figure 2-16 Difference substrate binding spectra upon binding of: a) C15; b) DHA to CYP102A1

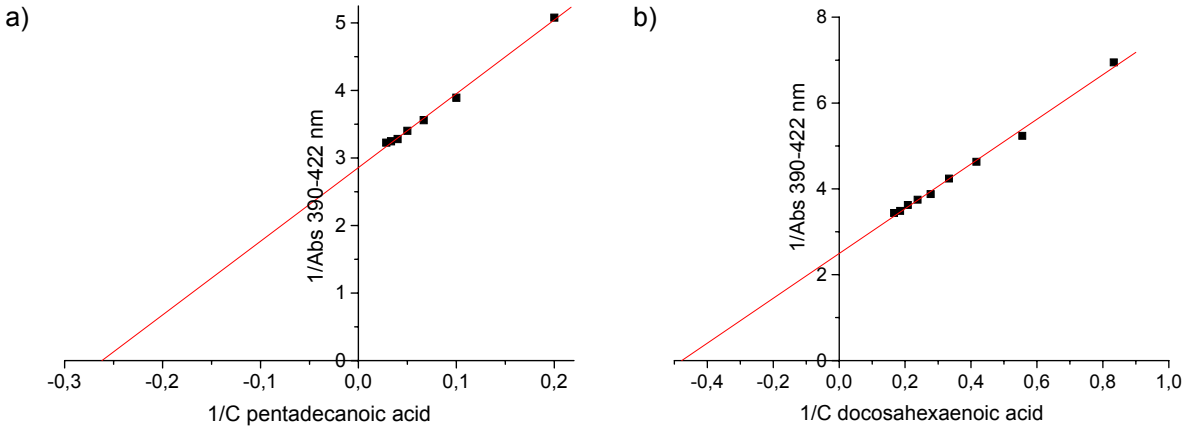

Figure 2-17 Reciprocal plot of the absorbance differences of CYP102A1 over substrate concentration

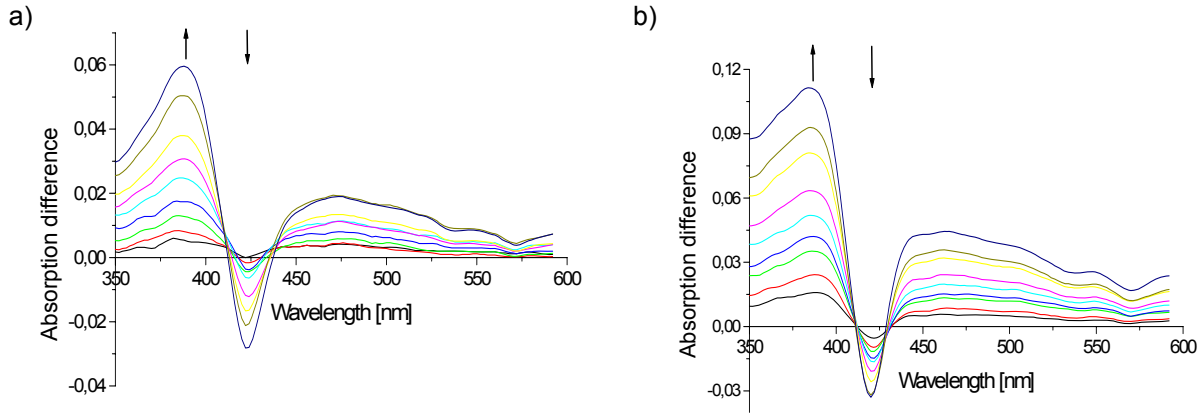

Figure 2-18 Difference substrate binding spectra upon binding of DHA to a) CYP102A2 b) CYP102A3

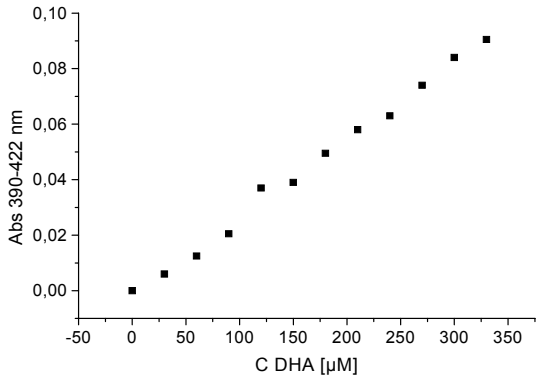

Figure 2-19 Absorption difference for CYP102A2 upon DHA binding

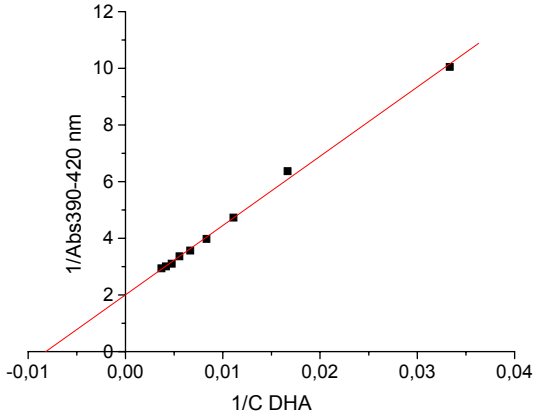

Figure 2-20 Reciprocal plot of the absorbance differences of CYP102A3 over DHA concentration

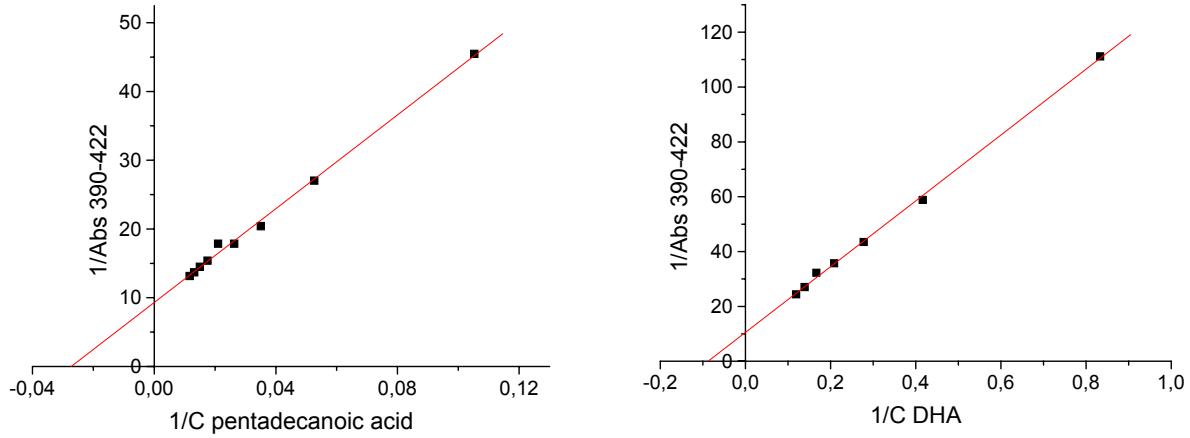

Figure 2-21 Reciprocal plot of the absorbance differences of CYP102A7 over substrate concentration

Apparent binding constants, $K_{D,}$ were calculated by plotting the absorption changes calculated for each difference spectrum against the substrate concentration in reciprocal mode (Figure 2-17, Figure 2-20 and Figure 2-21). For CYP102A1 the binding constants were calculated to be 3.8 µM and 2.1 µM for pentadecanoic acid and DHA respectively. For CYP102A7 they were calculated to be 36.7 and 11.4 µM. CYP102A2 and A3 the exhibited binding constants with pentadecanoic acid of 559 and 540 µM which were more than 100 times higher than for CYP102A1. The binding spectra of CYP102A3 with DHA yielded a binding constant of 122 µM. The differences in absorption upon substrate (DHA) binding of CYP102A2 did not

describe a hyperbolic curve but more closely a sigmoidal curve (Figure 2-19). However due to solubility problems of the substrate the maximum in spin state shift could not be reached and therefore the apparent binding constant could not be calculated. It was expected from literature (Gustafsson, Roitel et al. 2004) that the non hyperbolic curve did not reflect cooperative binding as observed in haemoglobin but binding of more than one DHA molecule in the substrate binding site of the enzyme.

2.1.8 Characterisation of Thermal Stability

An important property of proteins is their thermal stability. Because the P450 monooxygenases of the CYP102A family are comprised of two domains it was necessary to evaluate the stability of the discrete domains. The enzymes were incubated for 30 minutes at elevated temperatures and the loss in functionality was measured at room temperature after cooling of the samples for at least one hour at 4°C. These investigations were done using the whole enzymes and not the isolated domains.

2.1.8.1 Stability of the Heme Domain and Analysis of Co-factor Fluorescence

The stability of the monooxygenase domain is defined by its functional heme system which can be characterised by measuring the CO-difference spectrum.

The function of the reductase domain is to donate reduction equivalents to the monooxygenase domain by means of its co-factors FAD and FMN. Therefore loss in stability can be measured by the increasing fluorescence of the co-factors upon denaturation (Figure 2-22).

It is interesting to see, that CYP102A1 showed an opposite behaviour to either CYP102A2 or CYP102A3. In both enzymes the release of flavins occurred at much higher temperatures, 50 % of flavin release at 58°C and 59°C respectively, than for CYP102A1(49°C) indicating that the reductase domains are more stable. On the

other hand stability of the monooxygenase domain of CYP102A1 exceeded over monooxygenase stability of the other enzymes. Its 50 % inactivation was observed at ~56°C (for CYP102A2 and A3 51°C and 48°C respectively), while 50 % of the flavins have been released already at ~ 49°C

2.1.8.2 Thermal Stability of the Holoenzyme

To investigate if the more unstable domain is also responsible for stability under reaction conditions or if stability of the whole enzyme is a cumulative effect of both domains the surrogate substrate 12-*p*NCA was used. It could be shown for CYP102A1 that 50 % activity towards 12-*p*NCA were reached at ~ 49°C thus indicating the big influence of the more unstable reductase domain. On the other hand activities for CYP102A3 dropped to less than 50 % already after incubation at 46°C which is even a lower temperature than the critical temperature for the reductase domain. For construction of a more stable self-sufficient member of the CYP102A subfamily a chimeric enzyme consisting of the CYP102A1 monooxygenase domain and the CYP102A3 reductase domain was constructed.

a)

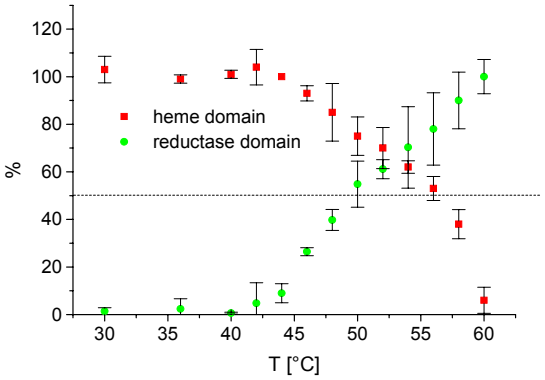

b)

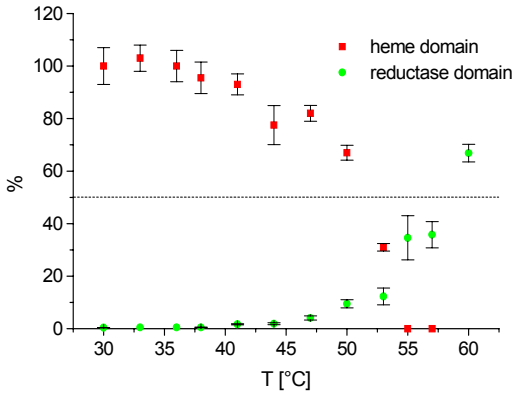

c)

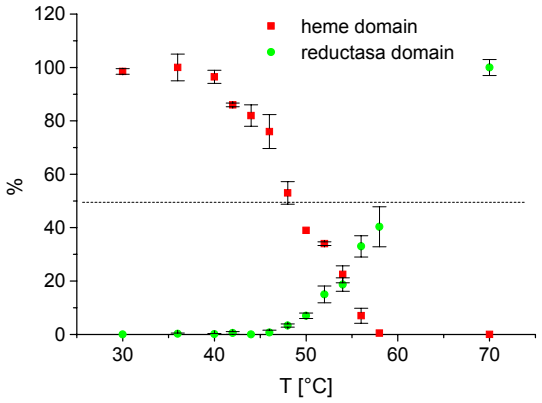

Figure 2-22 Stability of the heme domain and increase in co-factor fluorescence in % of the maximum for: a) CYP02A1; b) CYP102A2 and c) CYP102A3

2.2 Construction of Chimeric Enzymes

2.2.1 Cloning and Expression of a Chimera Consisting of the CYP102A1 Heme Domain and CYP10A3 Reductase Domain (A1A3)

The chimera was cloned in two steps. The monooxygenase domain of CYP102A1 including the natural linker was amplified from pET28aCYP102A1 using the oligonucleotides SEImonoLF and HBACYPA1RBam. The reductase domain of CYP102A3 was amplified using HBACYPA3FBam and HBACYPA3RecoR1. The *Bam*H1 site was introduced by PCR without altering the amino acid sequence. In the first step the monooxygenase domain was ligated into pET22Hb+ after digestion with *Nhe*I and *Bam*HI. The gene insertion was confirmed by control digest and then the reductase domain was ligated into pET22Hmono resulting in pET22HA1A3. The successful creation of the chimeric gene could be proven by digestion with three endonucleases, *Nhe*I, *Bam*HI and *Eco*RI resulting in three bands of ~5 kb (vector), 1.6kb (reductase) and 1.4 kb (monooxygenase) (Figure 2-23). Sequencing confirmed the correct sequence of the gene.

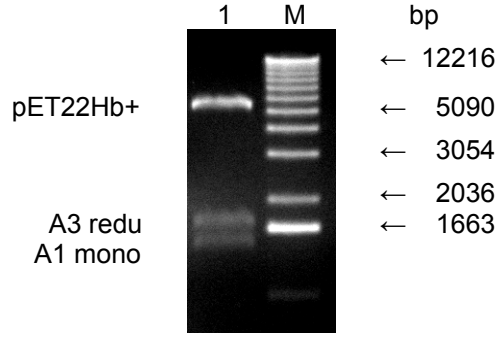

Figure 2-23 Control digestion of pET22HA1A3 with *Eco*RI, *Nhe*I and *Bam*HI

Additionally to the pET22Hb+ construct the chimeric gene was also introduced into pET28a+ (pET28aA1A3).

For expression the new plasmids pET22HA1A3 and pET28A1A3 were transformed into BL21 (DE3) and the fusion construct was expressed according to the improved protocol (4.2.2.3).

The yield of the chimeric P450 was between 500-650 nmol/L (as calculated from the CO-difference spectra) which was in good accordance with the yields of CYP102A3

and CYP102A1. A1A3 expressed from pET22HA1A3 was purified by anion exchange chromatography (IEX) while enzyme expressed from pET28A1A3 and carrying a His_6-tag was purified by Ni-sepharose. Figure 2-24 shows an example for a purification of CYP102A1, A3 and A1A3 by IEX chromatography. In all three cases the purification was successful resulting in almost pure P450 monooxygenases.

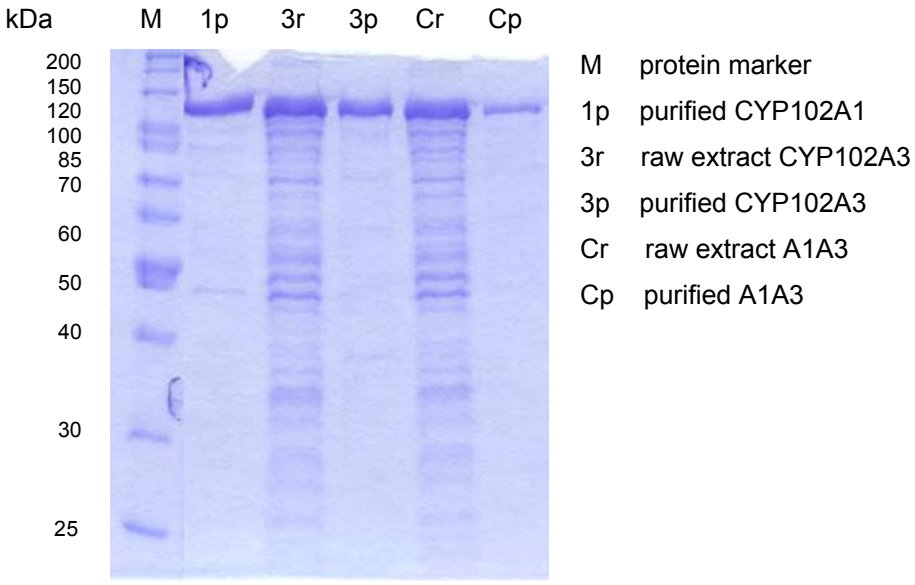

Figure 2-24 SDS gel of raw extract and the corresponding enzymes purified by IEX chromatography

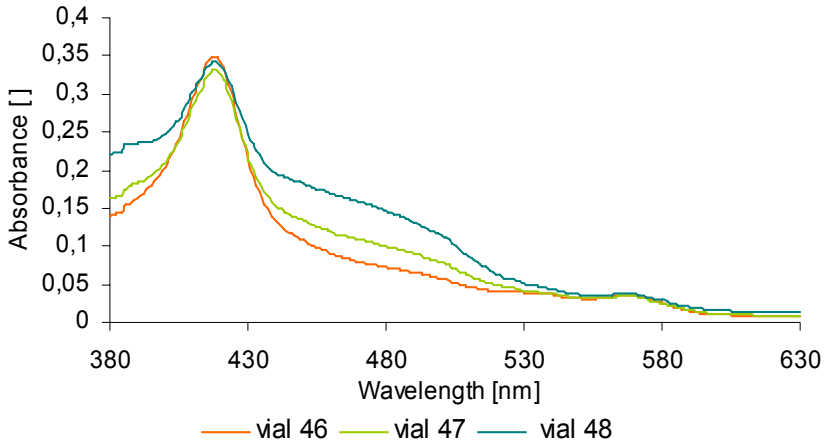

Figure 2-25 Spectra of A1A3 after purification by ion exchange chromatography

Interestingly the reduced and oxidised forms of the flavins were separated by IEX chromatography. The reduced (vial 46), partially reduced (vial 47) and oxidised (vial 48) forms of the enzyme were eluted consecutively (Figure 2-25). By measuring activity towards 12-*p*NCA it could be shown that all three states possessed the same specific activity.

2.2.2 Spectral Investigation

For spectral characterisation the enzyme purified by metal affinity chromatography was used. The chimeric enzyme A1A3 displayed absorption spectra analogous to those of the other P450 enzymes. The ferric form of A1A3 showed a Soret maximum at 418 nm and two visible bands between 500 and 600 nm. The reduced CO-bound form revealed the characteristic CYP102A1 maximum at 448 nm. The absence of a peak at 420 nm which is typical for disrupted P450 enzymes confirmed that the folding of the protein was not affected by the chimerisation and during purification. Interestingly CO binding seemed to be a relatively slow progress (Figure 2-26). It took nearly 30 minutes to get a fully formed CO-difference spectrum.

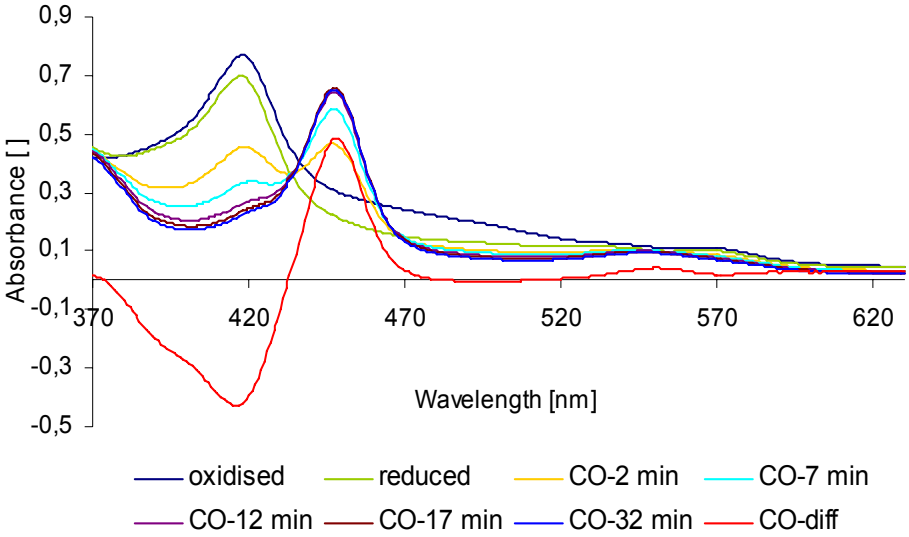

Figure 2-26 Absorption spectra of A1A3 before and after saturation with carbon monoxide

We could also show that after addition of 30 µM arachidonic acid the maximum absorption of the chimera was shifted from 420 nm to lower wavelength (390 nm) which is characteristic for the substrate bound form of the enzyme (Figure 2-27a).

By subtracting the initial spectrum without substrate from all of the following spectra we got the characteristic type I binding spectra with a maximum at 388 nm the minimum at 422 nm and an isobestic point at 407 nm (Figure 2-27b).

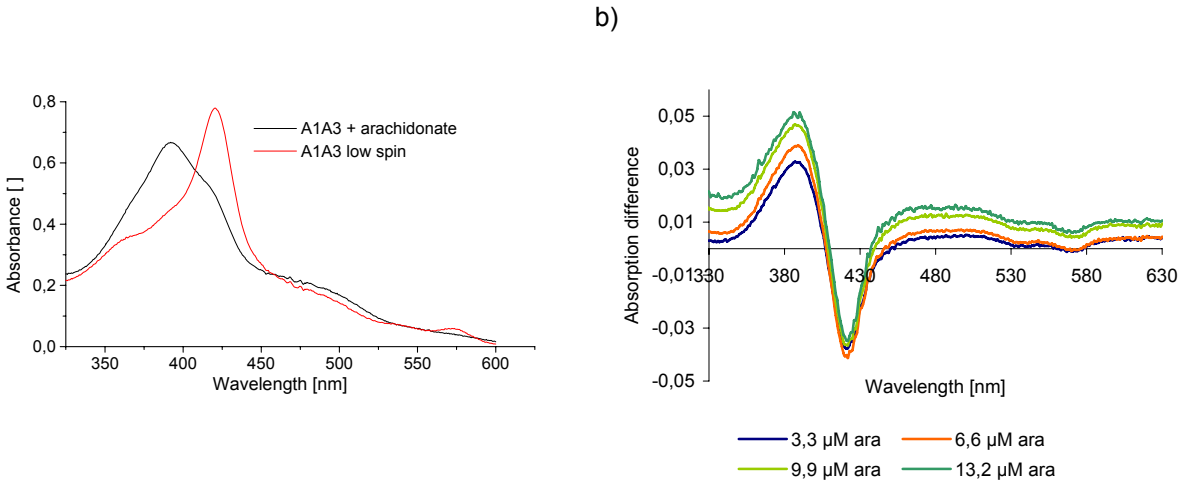

Figure 2-27 Spectral change upon substrate binding: a) Shift of the maximum to 390 nm; b) Binding spectra for different concentrations of arachidonic acid

The binding constants for pentadecanoic acid, docosahexaenoic acid and arachidonic acid to A1A3 were determined to be 3.9 µM, 2.9 µM and 1.0 µM respectively.

2.2.3 Activity Determination

The most important issue for the investigation of the chimera was to ensure that both foreign domains were expressed actively and that the reductase domain of CYP102A3 was able to transfer electrons to the heme iron of the CYP102A1 monooxygenase domain. The active conformation of the heme domain was proven by its ability to bind carbon monoxide as well as arachidonic acid. The functionality of the reductase domain was determined by cytochrome c reduction in an assay using 100 µM cytochrome c and 50 µM NADPH. CYP102A3 and the chimera exhibited turnover frequencies >1200 min^{-1}. As a last step the ability of the CYP102A3 reductase domain to transfer electrons to the heme iron of CYP102A1 within the chimera had to be confirmed. This was done by measuring activity towards 12-*p*NCA. In comparison to the activity of CYP102A1 towards 12-*p*NCA (~70 min^{-1}), CYP102A3 showed an activity of 55 min^{-1} and A1A3 exhibited an activity of 23 min^{-1}.

2.2.4 Thermal Stability

The thermal stability of A1A3 was determined by applying the same methods as for CYP102A1 and CYP102A3 (see chapter 2.1.8). The temperatures at which 50 % inactivation of the discrete domains of CYP102A1 and A3 was reached can be seen in Table 2-9. In comparison the stability profile of the chimera A1A3 is shown in Figure 2-28. The stability of the monooxygenase domain of A1A3 is identical to that of CYP102A1 (56°C) accompanied by a very stable reductase domain (58°C) as observed for CYP102A3.

Table 2-9 Stability of the discrete domains of CYP102A1 and A3 after incubation at elevated temperatures.

Enzyme domain [a]	T_{50} for 30 min incubation [°C] [b]
A1 holo	49
A1 mono	56
A1 redu	49
A3 holo	46
A3 mono	49
A3 redu	59

[a]: holo, stability of the whole enzyme measured by 12-pNCA activity; mono, stability of the monooxygenase domain measured by CO-difference spectra; redu stability of the reductase domain calculated for residual flavins in the protein; [b]: temperature resulting in 50 % inactivation.

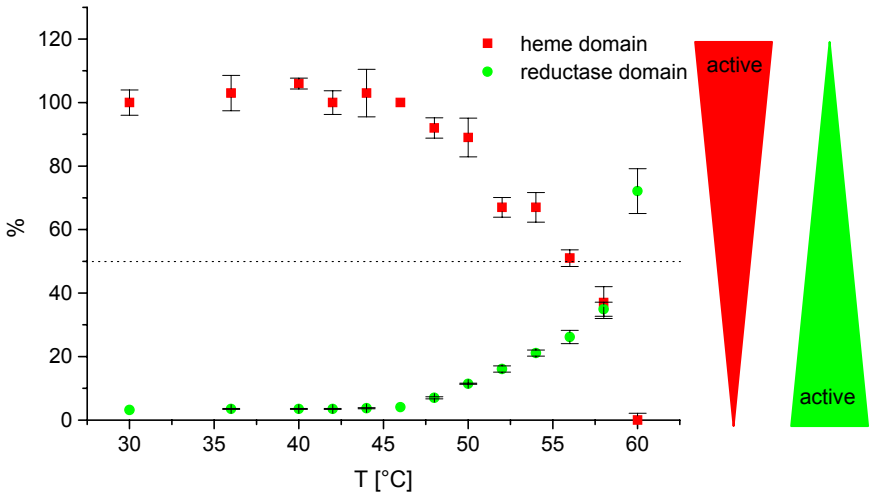

Figure 2-28 Stability of A1A3; functional heme and increase in co-factor fluorescence in % of the maximum

In the next step the distribution of the foreign domains to the thermal stability of the complete chimera was investigated.

2.2.4.1 Thermal Stability of Holoenzymes

Activity towards 12-*p*NCA was measured after incubation at elevated temperatures and cooling at room temperature. The *para*-nitrophenolate formation rate of the enzyme incubated at room temperature (23°C) was taken as 100 % activity (Figure 2-29). The activity of CYP102A3 decreased over the whole temperature range with about 50 % inactivation after incubation at 46°C. CYP102A1 activity increased after 30°C incubation followed by a slight decrease at 40°C, a second maximum is observable at 42°C dwindling at higher incubation temperatures to less than 50 % activity after incubation at 50°C. A1A3 exhibited behaviour similar to that of CYP102A1 but shifted to higher temperatures and with higher amplitude. The first minimum was reached at 42°C with a subsequent maximum at 50°C reaching more than 150 % activity, followed by a slow decrease to less than 50 % between 54 and 56°C. All enzymes exhibited no activity after incubation at 60°C.

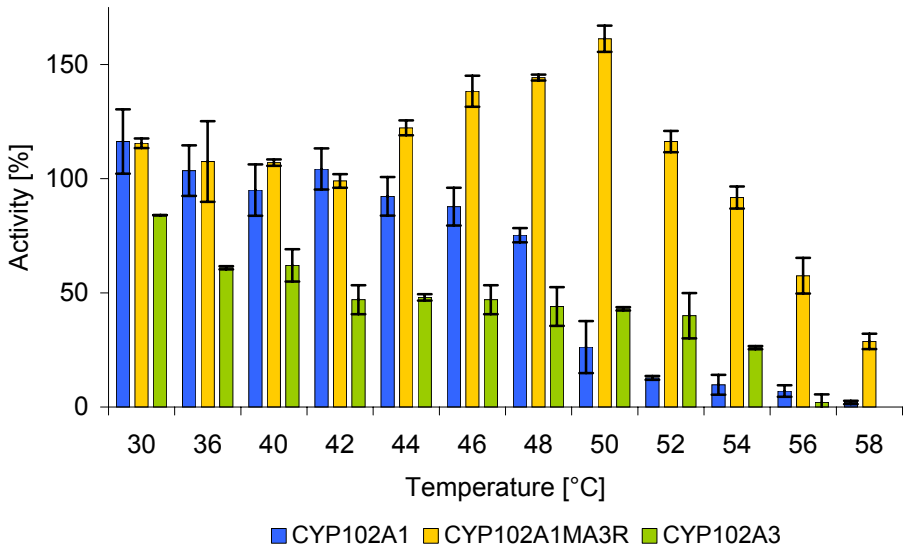

Figure 2-29 Activity of CYP102A1 and A3 and the chimera A1A3 towards 12-*p*NCA after incubation at elevated temperatures

2.2.4.2 Temperature Optimum

While the previous examination was performed at room temperature the next figure (Figure 2-30) displays the activity at a certain temperature after 15 minutes incubation time. Here the decrease in activity at increasing temperatures for CYP102A1 and especially CYP102A3 is more severe. The activity of A1A3 dropped again at around 41°C, but increased again and showed a maximum at 51°C. The activation effect was this time not as high as before, nevertheless reached 106 % of initial activity. As a result it could be proven that the chimera exhibited a higher temperature optimum at 51°C and therefore higher stability than the parental enzymes with an optimum at 23°C.

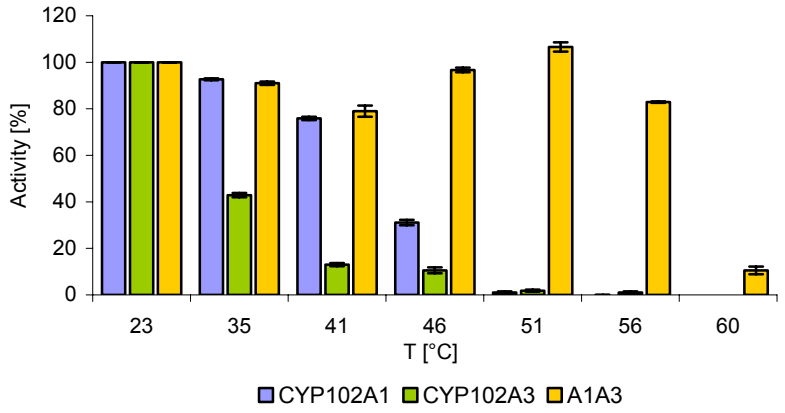

Figure 2-30 Temperature optimum for the hydroxylation of 12-pNCA with CYP102A1, A3 and A1A3

2.2.4.3 Inactivation Rate of CYP102A1 and A1MA3R

Because of the high temperature optimum of the chimera the inactivation rates for CYP102A1 and A1A3 were determined at 50°C (Figure 2-31). CYP102A3 was not used because of its low activity and stability at this temperature. With an inactivation rate of around 100 minutes the chimera was around 12 times more stable than CYP102A1 (~8 minutes).

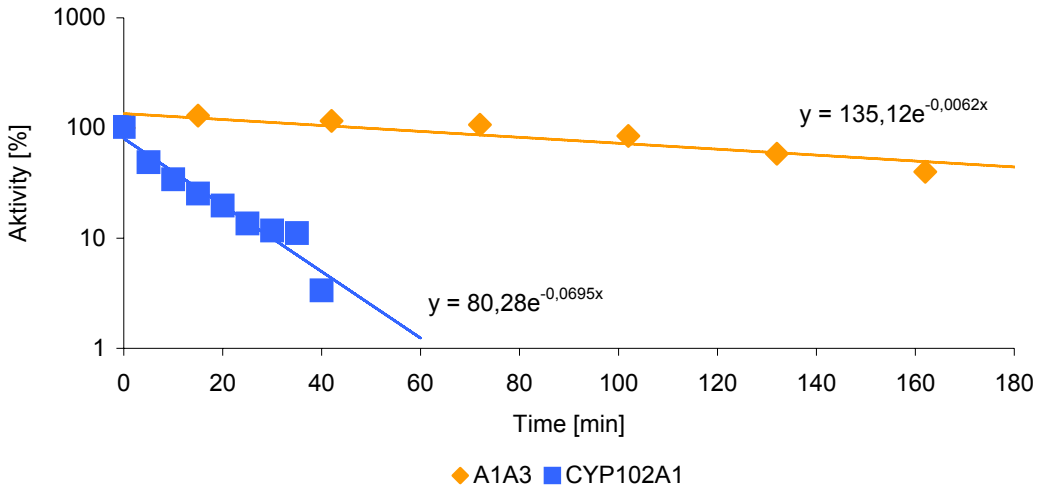

Figure 2-31 Inactivation rate for CYP102A1 and A1A3 at 50°C

2.2.4.4 Thermal Stability in the Presence of Substrate

Presence of substrate bound in the active site of an enzyme can influence its properties. Therefore we investigated the influence of the substrate 12-*p*NCA on thermal stability.

CYP102A1 and A1A3 were incubated for 30 minutes at elevated temperatures in the presence or absence of 2 % 10 mM 12-*p*NCA in DMSO. The residual activities were measured after cooling of the samples at room temperature according to the previously described protocol (2.2.4.1). Although the decrease in activity of A1MA3R after incubation at 30 to 40°C was no longer visible, the enzyme exhibited also in the presence of the substrate a continuous increase in hydroxylation activity up to 112 % at 45°C and still demonstrated 50 % activity after incubation at 56°C. The activation effect after incubation at elevated temperatures in this case was much lower than without substrate. While the chimera retained its stability in the presence of the substrate, the activity of CYP102A1 was much more severely affected resulting in a decrease of T_{50} from 50°C to 45°C.

2.2.5 Storage Stability

For determination of the storage stability the enzymes were incubated at 30°C and samples were taken at different time points. The foremost interest was in the activity of the P450 monooxygenases but stability of the discrete domains was also measured. In contrast to previous results of the measurements after incubation at elevated temperatures, the loss in activity over time was not reflected in the loss in stability of the domains. For example, after 47 hours incubation CYP102A3 completely lost its activity towards 12-*p*NCA (Figure 2-32), but retained 50 % of putative functional heme and showing nearly no loss of flavins. Although CYP102A1 was also completely inactivated in the same range as CYP102A3, after 49 hours, the course of deactivation was different. Activity of CYP102A3 decreased to less than 60 % after 6 hours followed by 18 hours showing nearly no loss and a second phase of rapid deactivation after 30 hours. In contrast, CYP102A1 exhibited a roughly hyperbolic course of deactivation. In this case the amount of potentially active heme was 87 % of the initial value, while 38 % of the flavins were still bound.

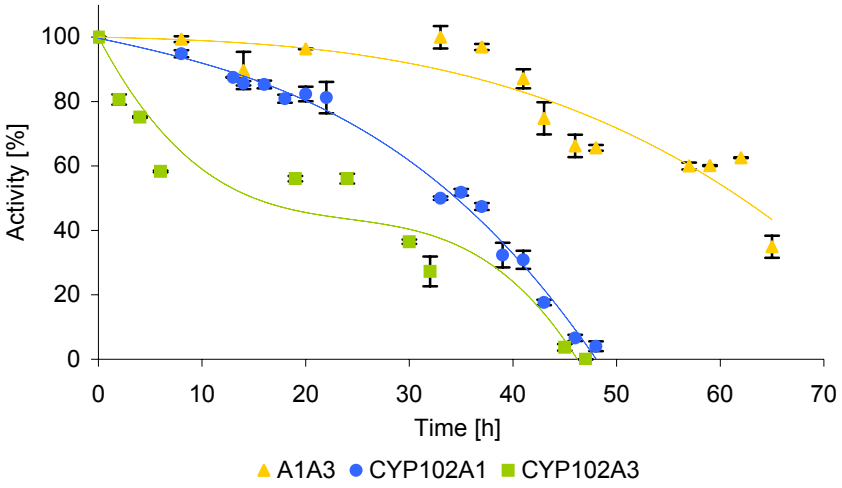

Figure 2-32 Storage stability of CYP102A1, A3 and A1A3 at 30°C measured with 12-pNCA

The chimeric A1A3 followed a similar course as CYP102A1 but showing extended stability with 35 % residual activity at the end of the experiment after 65 hours.

2.2.6 Process Stability

After exhibiting increased thermal stability in all prior investigations it was now necessary to examine if this stabilisation resulted also in higher process stability.

The process stability of CYP102A1 and A1A3 was determined over 12 hours by measuring the increase of absorbance due to *para*-nitrophenolate formation from 12-*p*NCA (Figure 2-33).

For co-factor regeneration an engineered $NADP^+$ dependant formate dehydrogenase from *Pseudomonas sp.* was used. The amount of product produced in the first 5 minutes after starting the reaction was taken as 1. The activity of both enzymes decreased dramatically after this initial high velocity, the amount of product was doubled (2) in the following 40 minutes and doubled (4) again after additional 105 min for CYP102A1and 165 min for A1A3. After six hours CYP102A1 had reached its maximum at the value of 4.8, while the chimera showed a constant increase of products for nearly 10 hours reaching a value of 7.5 after 11 hours and 45 min. Although the chimeric enzyme seems to be more stable than CYP102A1, the total turnover numbers reached only 30 % of the values calculated for CYP102A1 (720 and 2300 respectively).

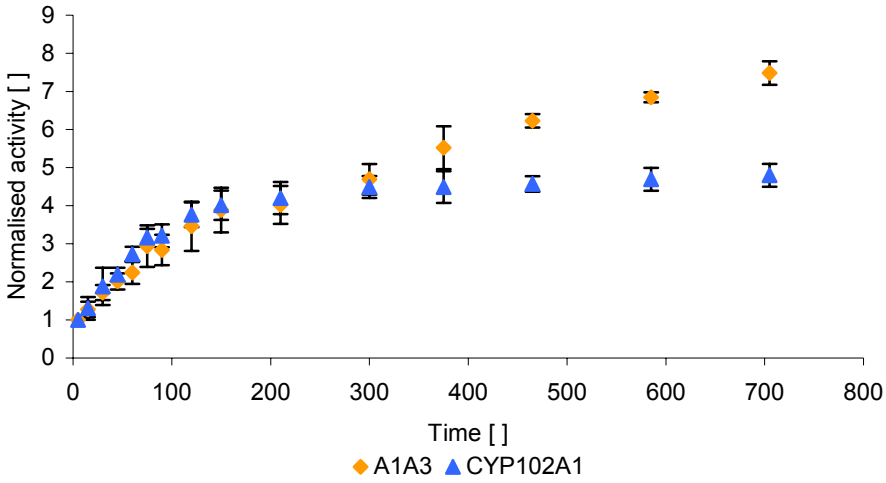

Figure 2-33 Process stability of CYP102A1 and A1A3

2.2.7 Circular Dichroism

The CD spectra measured in the far UV can be used to observe the structural composition and also the integrity of a protein. For CYP102A1 several crystal structures are solved and because of the similarity of the investigated P450 enzymes it can be expected that they share the same structural composition. Here the far UV was used to observe the structural changes upon heating of the enzyme. The following graph shows, that there are two effects, the maximum at ~ 180 nm decreases after 5 minutes incubation at 50°C and the trough between 210-220 nm increases over the measured time range indicating a loss in helical structures (Figure 2-34).

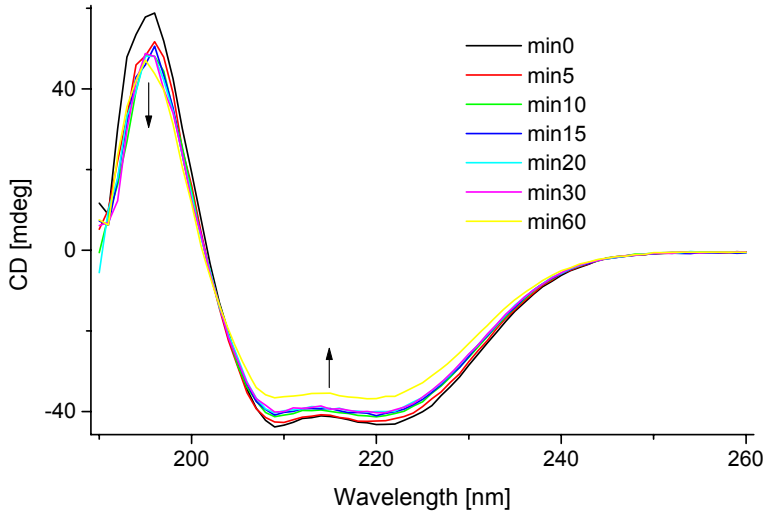

Figure 2-34 Changes in the far UV CD spectrum upon heating at 50°C of A1A3

The circular dichroism spectrum in the near UV/vis (300-600 nm) gives some information about the state of the heme and the heme surrounding. The following diagram shows a comparison between the near UV/vis CD spectra of CYP102A1, CYP102A3 and A1A3 (Figure 2-35). While CYP102A1 and the chimera exhibit nearly the same spectrum the spectrum of CYP102A3 looks a bit different. The shift of the maximal negative deviation to a lower wavelength, 402 nm instead of 410 and 410.5 nm for CYP102A1 and A1A3 respectively may be due to the fact that CYP102A3 is always expressed with partially inactive heme shown by its shoulder at 420 nm in the CO-difference spectrum.

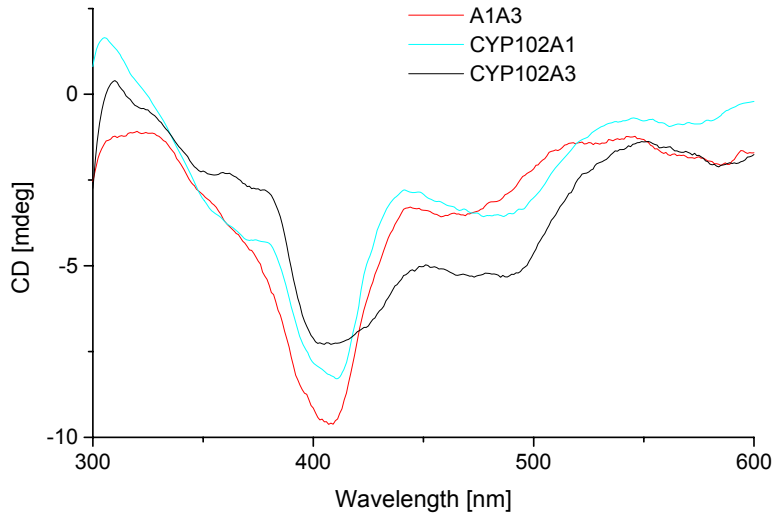

Figure 2-35 Circular dichroism spectra of CYP102A1, CYP102A3 and A1A3 in the near UV/vis

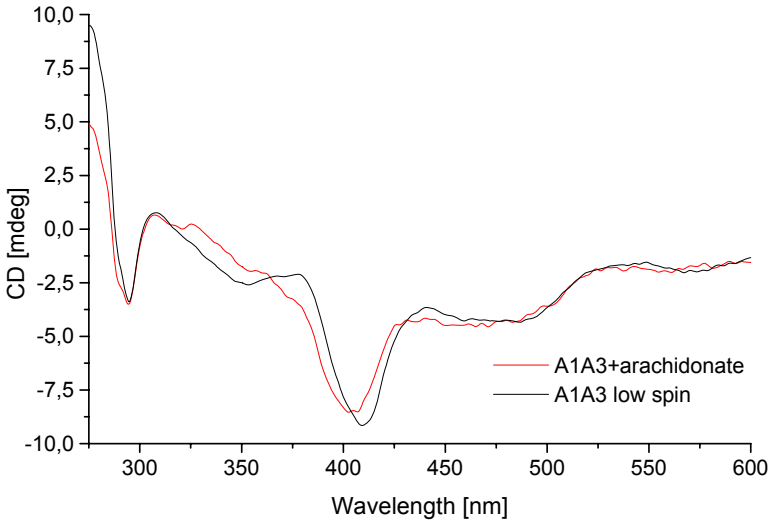

Figure 2-36 Near UV/Vis spectrum of substrate bound and substrate free A1A3

The CD spectrum of A1A3 was also recorded after addition of substrate (arachidonic acid) and exhibited a shift of the trough from 410.5 to 405 nm (Figure 2-36) which is in accordance to the substrate bound CD spectrum of CYP102A1 seen by Macdonald et al. (Macdonald et al. 1996).

2.3 A Thermostable Sulfite Reductase as Electron Transfer Protein for CYP102A1

The amino acid sequence of the CYP102A1 reductase domain (residues 485-1049) was used as template for a homology search within bacterial genome databases with a special focus on thermophilic microorganisms to find thermostable reductases. The homology search resulted in a homologous region within the genome of *Geobacillus stearothermophilus* DSMZ strain 13240 which was sequenced and published at the Advanced Centre of Genome Technology at the University of Oklahoma. However the identified open reading frame (ORF) with a length of 1170 base pairs (Figure 2-37) was not yet annotated.

```
>bstearo.Contig278
          Length = 32815
 Score =  204 bits (519), Expect = 2e-53
 Identities = 164/573 (28%), Positives = 267/573 (45%), Gaps = 10/573 (1%)
 Frame = +3
Query: 14    VLYGSNMGTAEGTARDLADIAMSKGFAPQVAT-LDSHAGNLPREGAVLIVTASYN-GHPP
71
             VLYGS  G A+  A         +GF  +V + LD     L +   +LIV +++  G PP
Sbjct: 11985 VLYGSQTGNAQKLAEKAGKALKERGFEAKVLSMLDFKPNELKKVETLLIVVSTHGEGDPP
12164
Query: 72    DNAKQFVDWLDQASADEVKGVRYSVFGCGDKNWATTYQKVPAFIDETLAAKGAENIADRG
131
             DNA  F ++L    A ++  +R+SV   GD ++    Q    F D+ L   G      R
Sbjct: 12165 DNAVSFYEFLHSKRAPKLNHLRFSVLALGDTSYEHFCQTGKDF-DKRLEELGGTRFYPRV
12341
Query: 132   EADASDDFEGTYEEWREHMWSDVAAYFNLDIENSEDNKSTLSLQFVDSAADMPLAKMHGA
191
             + D   D+E    +W + +  +++   N  +       +T  L    +A  M  A ++
Sbjct: 12342 DCDV--DYEEAAAKWLDGVLGELSKEANAHVG------ATPLLSAAATAPKMEPAVVYSR
12497
Query: 192   ---FSTNVVASKELQQPGSARSTRHLEIELPKEA-SYQEGDHLGVIPRNYEGIVNRVTAR
247
                F   V+ +  L   GS + TRHLE+ L      Y+ GD LG+ P+N   +V R+
Sbjct: 12498 KNPFPAEVLENINLNGRGSNKETRHLELSLEGSGLKYEPGDALGIFPKNDPELVERIIQE
12677
Query: 248   FGLDASQQIRLEAEEEKLAHLPLAKTVSVEELLQYVELQDPVTRTQLRAMAAKTVCPPHK
307
                +  + + ++ + E            V  L + +     +T    +A+  K
Sbjct: 12678 MKWNPEETVTIDKDGE------------VRSLREALTSHFEIT-VLTKALLQKLATLSKN
12818
Query: 308   VELEALLEK-QAYKEQVLAKRLTMLELLEKYPACEMKFSEFIALLXXXXXXXXXXXXXXX
366
              EL+AL+      K +  AK   +L+ L  +   +    + I++L
Sbjct: 12819 SELQALVAPGNEAKLKEYAKGRDLLDALRDFGPWDATLQQLISILRKMPPRLYSIASSLA
12998
Query: 367   VDEKQASITVSVVSGEAWSGYGEY-KGIASNYLAE-LQEGDTITCFISTPQSEFTLPKDP
424
                +  +T+  V  E+   +G   KG+ S + AE +Q GDT+  F+  P   F LPKDP
```

```
Sbjct: 12999 AYPDEVHLTIGAVRYES---HGRLRKGVCSTFCAERVQIGDTLPVFVQ-PNPNFKLPKDP
13166
Query: 425   ETPLIMVGPGTGVAPFRGFVQARKQLKEQGQSLGEAHLYFGCRSPHEDYLYQEELENAQS
484
              +TP+IM+GPGTGVAPFR F+Q R+ +  +G+S     L+FG +    D+LYQ E
Sbjct: 13167 DTPIIMIGPGTGVAPFRAFMQEREAIGAKGKSW----LFFGDQHFMTDFLYQTEWLAWLK
13334
Query: 485   EGIIT-LHTAFSRMPNQPKTYVQHVMEQDGKKLIELLDQGAHFYICGDGSQMAPAVEATL
543
               G++T +  AFSR   + K YVQH M +  K+L   L++GA  Y+CGD   MA  V  TL
Sbjct: 13335 SGVLTKMDVAFSR-DTEKKVYVQHRMLERSKELFGWLEEGAVVYVCGDKQHMARDVHQTL
13511
Query: 544   MKSYADVHQVSEADARLWLQQLEEKGRYAKDVW 576
              ++       +S   A  ++ +++++ RY +DV+
Sbjct: 13512 IEIIEKEGGMSREQAEAYVTEMQKQKRYQRDVY 13610
```

Figure 2-37 Alignment between the reductase domain of CYP102A1 and a putative reductase from *Geobacillus stearothermophilus*

The gene shows highest homology (83 %) to the α-subunit of a sulfite reductase of *Bacillus subtilis strain 168 (yvgR)*. The homology with the reductase domain of CYP102A1 is 45 %.

2.3.1 Cloning and Expression of the α-Subunit of the *Geobacillus stearothermophilus* Sulfite Reductase Domain (Gstredu)

2.3.1.1 Isolation of Genomic DNA and Cloning of the *Gstredu* Gene

Geobacillus stearothermophilus was cultivated at 60°C overnight and the genomic DNA was isolated according to the protocol (4.2.1.1). For amplification of the *gstredu* gene the two oligonucleotides SEIGstReF and SEIGstReNot1 were used in a hot-start PCR. The genomic DNA (0.85 µg/µl) was used in 5-, 10- or 50-fold dilution (Figure 2-38).

The PCR product of the expected size of ~1600 bp was isolated and digested with *Eco*RI and *Not*I and ligated into pET22b+ digested with the same restriction endonucleases.

After transformation and isolation of the plasmid DNA, positive clones were identified by analytical restriction analysis using *Eco*RI and *Not*I. After sequencing of positive clones one clone was selected for further experiments and named pET22bGstredu.

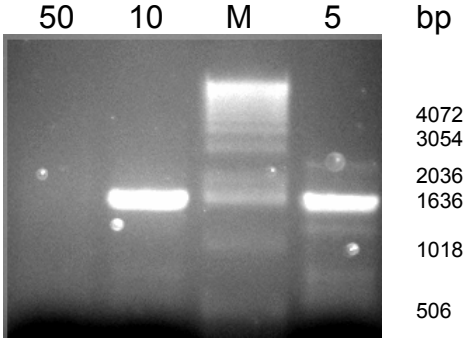

Figure 2-38 PCR products of *gstredu* obtained from different amounts of genomic DNA (5-, 10-, 50-fold dilution)

2.3.2 Partial Purification and Preliminary Characterisation of the Gstredu

The plasmid obtained from cloning was transformed into *E. coli* BL21 (DE3) for expression. The same improved protocol as for expression of the P450 monooxygenases was applied. Because this enzyme originated from a thermophilic species heat precipitation was tried as a first purification step. The cell lysate was incubated at 60°C for increasing time intervals and cytochrome c reduction was measured as control. It could be shown that the Gstredu is strictly NADPH dependant as was expected from the amino acid sequence exhibiting higher homology with NADPH dependant enzymes than with NADH dependant reductases. *E. coli* cell lysate transformed only with the empty vector was used as control for cytochrome c reduction resulting in less than 1 % activity compared to the Gstredu containing lysate. This host dependant activity completely disappeared upon incubation at 60°C due to inactivation of intrinsic *E.coli* reductase activity. In contrast the activity of the Gstredu increased after incubation at 60°C to 150 % after 20-30 minutes (Figure 2-39).

Figure 2-40 shows the protein composition of *E. coli* cells before and after induction of expression of Gstredu. In comparison to the lane before induction in the lane after overnight expression a band occurs at the expected size of around 65 kDa. After 30 minutes incubation at 60°C many host proteins have disappeared.

The temperature optimum of the Gstredu was determined using the cytochrome c reduction assay. The optimum was determined to be around 60°C. Remarkably high was the activity also between 70 to 80°C (Figure 2-41).

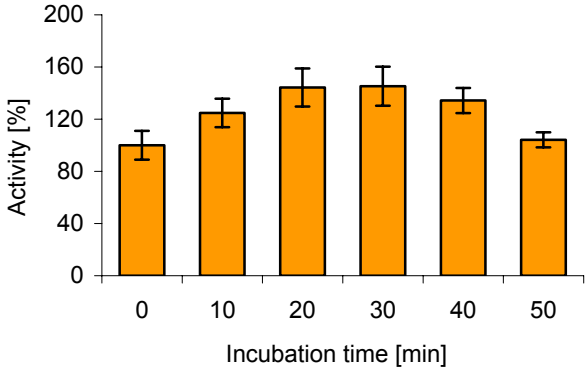

Figure 2-39 Influence of incubation at 60°C on cytochrome c reduction by Gstredu

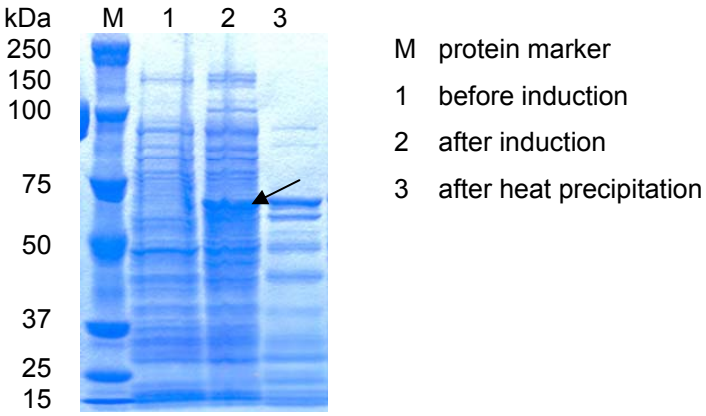

Figure 2-40 SDS gel of Gstredu expression

The spectra of the reductase were recorded for the oxidised, partially reduced (by NADPH) and complete reduced form (by sodium dithionite) (Figure 2-42).

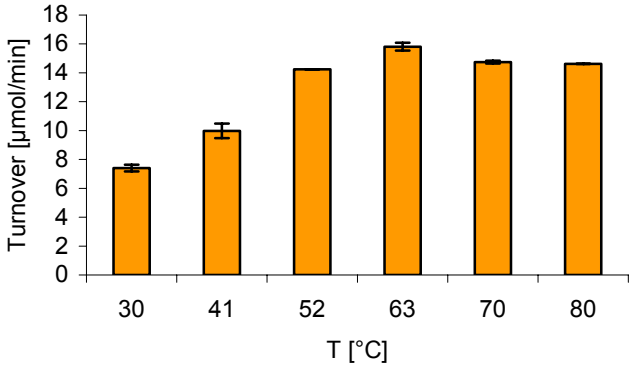

Figure 2-41 Temperature optimum of Gstredu determined by measuring cytochrome c reduction

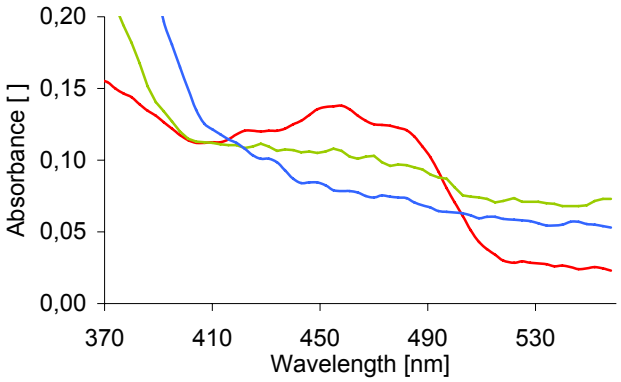

Figure 2-42 Spectral analysis of the α-subunit of sulfite reductase from *Geobacillus stearothermophilus*

Red line oxidised reductase, green line partial reduction after addition of NADPH and blue line after complete reduction with sodium dithionite.

The Gstredu demonstrated a characteristic spectrum for a sulfite diflavin reductase with a maximum at 454 nm and two shoulders at 422 and 476 nm. After reduction with NADPH these peaks decrease and after reduction with sodium dithionite both flavins exist in their hydroquinone form showing no absorption between 420 and 500 nm.

2.3.3 Construction of Chimeric Proteins between the Monooxygenase Domain of CYP102A1 and the Gstredu

The chimeric enzyme was constructed by amplification of the CYP102A1 monooxygenase gene using the oligonucleotides SEIMonoLNhe1 and SEIMonoLR. The resulting gene product was then cloned together with the gene for Gstredu into pET28a+. Figure 2-43a shows the digested gene products, lane1 the CYP102A1 monooxygenase domain (*Nhe*I and *Eco*RI), lane 2 the *gstredu* gene (*Eco*RI and *Not*I) and lane 3 the digested pET20a+ vector (*Nhe*I and *Not*I). After ligation and transformation the positive clones were identified by triple digestion of the resulting plasmids (Figure 2-43b). The correct cloning was confirmed by sequencing and one clone was then named pET28A1GR and used for further investigations.

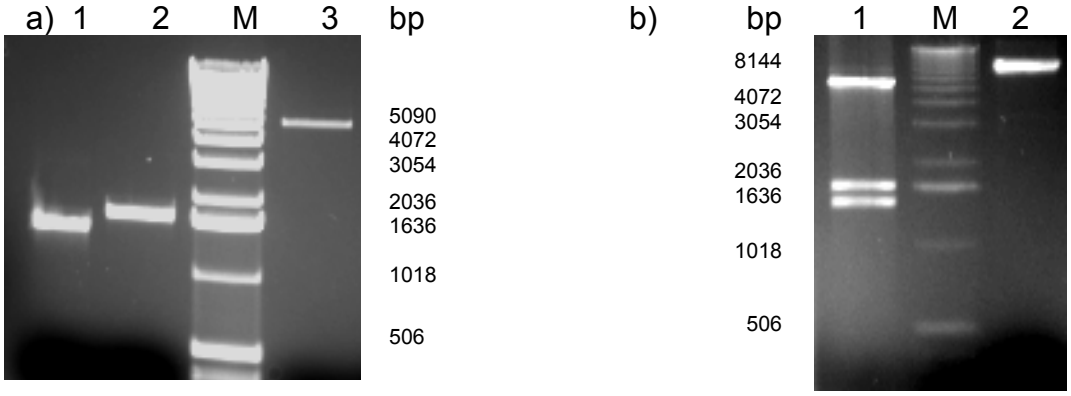

Figure 2-43 a) Agarose gel of the digested CYP102A1 monooxygenase and *Gstredu* gene and the pET28a+ vector (a) lane1 CYP102A1 monooxygenase, lane 2 Gstredu and lane 3 pET28a+; b) Control digestion of pET28A1GR using *Nhe*I, *Eco*RI, and *Not*I (lane1) and the undigested pET28A1GR (lane2)

2.3.4 Expression and Purification

CYP102A1 and the chimera were expressed in *E. coli* BL21 (DE3), resulting in 80-120 mg correctly folded P450 monooxygenase per litre cell culture according to CO-difference spectra (670-1000 nmol/L). Although the chimera was expressed from pET28a+ with a His_6-tag it was not possible to purify the enzyme using metal affinity chromatography (IMAC). Figure 2-44 a) shows the protein composition *of E. coli* cell lysates before (lane 1) and after induction (lane 2) as well as after washing with 50 mM imidazole on a Ni-NTA column (lane3) and elution with 250 mM imidazole. While lane 3 looks nearly identical with lane 2 the eluate exhibits an accumulation of several smaller proteins (40-80 kDa) instead of the target enzyme. Therefore the chimera A1GR was then purified by ion exchange chromatography using the same protocol as for other P450 monooxygenases as described before. Figure 2-44 b) presents the different steps of purification with the cell lysate in lane 1, the flow through in lane 2 while lane 3 and 4 show the purified enzyme at different amounts of protein (10 and 5 µg) The recovery rate was determined to be ~75 % yielding approximately 80 % pure enzyme.

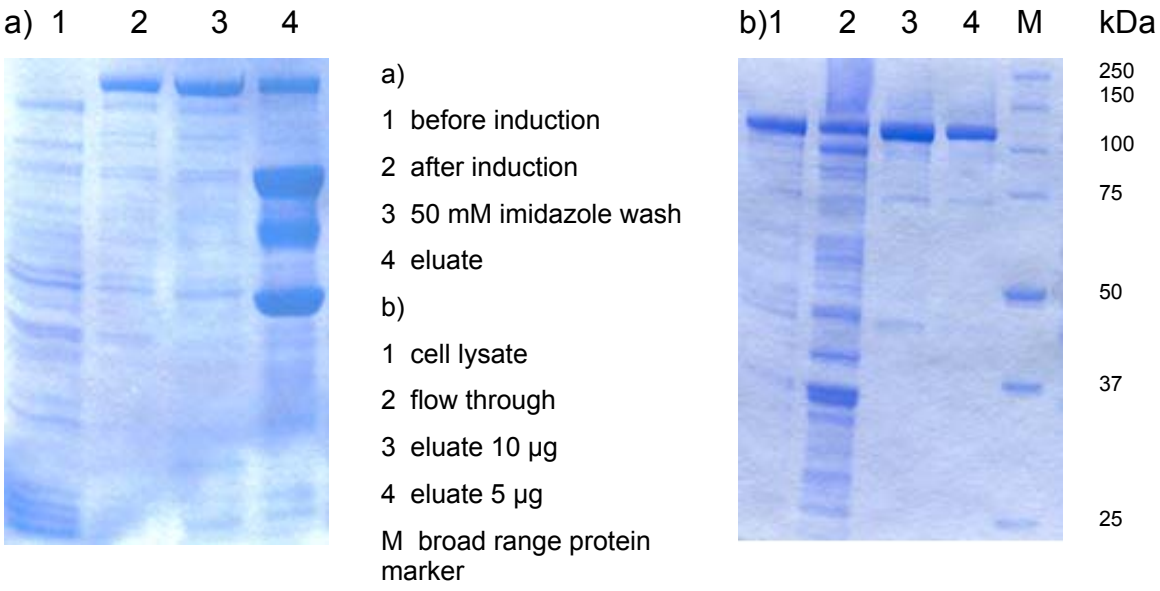

Figure 2-44 Comparison of the purification of A1GR using IMAC (a) and IEX (b)

2.3.5 Characterisation of the Chimera

2.3.5.1 Spectral Analysis of A1GR

The spectrum of the chimera in the oxidised state shows the same slope progression as oxidised CYP102A1 with an additional peak at 390 nm which can also sometimes be seen with CYP102A1 due to partially high spin state of the heme iron (Figure 2-42).

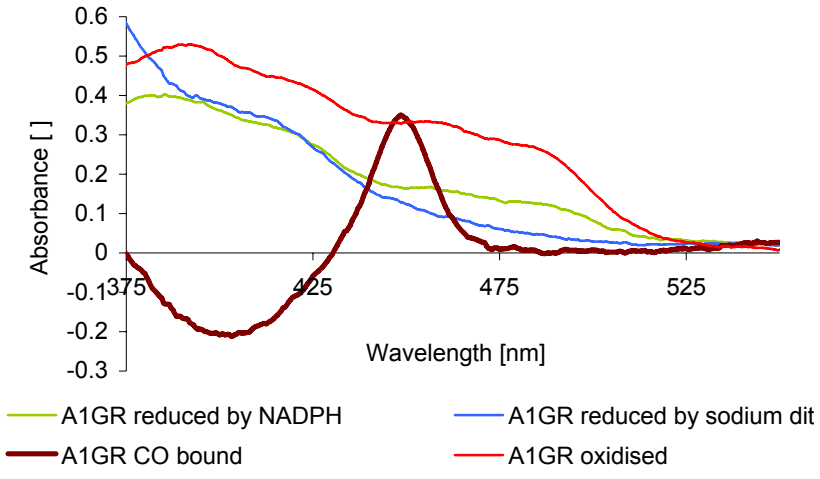

Figure 2-45 Absorption spectra of A1GR

The spectrum shows the characteristic P450 absorption at 420 nm (low spin heme iron) followed by two shoulders at 460 and 485 nm provoked by the two flavins. After addition of NADPH reduction of the flavin absorbance is also observable. These peaks vanish completely after reduction with sodium dithionite. The carbon monoxide difference spectrum of the chimera shows a discrete peak at 448 nm like CYP102A1 without a shoulder at 420 nm.

2.3.5.2 Stability of the Reductase Domain at 45°C

By measuring the increase of fluorescence due to the release of flavins during incubation at 45°C it could be shown that the reductase domain in A1GR exhibits the same stability as the Gstredu on its own. In contrast CYP102A1 starts to release its flavins already after 10 to 20 min incubation time (Figure 2-46).

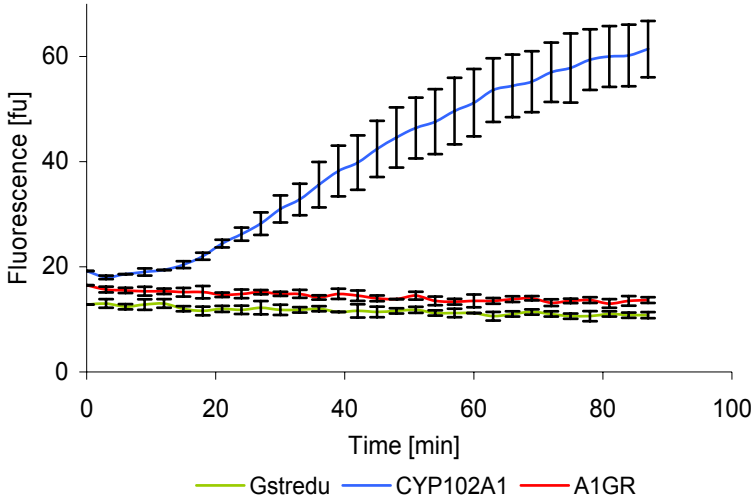

Figure 2-46 Increase of flavin fluorescence upon incubation at 45°C

2.3.5.3 Electron Transfer under Anaerobic Condition

First evidence for the ability of the Gstredu to transfer electrons to the CYP102A1 monooxygenase was obtained from the NADPH dependant reduction of the heme iron with subsequent CO-difference spectra analysis. Therefore the chimera and CYP102A1 were incubated in nitrogen-saturated buffer supplemented with substrate (tetradecanoic acid) and co-factor (NADPH). After reduction one part of the reaction mixture was bubbled with CO and after 30 min difference spectra were recorded.

This was also done after incubation of the enzyme at 35°C and 45°C for 30 minutes. In contrast to the chimera the CYP102A1 reductase in the WT enzyme sequentially loses its ability to reduce the heme iron resulting in 50 % loss of reduction activity after incubation at 45°C (Figure 2-47). As a control for complete reduction CO-difference spectra were also recorded using sodium dithionite for reduction, showing the same values as were obtained by NADPH.

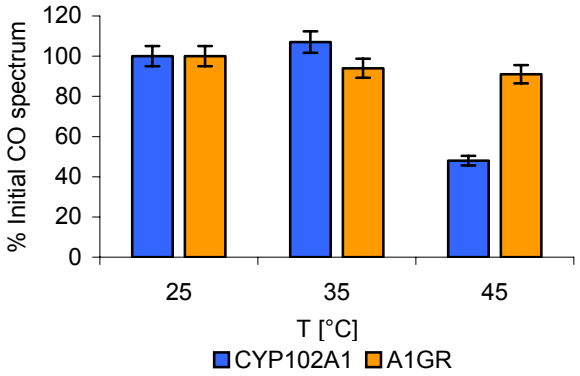

Figure 2-47 Electron transfer between the reductase and monooxygenase domains of CYP102A1 and A1GR

Amount of reduced carbon monoxide bound heme as evidence for interdomain electron transfer

2.3.5.4 Identification of Substrates by Binding Spectra

The next step was to investigate the ability of A1GR to hydroxylate substrates. In a first attempt 12-*p*NCA was used as a substrate but no product formation could be detected. Therefore binding spectra with several substrates and inhibitors were collected to investigate if the reductase domain has an influence on the structure of the substrate binding site.

While it was not possible to record binding spectra for A1GR using 12-*p*NCA or naphthalene the addition of imidazole yielded a standard inhibitor spectrum with a minimum at ~393 nm an increase of absorbance at 434 nm and an isobestic point at 421 nm (Figure 2-48). The use of the natural substrates, long chain fatty acids, introduced a typical Type I binding spectrum associated with substrate binding although the maximum is slightly shifted from 390 to 384 nm but with an isobestic point at 408 nm and a minimum at 420 nm (Figure 2-49). From these spectra the

binding constants for CYP102A1 and A1GR with hexadecanoic acid were calculated. With an K_D of 22 µM the binding constant for A1GR was around four times lower than for CYP102A1, K_D= 105µM.

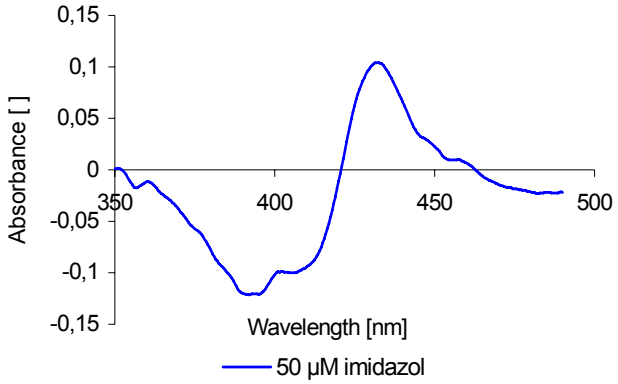

Figure 2-48 Type II inhibitor spectrum of A1GR with imidazole

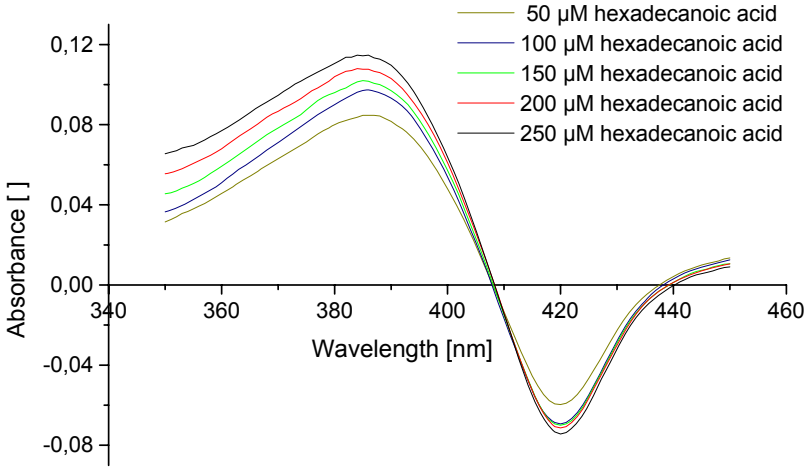

Figure 2-49 Substrate binding spectra of A1GR with hexadecanoic acid

2.3.5.5 Fatty Acid Hydroxylation

Due to their binding ability to A1GR tetradecanoic- and hexadecanoic acid were used to investigate substrate conversion and stability.

To measure conversion rate and to determine coupling efficiency for CYP102A1 (0.05 µM) and A1GR (2 µM), both enzymes were incubated with tetradecanoic- and

hexadecanoic acid and NADPH in a 6 ml approach. One ml was used to measure NADPH consumption over 1 minute while the residual 5 ml were used to determine the product formation at different time points (3,6,9,12,15 min) using GC/MS analysis. The product formation rate for A1GR was constant over the whole time with ~0.3 min^{-1} for both substrates and a coupling efficiency of less than 10 %. Due to the high activity of CYP102A1 the rate was already decreasing between the first and second time point and was therefore only calculated from the first time point after 3 minutes to be ~150 min^{-1} with 65-70 % coupling.

Despite the low activity and the high uncoupling we investigated the thermal stability of the chimera. CYP102A1 and A1GR were incubated for 30 min at the indicated temperatures with subsequent cooling. Hydroxylation of tetradecanoic- and hexadecanoic acid was performed at room temperature for 15 minutes. After extraction, substrate and products were derivatised and analysed by GC/MS. Product formation after incubation at 30°C was defined as 100 % hydroxylation activity.

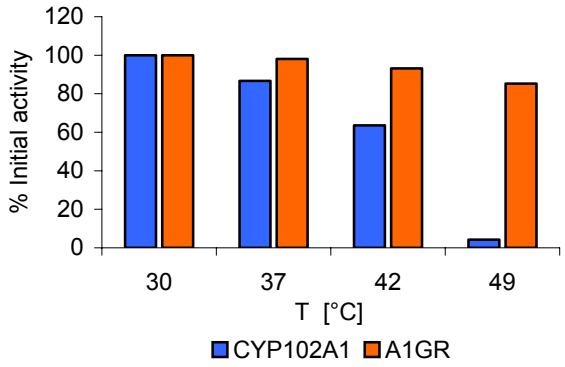

Figure 2-50 Relative activity of CYP102A1 and A1GR towards hexadecanoic acid after incubation at elevated temperatures

As can be seen from Figure 2-50 the chimera retained its activity towards hexadecanoic acid over the whole temperature range while CYP102A1nearly completely lost its activity after incubation at 49°C. The results for hydroxylation of tetradecanoic acid were identical (data not shown).

3 Discussion

3.1 Expression

In this work it was possible to increase the expression level of all P450 monooxygenases and the chimeric enzymes in *Escherichia coli*. Two effects could be observed, first of all the high impact of the choice of cloning vector. The low expression of CYP102A3 in pET20b+ is probably due to the *pel*B leader sequence which is fused to the N-terminus in this construct. While this leader sequence allows for expression of some proteins in the periplasmatic space, it probably hinders the functional expression of the monooxygenase. By cloning the CYP102A3 gene before the leader sequence in pET22b+ this was excised and the yield could be increased around five-fold. The other effect is the expression temperature and the use of recombinant *E. coli* cells for inoculation of the main culture that are still in the exponential phase. It was already reported by Barnes that lower expression temperature and moderate shaking speed result in higher expression of eukaryotic P450s in *E. coli* (~500 nmol/L) (Barnes 1996). By reduction of the temperature after induction of expression from 37°C to 25°C the whole metabolism of the host is slower therefore allowing the P450 monooxygenases time to fold correctly resulting in a higher yield especially in comparison to host proteins.

The observation that low shaking speed yielded a better expression level indicated that the oxygen content in the medium could be an important factor influencing the expression. Especially CYP102A3 was extremely susceptible to inactivation effect due to high oxygen content: when the monooxygenase domain of CYP102A3 was expressed in buffled flasks all of the P450 was inactivated (unpublished data). A possible explanation for this observation is the oxidative inactivation of cytochrome P450 (Karuzina and Archakov 1994).

3.2 Purification

The enzymes of the CYP102A subfamily show high conservation of their amino acid sequence and protein structure. However, there seems to be a difference in the structure at the N-terminal end of these enzymes. We constructed variants of all

investigated P450 enzymes with an N-terminal His_6-tag for simple purification. While CYP102A1-A3 could be easily purified using Ni-NTA or Ni-sepharose columns CYP102A7 did not bind on the column. The same effect was observed for the A1GR chimera which also eluded purification by metal affinity chromatography.

3.3 Product and Substrate Spectra

Examination of the biochemical properties of the CYP102A enzymes revealed distinctive differences. They all accept middle to long chain saturated fatty acids and also polyunsaturated fatty acids as substrates. Experiments have shown that CYP102A1 to CYP102A3 show highest activity towards polyunsaturated fatty acids, two- to four-folds higher than towards the best saturated fatty acid (C14 or C15). In contrast, CYP102A7 exhibits highest activity towards myristic acid (C14) showing the highest activity towards saturated fatty acids at all. The distribution of activities towards saturated fatty acids of different chain length for CYP102A1 is consistent with data previously reported. Activity towards tetradecanoic acid is highest and decreases with longer or shorter chain length (Boddupalli et al. 1990). Values previously reported for the *Bacillus subtilis* P450 monooxygenases vary from slightly to great depending on publication. Gustafsson et al. reported, for example, that dodecanoic acid is the preferred saturated fatty acid for CYP102A2, while tetradecanoic acid is oxidised with much lower activity (2.5 %) (Gustafsson, Roitel et al. 2004). In contrast, Budde et al. reported that tetradecanoic acid is the preferred saturated fatty acid for this enzyme, which was reproduced in the present work (Budde, Maurer et al. 2004).

For CYP102A3 the substrate profile between Gustafsson and this work is also not compatible. Slight differences in the profile can be explained by different reaction conditions, e.g. temperature, fatty acid concentration due to different kinetic constants one or the other fatty acid is favoured. The differences concerning CYP102A2 are however not explainable especially the k_{cat} of tetradecanoic acid which is about 10 to 20 times lower than the activities measured under non-saturated conditions.

The results from this investigation have shown that each enzyme can be identified by its hydroxylation pattern of the saturated fatty acids. Outstanding is the ability of CYP102A3 to hydroxylate palmitic acid (C16) to about 25% at position ω-7 while all the other enzymes produce as main products ω-1 to ω-3 hydroxy products with only minor hydroxylation at position ω-4. This was neither reported by Lentz et al 2004 nor Gustafsson et al 2004 probably due to the mode of measurement (Gustafsson, Roitel et al. 2004; Lentz, Urlacher et al. 2004). Another interesting observation is that, for example CYP102A1 changes its preferences for each fatty acid while for CYP102A2 the preferences do not change very much. An explanation for this behaviour could be that the fatty acids are proposed to be fixed at the carboxy-terminal end in the substrate binding site of CYP102A1 by R47 and the ω-end of the fatty acid has to fold differently according to its chain length in the vicinity of the heme. In CYP102A2 the situation might be different, there is no amino acid in the entrance to bind the carboxy-group that is free to stick out of the entrance at longer chain length and the space near the heme just allows the fatty acid a very restricted conformation.

Next to fatty acids the four enzymes show activity to several other substrates. CYP102A1 converts, for example beta-ionone to 4-hydroxy beta-ionone, while CYP102A2 is extremely active towards iso- and anteiso branched chain fatty acids. Surprisingly 7-ethoxycoumarin, normally a substrate for microsomal P450 monooxygenases is deethylated by CYP102A7. It was interesting for practical use of this enzyme to test if other microsomal substrates could also be accepted, but none of the following compounds, 7-ethoxy resorufin, testosterone, Reichstein S and dextromethorphan were oxidised by CYP102A7. If we look at the shapes of the substrate binding sites of CYP102A1-A3 and CYP102A7 which were determined from the modelled structures of CYP102A2,A3 and A7 and the crystal structure of CYP102A1 we can see that they look rather different although the structures were modelled on CYP102A1 as the template (courtesy from Tuan A. Do) (Figure 3-1a). The cartoon (Figure 3-1b) clearly shows that CYP102A2 has the narrowest substrate binding site even with some kind of bottle neck, explaining the strict product spectrum and the restriction to fatty acids as substrate. The SBS of CYP102A3 exhibits an additional cavity where long chain fatty acids can bend so exposing carbon atoms to the reactive centre which are far from the ω-end. Interesting is here that a mutant of

CYP102A1, R47A/F87V/L188Q also shows an additional cavity in a comparable position as in CYP102A3 and as it has been reported previously also hydroxylates longer fatty acids at positions far from the ω-end, up to ω-8. CYP102A7 has a narrow access to the heme but the broadest SBS. This may explain why 7-ethoxycoumarin is a substrate of CYP102A7 but not naphthalene which is of nearly the same size. In 7-ethoxycoumarin the ethoxy-group may point to the heme and can be attacked, while naphthalene is very rigid without side chains accessing the reactive centre.

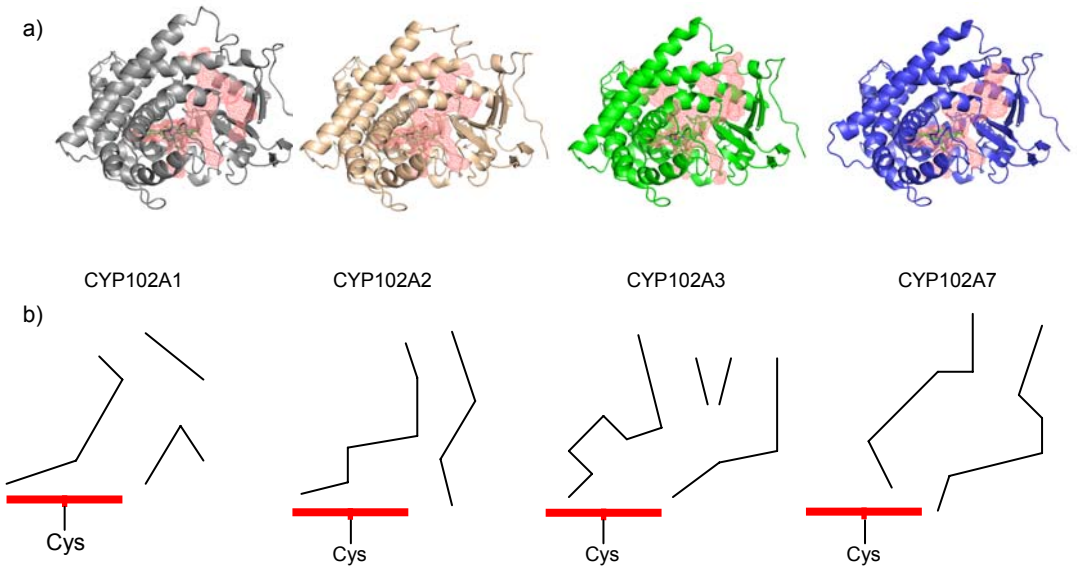

Figure 3-1a) The modelled substrate binding sites of CYP102A1-3 and CYP102A7 by courtesy of Tuan A. Do; b) Cartoon of the SBS, in red the plane of the heme

These observations may help to understand some of the properties of these enzymes but are still speculative because on the one hand these are only models and therefore resemble mostly the structure of the template and on the other hand crystal structures of CYP102A1 with and without substrate indicate that there is a great mobility in these type of enzymes especially of the substrate binding region proposing an induced fit model. Additionally it should not be neglected that all structures were obtained without the reductase domain and as it was shown by Boddupalli in 1992 the binding constants of the free monooxygenase domain of CYP102A1 and the fusion enzyme differ greatly which indicates structural effects of

the reductase domain on the SBS: This proposition can also be supported by this work where the chimera of the CYP102A1 monooxygenase domain with the Gstredu exhibits opposed preferences for palmitic and myristic acid (Boddupalli et al. 1992).

Closer investigation of CYP102A2, A3 and A7 especially of the crystal structures with different substrates and/or the intact reductase domain could lead to a more detailed explanation of these properties.

3.4 The Natural Substrate?

There are some publications speculating about the natural substrates of the P450 monooxygenases from the CYP102A subfamily. One interesting preposition for the natural substrate of CYP102A1 and A3 are polyunsaturated fatty acids. These enzymes may play a crucial role in detoxification of polyunsaturated fatty acids, because even low concentrations of these compounds are lethal for *Bacillus megaterium* or *B. subtilis* (Macdonald, Smith et al. 1996; Palmer, Axen et al. 1998). This idea can be strengthened by the high activity and extremely low binding constants of CYP102A enzymes towards polyunsaturated fatty acids. Cryle and Gustafsson favour branched fatty acids as the natural substrate of CYP102A1 or A2 (Gustafsson, Roitel et al. 2004; Cryle et al. 2006). High content of branched fatty acids in the membrane of *Bacillus strains* (>90%) encourages this argumentation (Kaneda 1977). The ratio of branched and also saturated and unsaturated fatty acids plays an important role in membrane stability and adaptation to different environments (Suutari and Laakso 1992). There is also some support for the influence of membrane composition on sporulation, however while CYP102A2 exhibits rather high activities towards branched fatty acids the velocities for CYP102A1 are more moderate and also the content of branched chain fatty acids in *Bacillus megaterium* are lower than in *B. subtilis*. The roles of CYP102A4, A5, A6 and also A7 in their specific organisms remain to be investigated.

3.5 Temperature Stability and the Chimera A1A3

Next to the differences of substrate and product spectra the four P450 monooxygenases have different properties concerning temperature stability.

When we investigated the stability of the discrete domains in CYP102A1 the reductase domain was less stable than the monooxygenase domain, while for CYP102A2 and CYP102A3 the situation was vice versa. The difference was in both cases about 10°C. This led to the idea to combine the both stable domains to create an enzyme with increased thermal stability. The combination of the CYP102A1 monooxygenase domain with the CYP102A3 reductase domain yielded a protein (A1A3) exhibiting the characteristic spectra for this type of P450 monooxygenase – reductase fusion enzymes. It was expressed at high yield (133 mg/L) without a shoulder at 420 nm in the CO-difference spectrum which is a sign for non-functional heme caused by removal of the thiolate binding (cysteine 400) of the iron (Omura 2005). The thermal stability of both domains in A1A3 mirrored the stability of the discrete domains of the parental enzymes as was expected. Long term storage stability was also increased by a factor of about two. Additionally the chimera displayed an unusual behaviour after incubation at elevated temperatures. It is well known that the CYP102A enzymes show increased activity after incubation at 30-37°C but the chimeric enzyme exhibited first a decrease of activity after incubation at around 40°C and then an increase up to more than 150 % after incubation at 50°C (Noble et al. 1999; Lentz, Urlacher et al. 2004). Activity was always measured using 12-*p*NCA a surrogate substrate. In CYP102A1 and A3 overall stability seemed to be dependant on the stability of the less thermostable domain. The high activation of the chimera could be due to a rearrangement of the monooxygenase to the reductase domain upon heating or of a disaggregation of non-functional multimers to functional dimers (Neeli, Girvan et al. 2005). The activity of the chimeric enzyme towards 12-*p*NCA was 50-65 % of that measured for CYP102A1, but activity towards fatty acids was only in the range of ten percent although the product pattern was unaltered. An explanation for this different behaviour could be, that the activity towards 12-*p*NCA is mainly restricted by binding and release of the substrate (binding constant) which is the same in the chimera, while the velocity of fatty acid conversion depends on the electron transfer rate, which may be hampered in the chimeric enzyme because of a

wrong orientation of the two foreign domains. This observation was confirmed by the similarity of the binding constants for CYP102A1 and A1A3 with pentadecanoic (C15) and docosahexaenoic acid (DHA) of 3.8 µM vs. 3.9 µM for C15 and 2.1 µM vs. 2.9 µM for DHA respectively.

The CD spectra recorded in the near UV/Vis region for A1A3 revealed that the surrounding of the heme in fact has the same active organisation as in CYP102A1. It had been shown previously that mixing of the two domains of CYP102A1 expressed independently did not result in the same CD spectrum as for the holoenzyme and therefore did not result in the correct structural basis for efficient electron transfer which was also proven by the extremely low activity (~0.1 %) resulting from mixed domains (Munro et al. 1994).

3.6 A1GR

Recent publications showed that it is possible to construct functional chimeric enzymes between CYP102A1 and Nitric oxide synthase (Fuziwara, Sagami et al. 2002). While some older publications deal with the acceptance of *E. coli* sulfite reductase as electron partner for microsomal P450s. Therefore we constructed a chimeric enzyme comprised of the monooxygenase domain of CYP102A1 and the α-subunit of a sulfite reductase isolated from the thermophilic *Geobacillus stearothermophilus*. This reductase domain exhibited high thermal stability and was able to reduce cytochrome c at 60°C with high activity. In the chimeric enzyme A1GR the reductase was able to reduce the heme iron of the monooxygenase domain and also to deliver reduction equivalents for the hydroxylation of myristic and palmitic acid also at temperatures (45°C) were the wild type CYP102A1 was highly diminished in its activity. In contrast to the chimeric enzyme between CYP102A1 and CYP102A3 where substrate and product spectra were unaltered the sulfite reductase seemed to have an influence on the structure of the monooxygenase domain. On the one hand the N-terminal His_6-tag now seemed to be buried in the enzyme so that it was no longer possible to use metal affinity chromatography for purification, on the other hand A1GR could not hydroxylate any of the *p*NCAs. Additionally the preference for the fatty acids was switched, while CYP102A1 preferred myristic acid over palmitic

acid the chimera A1GR preferred palmitic acid. The drawback for further investigation of differences in substrate or also product spectra was the low activity of A1GR accompanied by a high uncoupling rate. Together with the experiments on NOS/CYP102A1 fusion enzymes these investigations showed the conserved function of the diflavin reductases, that they are interchangeable although at lessened activities. Up to now there exists no crystal structure of the CYP102A1 fusion protein, therefore no concrete information where the reductase interacts with the monooxygenase domain and which amino acids are important for electron transfer. Deeper inside of this relationship in future investigations would greatly help to construct chimeric stable enzymes.

4 Materials and Methods

4.1 Materials

4.1.1 Instruments

Instrument	Characteristics	Company
Devices for agarose gel electrophoresis	DNA Sub Cell™	BioRad Laboratories,
	Mini Sub™ DNA Cell	USA
	Mini Sub™ Cell GT	
	BWM 9X Monitor	Javelin Electronics, USA
	UV-lamp table	MWG-Biotech, Germany
Balances	Basic, MCI Research RC 210 D	Sartorius Germany
	Precision Advanced	OHAU® USA
Centrifuges	Eppendorf Centrifuge 5417 C	Eppendorf, Germany
	Eppendorf Centrifuge 5415 R	
	Eppendorf Centrifuge 5415 R	
	Sorvall RC – 5B (Rotor: SA 600)	Sorvall Germany
Circular dichroism spectrometer	Chirascan	Applied Photophysics, UK
FPLC	Äkta Explorer	Amersham Bioscience, Germany
Fluorimeter	Fluostar 403 fluorimeter	BMG LabTechnologies Germany
GC/MS	GC/MS QP2010	Shimadzu, Germany

Incubators	WTE	Binder, Germany
	HT-incubator Multitron	Infors AG, Switzerland
	Certomat R Incubator	Braun, Germany
	UM 500	Memmert, Germany
Microwave oven	Micro-Chef FM A935	Moulinex, Germany
Power supplies	Power Pac 3000	BioRad, USA
Power supplies	Power Pac 300	
	Model 200/2.0 Power supply	
PCR-Cycler	Master Cycler Gradient	Eppendorf, Germany
	Robocycler® Gradient 40	Stratagene®, Germany
pH-Meter	Digital pH Meter pH525	WTW, Germany
Device for Polyacrylamide gel electrophoresis	Minigel-Twin G42	Whatman Biometra®, UK
	Model 583 Gel Dryer	BioRad, USA
Rotors	A-4-62, F34-6-38	Eppendorf, Germany
	SS34, SLA-3000	Sorvall, Germany
Sonifier	Sonifier 250	Branson, USA
Spectrophotometer UV/VIS	Ultrospec 3000	Pharmacia Biotech, Germany
	Spectramax 340 PC for Microtiter plates	Molecular Devices, USA
	EvolutionTM100 UV-Vis	Thermo Electron Corporation, Germany
	Cary 50 Bio UV-VIS	Varian, Germany

Vacuum concentrator	SpeedVac Concentrator 5301	Eppendorf, Germany
Vortex	Vortex Genie 2	Scientific Industries, USA
Thermomixer	Thermomixer 5436	Eppendorf, Germany

4.1.2 Chemicals

Supplier	Material
ARK scientific GmbH, Darmstadt Germany	Oligonucleotides
Applichem, Darmstadt Germany	IPTG
BIO-RAD Laboratories, Richmond, USA	LMW protein standard
Boehringer Mannheim, Mannheim Germany MBI Fermentas, St. Leon-Rot Germany	Restriction endonucleases, T4-DNA ligase
DIFCO-laboratories, Detroit, USA	Yeast extract, Tryptone, Bacto-tryptone, Bacto-yeast extract
Fluka Chemie, Buchs, Schweiz	Agar, Ampicillin, Bromphenolblue, Coomassie Brilliant Blue, EDTA, Ethidium bromide, Lysozyme, NaCl, , SDS, Tris-(hydroxymethyl)-aminomethane, Na_2HPO_4, NaH_2PO_4, K_2HPO_4, KH_2PO_4, NaOH, KAc, Acetic acic, Sodium dithionite

Gibco BRL GmbH, Eggenstein Germany	1 kb-Ladder (DNA standard)
MBI Fermentas, St. Leon-Rot Germany	Restriction endonucleases, T4- DNA ligase, *Taq*-polymerase
Merck, Darmstadt Germany	Glacial acetic acid, TLC plates (0.2 mm, Silica 60 F_{254}),
GATC Konstanz Germany	DNA sequencing
Pharmacia LKB, Freiburg Germany	Source Q, PD10, Ni-Sepharose
Qiagen GmbH, Hilden Germany	Midi Plasmid Kit, Spin Mini Plasmid Kit, QIAquick Gel Extraction Kit, Ni-NTA
Riedel-de-Haën, Seelze, Germany	DMSO, Ethylacetate, Glycine
Schleicher & Schuell, Dassel Germany	Paper filters
Serva Feinbiochemika GmbH, Heidelberg Germany	Agarose
Sigma Chemie GmbH, Deisenhofen Germany	Ammoniumpersulfate, PMSF, Acetone, Methanol, Diethylether, Dichloromethane,
Stratagene, Heidelberg, Germany	*Pfu*-polymerase, *Pfu* turbo-polymerase
Tosoh Haas, Stuttgart, Germany	DEAE sepharose 650 M

4.1.3 Buffers and Commonly Used Solutions

4.1.3.1 Common Buffers

TE buffer:	Tris	10	mM
(pH 8.0)	EDTA	1	mM
Potassium Phosphate Buffer:	K_2HPO_4 1M	40.1	ml
(0.05 M, pH 7.4)	KH_2PO_4 1M	9.9	ml
buffer A	H_2O	950	ml
Potassium Phosphate Buffer:	K_2HPO_4 1M	~48	ml
(0.05 M, pH 8.1)	KH_2PO_4 1M	~2	ml
buffer B	H_2O	950	ml

4.1.3.2 Buffers and Solutions for Agarose Gel Electrophoresis

1 % agarose gel:	Agarose	4.0	g
	1 x TAE (Tris-acetate)	400	ml
50 x TAE buffer:	Tris base	242	g/L
	glacial acetic acid	57	ml
	EDTA (0.5 M, pH 8.0)	100	ml
6 x DNA loading buffer:	glycerol	30	% (w/v)

	bromphenol blue	0.2	% (w/v)
	EDTA (pH 7.5)	5	mM

4.1.3.3 Buffers and Solutions for Polyacrylamide Gel Electrophoresis

4 x Lower Tris (200 ml):	Tris base	36.46	g
pH 8.8	SDS	0.8	g
4 x Upper Tris (200 ml):	Tris base	12.11	g
pH 6.8	SDS	0.8	g
Resolving gel (12.5 %)	acrylamide: bisacrylamide 37.5:1 (30 %)	3.33	ml
	Lower Tris 4 x	2.0	ml
	$H_2O_{bidest.}$	2.67	ml
	TEMED	4.0	µl
	ammonium persulfate (10 % (w/v))	40.0	µl
Stacking gel (3.9 %)	acrylamide : bisacrylamide 37.5:1 (30 %)	0.52	ml
	Upper Tris 4 x	1.0	ml
	$H_2O_{bidest.}$	2.47	ml

	TEMED	4.0	µl
	ammonium persulfate (10 % (w/v))	40.0	µl
5 x Tris glycine buffer	Tris	15	g/L
pH 8.3	glycine	72	g/L
	SDS	10	% (w/v)
6 x Loading buffer	Tris/HCl (pH 6.8)	320	mM
	glycerol	50	% (v/v)
	SDS	10	% (m/v)
	β-mercaptoethanol	25	% (m/v)
	bromophenol blue	0.1	% (m/v)

Staining with Coomassie Brillant Blue:

staining solution:	Coomassie Brillant Blue R-250	0.1	% (m/v)
	methanol	30	% (v/v)
	glacial acetic acid	10	% (v/v)
destaining solution:	methanol	30	% (v/v)
	glacial acetic acid	10	% (v/v)

4.1.3.4 Media

All media were autoclaved immediately after preparation. For agar plates 14 % (m/v) agar were added to the medium prior to autoclaving. Specific selection markers were added after cooling to less than 50°C.

LB-Medium	tryptone	10	g/L
pH 7	yeast extract	5	g/L
	NaCl	5	g/L
TB-Medium	tryptone	12	g/L
	yeast extract	24	g/L
	glycerol	4	ml/L
	potassium phosphate buffer 0.89 M, pH 7.4	10	% (v/v)
Tfb I (200 ml)	KOAc	0.588	g
	RbCl	2.42	g
	$CaCl_2$	0.294	g
	$MnCl_2 \cdot 4\ H_2O$	2	g
	87 % Glycerin	34.48	ml
	with acetic acid	pH 5.8	

Tfb II (50 ml)	MOPS	0.105	g/50 ml
	$CaCl_2$	0.55	g/50 ml
	RbCl	0.061	g/50 ml
	87 % Glycerin	8.6	ml/50 ml
	adjust with diluted NaOH	pH 6.5	

Medium 220	Peptone from casein	15	g/L
pH 7.3	Peptone from soy meal	5	g/L
	NaCl	5	g/L

4.1.3.5 Antibiotics and Others

1000 x phenylmethylsulfonyl fluoride (PMSF) 1 mM in ethanol

The following solutions were made with H_2O_{bidest} and filter sterilised (0.2 µM) prior to use. For storage they were frozen at -20°C.

1000 x Ampicillin 100 g/L

1000 x Kanamycin 30 g/L

2000 x isopropyl-beta-D-thiogalactopyranoside (IPTG) 1 M

4.1.4 Bacterial Strains

Geobacillus stearothermophilus strain 13240 was obtained from the DSMZ and grown at 60°C in medium 220 (Caso Agar) according to a DSMZ protocol.

E. coli strain DH5α [F'/endA1 hsdR17 (r_K—m_K+) glnV44 thi-1 recA1 gyrA (Nal^r) relA1 Δ(lacIZYA-argF)U169 deoR [Φ80 dlac Δ(lacZ)M15]] (Clontech) was used as host for the subcloning steps

E. coli BL21 (DE3) [F— ompT gal [dcm] [lon] $hsdS_B$ (r_B- m_B—; an E. coli B strain) with DE3, a λ prophage carrying the T7 RNA polymerase gene] (Novagen) was used for gene expression.

4.1.5 Vectors

pET 28a+	EMD Biosciences (Novagen)
pET22b+	EMD Biosciences (Novagen)
pET20bCYP102A3	Dr. Oliver Lenz
pET28bCYP102A2	Dipl. Chem. Michael Budde
pET28aCYP102A1	Dr. Steffen Maurer
pET28aCYP102A7	Dipl. Chem. Asta Chimene

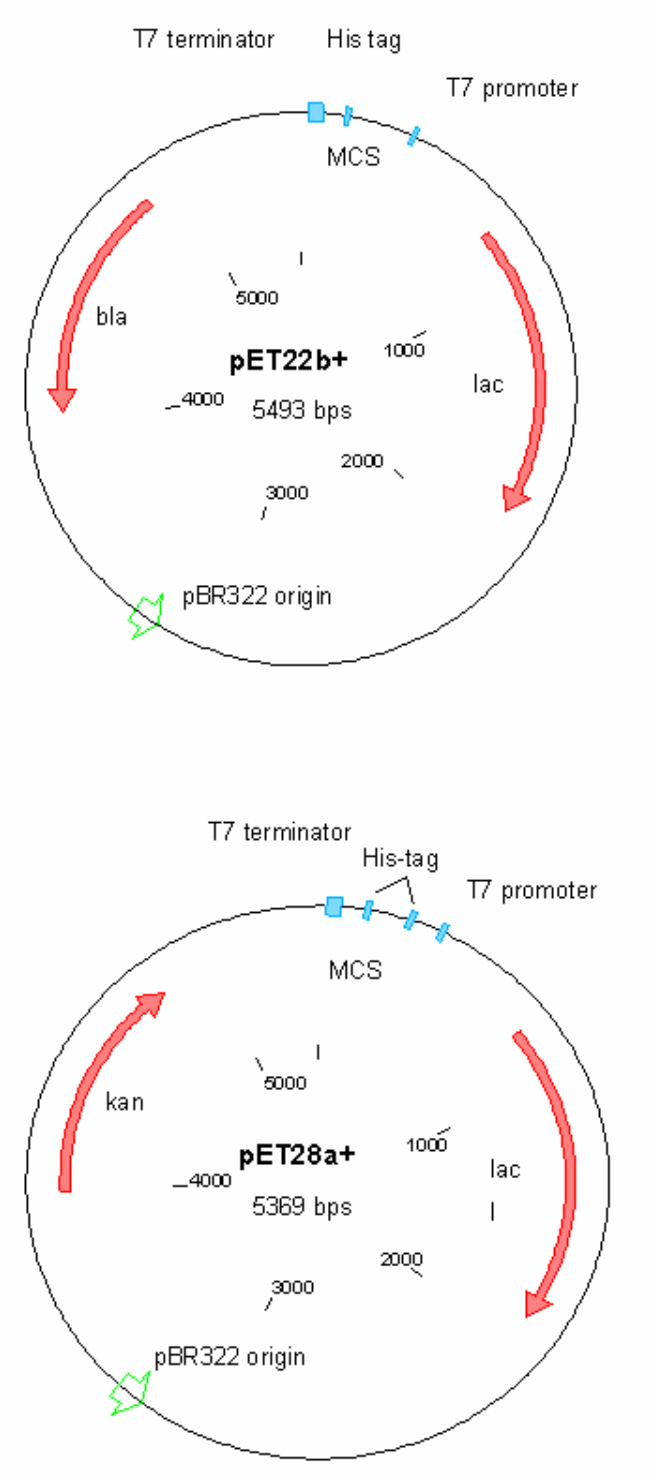

Figure 4-1 Schematic view of pET22b+ and pET28a+

4.1.6 Oligonucleotides

Oligonucleotides (Sigma-Aldrich, ARK) were dissolved in TE Buffer to a final concentration of 100 pmol/µl.

Primer name:	sequence 5'-3'
SEIMonoLNhe1	CTA GCT AGC ATG ACA ATT AAA G
SEIMonoLR	GGA ATT CGT ATT ATG AGC GTT TTC TGC CTT TTT GCG
SEIGstReF	GGA ATT CTG TGA CGG TAT TGT ACG
SEIGstReNot1	ATA AGA ATG CGG CCG CTT AGT AGA CGT CGC G
HBACYPA1RBam	CGG GAT CCG TAT AGC ACA AG
SeiCypA3Nhe1F	CTA GCTAGC ATG AAA CAG GC
Spf_pET28a_BM_R	CTAGAATTCTTACCCAGCCCACACGTCTTT
HBACYPA3FBam	CGG GAT CCA ATC TTG GG
HBACYPA3RecoR1	GGA ATT CTT ACA TTC CTG TC
SEIpET22NheF	CGG CAG CAG GTA TTT GCT AGC TAT ATC TCC TTC
SEIpET22NheR	GAA GGA GAT ATA GCT AGC AAA TAC CTG CTG CCG
SEIGRBam-F	CTT TAA GTT GCC GAA GGC TCC CGA CAC GCC GAT C
SEIGRBam-R	GAT CGG CGT GTC GGG AGC CTT CGG CAA CTT AAA G
SEIGstreduBamH1F	GCG GAT CCC AAA CCG G
SEIA1F393XF	GCG TTT AAA CCG SWT GGA AAC GGT CAG
SEIA1F393XR	CTG ACC GTT TCC AWS CGG TTT AAA CGC
SEIA1GReco-2F2	GAA AAC GCT CAT AAT ACG ccT ctT cTG _GTA TTG TAC GGC

	TCG CC
SEIA1GReco-2R2	GG CGA GCC GTA CAA TAC CAG AAG AGG CGT ATT ATG AGC GTT TTC
A1Primer R1	GGC TAT CAT GCG ATG ATG GT
A1Primer R2	GGA AAA GAT CCA GAA ACG GG
A1Primer R3	ATT CCT CAG CTT CAC CGT GA
A1Primer R3,5	CTT GGC GGT ATT CCT TCA C
A1Primer R4	ATT TGC ACC GCA GGT CGC AA
A1Primer R5	TTC AAT TTG TCG ACA GCG CC
A1Primer R6	TCG CGC AAT GGC TGC TAA AA
A1Primer R7	CTG CCA AAA GAC CCT GAA AC
A3Primer S1	CTA TCA TTC TAT GAT GCT G
A3Primer S2	CTT ACA CATCCG GAA AAA C
A3Primer S3	CTG TGA AAC CGC GAA AAA
A3Primer S4	GCG AGT CTT GGG AAA ACC
A3Primer S5	GCT GGA ACA GCT CGT TCC
A3Primer S6	GAG AAG AGC TGG ATC AAG
T7-Promotor-Primer	TAA TAC GAC TCA CTA TAG GG
T7-Terminator-Primer	GCT AGT TAT TGC TCA GCG G

4.2 Methods

Standard procedures for molecular biology were performed as described by Sambrook et al. (Sambrook 2000)

4.2.1 DNA Methods

4.2.1.1 Isolation of Genomic DNA

Isolation of genomic DNA was accomplished by phenol/chloroform extraction and isopropanol precipitation after cell lysis with lysozyme.

150 ml Medium 200 were inoculated with a fresh colony of *Geobacillus stearothermophilus* and cultivated for 20 hrs at 65°C, 160 rpm in a shaking incubator. After centrifugation of 35 ml culture (10 min 3220 rcf) the pellet was resuspendet in 15 ml lysis buffer (30 mM Tris; 50 mM EDTA; 50 mM NaCl; pH 8.5 mg lysozym) and incubated for 30 min at 30°C. Before a second incubation period at 37°C for 45 min 1.5 ml of 10 % SDS solution were added. Proteins were removed by two times extraction of the cell lysate with phenol/chloroform (0.7 volumes) with subsequent extraction with the same volume of chloroforme. The DNA in the aquous phase was precipitated through addition of 10 % (v/v) sodium acetate (pH 4.8) and 0.6 volumes isopropanol. After centrifugation and removal of the liquid phase the DNA was washed twice with 2 ml ice cold 70 % ethanol. The DNA was then dried 15 min at 30°C using a speed vac and resuspended in 1 ml TE buffer.

4.2.1.2 Plasmid Isolation

Highly pure plasmid DNA was obtained by means of QIAprep® (Quiagen) or GenElte™ Plasmid miniprep (Sigma) kit. These procedures are based on alkaline lysis of bacterial cells, followed by purification of the DNA by ion-exchange chromatography (Birnboim and Doly 1979).

After harvesting the cells from a 4 ml overnight culture by centrifugation, the plasmid isolation was carried out according to the instructions of the manufacturers. Elution was initiated by addition of 75 µl of a 1:5 dilution of the respective elution buffer. Plasmid DNA was stored at -20°C.

4.2.1.3 Digestion of DNA with Endonucleases

DNA digestions were carried out according to the instructions of the manufacturer. Normally 0.1-10 μg DNA were restricted by 1-10 U of endonuclease. Specific enzyme buffers provided with the enzymes were used at specified concentrations to achieve the best results. Usually double digestions were performed. If buffer concentrations differed enzymes were used subsequently. Restriction digestions were performed in 20-50 μl scale. Incubation times and temperatures were depended on the enzymes used, typically 1-4 hours at 37°C. The digested DNA was analysed by agarose gel electrophoresis. Preparative digestions were isolated by gel extraction.

4.2.1.4 Ligation of DNA

To ligate digested and purified DNA stretches new bonds between phosphate residues located at the 5' termini of double-stranded DNA and adjacent 3'-hydroxyl moieties have to be formed. These phosphodiester bonds between adjacent 5'-phosphate and 3'-hydroxyl residues can be catalysed *in vitro* by DNA ligases.

A typical ligation mixture was either incubated 1 hour at room temperature or 16 hours at 16°C. The ligation mixture was comprised by a 2-5-fold molar excess of foreign DNA towards plasmid DNA at the appropriate buffer concentration and 1 U T4 DNA ligase in 20 μl scales.

4.2.1.5 Agarose Gel Electrophoresis

An effective method to separate DNA fragments for analytical as well as preparative purposes by means of size differentiation is agarose gel electrophoresis. Due to the negative charge of DNA molecules, they migrate in an electrical field towards the anode the rate depending on size and conformation of the DNA and also on pore size. Larger molecules migrate more slowly than smaller molecules because of greater frictional drag. To visualise the DNA ethidium bromide, a fluorescent dye, is often used. It intercalates between stacked base pairs and upon ultraviolet illumination makes DNA visible.

For DNA fragments between 1000 and 8000 bp length 1 % melted agarose solution in 1xTAE was poured into the mould after addition of 0.01 % ethidium bromide. After

complete setting of the gel it was transferred into the electrophoresis tank and covered with 1 x TAE buffer. DNA samples (5-50 µl) with DNA loading buffer (5:1) were loaded on the gel. As size standard a 1 kb-ladder was used. Electrophoresis was performed at 90 V for 40 min. The gel was examined by ultraviolet light and documented.

4.2.1.6 DNA Isolation from Agarose Gels

The extraction of DNA from agarose gels using the QIAquick Gel Extraction kit applies to the same principle as plasmid isolation with the difference that the gel piece with the desired DNA fragment has to be melt in a special buffer prior to application on the column. Elution was initiated by addition of 35 µl of a 1:5 dilution of elution buffer (10 mMTris-Buffer, pH 8).

4.2.1.7 DNA Quantification

Quantification of DNA is based on its specific absorption at 260 nm, where an OD of 1 corresponds to approximately 50 µg/ml for double-stranded DNA. The quality, purity of the DNA can be estimated by ratio between the readings at 260 nm and 280 nm (OD_{260}/OD_{280}). Pure DNA preparations have OD_{260}/OD_{280} values between 1.7 and 2.0.

4.2.1.8 Polymerase Chain Reaction

The polymerase chain reaction is used to amplify a segment of DNA that lies between two regions of known sequence. Two oligonucleotides (complimentary to the 3'- and 5'-termini of a DNA segment) are used as primers for a series of synthetic reactions that are catalysed by a DNA polymerase. The reaction consists of three steps:

Denaturation: Through heating at temperatures higher than 92°C the template DNA is separated into its complementary single strands.

Annealing: The reaction mixture is then cooled to a temperature around 5°C lower than the melting temperature of the oligonucleotides this allows them to anneal to their target sequence.

Elongation: At temperatures between 68-72°C depending on the used enzyme the annealed primers are extended by the DNA polymerase. Synthesis is always in the 5'→3' direction under consumption of desoxyribonucleotide-5'-triphosphates (dNTPs).

These 3 steps are repeated 15-40 times and each new synthesized DNA fragment can be used as a template for the next round of PCR so that it results in an exponential increase of PCR products under optimal conditions.

Either plasmid DNA or genomic DNA were used as templates. For PCR reactions resulting in fragments used for further cloning the high fidelity *Pfu*-polymerase (from Pyrococcus) was used to exclude the introduction of mutations. For colony PCR the cheaper and faster *Taq*-polymerase (from *Thermus aquaticus*) was the enzyme of choice.

Colony PCR is a fast and easy method to investigate if a bacterial colony contains a plasmid with the gene of interest. Therefore an extremely small amount of a bacterial colony was picked and streaked on the lid of a PCR tube and also on a new agar plate. A PCR mastermix was prepared, for each colony PCR 20 µl of the mastermix were used. If the gene of interest is very big it is sometimes necessary to amplify only a small piece of 500 to 1000 kb. Either hot start PCR or normal PCR programs were used. The clones containing the gene of interest were the identified by agarose gel filtration analysis.

Oligonucleotides had to be constructed according to the DNA sequence of choice (8-10 binding bases) and the endonuclease restriction site used for further cloning, 6-8 bases plus 1-8 bases overhang assuring complete restriction of this site. The melting temperatures of the two oligonucleotides used in one reaction should be nearly similar in the range of 48-60°C.

Because the polymerases are magnesium dependant the reaction mixture has always to contain a source of magnesium ions. The specific buffers for the polymerases supplied with the enzymes used here already contained MgCl at the necessary concentration.

PCR reactions were either performed at 20 or 50 µl scale a typical reaction mixture contained the following components (100 µl mastermix):

Component	Volume [µl]	Final concentration
10 x polymerase buffer	10	1 x
dNTP mix (2,5 mM each)	4	0.01 mM each
sense primer	2	0.2 µM
antisense primer	2	0.2 µM
DNA template	variable	ca. 20-100 ng
DNA polymerase	1	2.5 U
H_2O	variable	-
Total volume	100	

PCRs were performed in a thermocycler (Eppendorf) using the following general program:

Cycle	Denaturation	Annealing	Extension
Initial denaturation	95°C, 1 min		
PCR cycles (25)	95°C, 1 min	45-55°C, 30 s	70°C, 2 min /1 kb
Final extension			70°C, 6 min

Hot Start PCR was used for genomic DNA as template with the initial denaturation lasting for 10 min after which the polymerase was added.

4.2.1.9 QuikChange™ PCR (Stratagene) for Site Directed Mutagenesis

QuikChange™ PCR (QCPCR) can be used to change, delete or introduce some bases in a gene already cloned into a vector. Therefor complementary primers are

selected containing the desired mutation in the middle flanked by 12-20 bases complementary to the gene of interest. The principle of QCPCR is the amplification of the complete plasmid while the desired mutation is introduced. The products of one QCPCR cycle are linear and can not act as template in the following cycles; thus increase of products is not exponential. After the QCPCR the whole mixture is treated with *Dpn*I. This endonuclease, specific for methylated and hemimethylated DNA is used to digest template DNA. DNA isolated from almost all *E. coli* strains is dam methylated and therefore, in contrast to the newly synthesized strands, susceptible to *Dpn*I digestion. Due to the length of the oligonucleotides their melting temperature lies often in the range of 60-80°C. To avoid unspecific binding at lower annealing temperatures DMSO is added to the reaction mixture at a concentration of 10 % (v/v).

The following table shows a typical reaction mixture (50µl total volume).

Component	Volume [µl]	Final concentration
10 x polymerase buffer	5	1 x
DMSO	5	10 % (v/v)
dNTP mix (2,5 mM each)	1	5 µM each
sense primer	1	0.2 µM
antisense primer	1	0.2 µM
Plasmide	1	ca. 50 ng
DNA polymerase	1	2.5 U
H_2O	35	-

PCRs were performed in a thermocycler (Eppendorf) using the following general program:

Cycle	Denaturation	Annealing	Extension
Initial denaturation	95°C, 1 min		
PCR cycles (15)	95°C, 30 sec	52-58°C, 1 min	70°C, 2 min/1 kb
Final extension			70°C, 6 min

4.2.2 Microbiological Methods

4.2.2.1 Cultivation and Storage of Bacteria

Long-term storage of cells was performed in form of glycerol stocks. To 1 ml of overnight culture 0.5 ml sterile 87 % glycerol was added. The mixture was vortexed to ensure that the glycerol was evenly dispersed and then stored at -80°C. To recover the bacteria, the surface of the frozen culture was scraped with a sterile inoculation needle, and then streaked onto the surface of an LB agar plate containing the appropriate antibiotics.

4.2.2.2 Transformation of RbCl Competent Cells by the Heat Shock Method

Cells which are capable of taking up DNA are called competent. The following method of transformation is very fast and easy and the cells can be readily frozen for later use.

4.2.2.2.1 Preparation of E. coli Competent Cells by the RbCl Method

A fresh overnight culture of bacteria was diluted 1:100 into 100 ml prewarmed LB broth and the cells incubated at 37°C with shaking (225 rpm) to an OD_{600} 0.4-0.5. The cells were pelleted at 6000 rpm for 10 min in a centrifuge. They were resuspended in 40 ml of ice-cold TfbI buffer and incubated for 15 min on ice. After a second centrifugation step the cells were resuspended in 4 ml TfbII. Following another 15 min on ice the cells were divided into 200 µl aliquots and either immediately used or frozen in liquid nitrogen and stored at -80°C.

4.2.2.2.2 Transformation of E. coli

The competent *E.coli* cells were thawed on ice if necessary. For transformation 0.5 µl (50-200 ng) plasmid were added to 100 µl competent cells or 20 µl ligation mixture/QCPCR product were added to 200 µl competent cells and incubated on ice for at least 30 minutes. After heat shock for 45 seconds at 42°C and cooling on ice for 2 minutes 600 µl LB medium were added to the cells. After 45 minutes incubation at 37°C to allow expression of the antibiotic-resistance gene the mixture was centrifuged for 1 min at 6000 rpm and the supernatant discarded. The pellet was resuspended in the remaining supernatant and spread on LB agar plates containing the appropriate antibiotic.

4.2.2.3 Heterologuos Protein Expression in *E. coli*

Over-expression was carried out in *E. coli* BL21 (DE3) cells, in which the *lac* promoter controls expression of the T7 polymerase gene. Precultures for the wild type enzymes and the chimeric proteins were cultivated in 5 ml Luria-Bertani medium, supplemented with 30 µg/ml kanamycin (or 100 µg/ml ampicillin for pET 22b+-derivatives) inoculated from either fresh colonies or glycerol stocks. After 4 hours precultures were transferred to 2 L shaking flasks containing 400 ml TB medium. When the optical density reached OD_{600} ~ 0.6-0.8 protein expression was induced by addition of Isopropyl-ß-D-thiogalactopyranosid at final concentration 0.5 mM and the cultivation conditions were changed from 37°C and 200 rpm to 25°C and 120 rpm for approximately 16 hours.

The cells were harvested by centrifugation at 10000 *g* for 15 min at 4°C and the pellets stored at -20°C until further use.

4.2.2.4 Cell Lysis by Sonification

The cell pellets were resuspended 1:4 (m:v) in 50 mM potassium phosphate buffer pH 7.5 containing 0.1 mM phenyl-methane-sulfonyl-fluoride (PMSF) and broken by sonication with four bursts of sonication for 2 min with at least 4 min cooling on ice.

The cell debris was separated from the cell lysate by centrifugation at 8000 *g*, 4°C for 60 min.

4.2.3 Biochemical Methods

4.2.3.1 Determination of Protein Concentration

The BCA™ Protein Assay Kit was used to determine the concentration of proteins. The principle of this method is the reduction of Cu^{2+} to Cu^{+} by proteins under alkaline conditions. The reaction of Cu^{+} with bicinchonic acid leads to a purple product which can be quantified at 562 nm.

The reaction was performed in microtiterplates using 2-4 dilutions of each sample in duplicates always accompanied by six BSA standards of different concentration (50-2000 µg/ml). To 20 µl sample 200 µl BCA working solution prepared according to the manual were added and incubated for 30 minutes at 37°C. Concentrations were calculated according to the slope of the standard curve generated after measuring absorbance at 562 nm using the Spectramax 340 PC microtiterplate reader.

4.2.3.2 SDS-Gel Electrophoresis

The sodium dodecyl sulfate polyacrylamide gel electrophoresis (SDS-PAGE) technique is used to assess the purity and estimate the molecular weight of a protein (Laemmli 1970). Proteins migrate to the anode of the gel when an electric current is applied. The rate at which the proteins move in the gel is affected by the number of SDS-molecules bound to each protein. SDS confers a negative charge to the polypeptide in proportion to its length, so that smaller proteins after complete denaturation move faster. To analyse the P450 proteins the concentration of acrylamide in the resolving gel was 10 or 12.5 % while the stacking gel contained always 4 % acrylamide.

First the resolving gel was prepared and poured between two glass-plates and allowed to polymerise after overlaying with isopropanol. Then the stacking gel was prepared and poured on the resolving gel after removing residual isopropanol and

the comb was inserted in the stacking gel. After the second polymerisation step the comb was removed and the gel mounted in the electrophoresis chamber.

The samples were prepared by addition of 30-60 % SDS gel-loading buffer and subsequently heating at 95°C for 5 min. The concentration of proteins varied between 2-15 µg/10µl according to the purity of the sample in respect to the enzyme of interest. Finally they were loaded into the wells and a protein standard (broad range or low molecular weight) was added. Electrophoresis was carried out for 90 minutes at 30 mA. Staining of the gel was performed for one hour in fresh Coomassie staining solution after dismantling of the gel. The excess of dye was allowed to diffuse from the gel for two to three hours in destaining solution. For storage the gels were dried between a filter paper and cellophane foil at 80°C under vacuum.

4.2.3.3 Protein Purification

4.2.3.3.1 Ion Exchange Chromatography

IEX chromatography separates proteins with differences in charge. The separation is based on the reversible interaction between a charged protein and an oppositely charged chromatographic matrix. Proteins bind as they are loaded onto a column. Elution is usually performed by an increase in salt concentration or changes in pH.

The enzymes expressed from pET22b+ were purified by ion exchange chromatography. After centrifugation the supernatants were loaded on either a 20 ml DEAE 650M anion exchanger column (Tosoh Haas) or 17.5 ml Super Q 25 column (Pharmacia). After washing with buffer A, a linear gradient of NaCl between 0 and 500 mM over 8 column volumes was applied. The proteins were eluted between 180 and 250 mM salt concentration for both columns.

4.2.3.3.2 Metal Affinity Chromatography

Those proteins, expressed from pET28a+ or pET28b+, contained an N-terminal His_6-Tag and were purified by the method of immobilised metal affinity chromatography either on Ni-NTA columns from Quiagen or Ni-Sepharose from Pharmacia, the latter showing higher binding capacity and less stripping of Ni-ions. The columns were equilibrated with buffer A containing 500 mM NaCl and 20 or 25 mM imidazol. The cell lysates were diluted with buffer A containing 1 M NaCl and brought to the same

imidazol concentration as was used for equilibration. Usually 4 ml columns were used to purify 20 ml of cell lysate containg 10-30 µM P450. After sample application the columns were washed with 4 column volumes of buffer A containing 500 mM NaCl and 25 or 50 mM imidazol and again with the same volume of the same buffer with 40 or 62.5 mM imidazol. Finally the enzymes were eluted by the addition of buffer A containing 500 mM NaCl and 250 or 500 mM imidazol. Elution volumes were between 3 and 6 ml of highly concentrated P450 enzymes. Before application the eluates were dialyzed against buffer A using dialysis tubing with 15 kDA cutoff. Enzymes were used either directly, stored in the fridge for short time (2 weeks) or mixed with glycerol to give a 50 % solution and frozen at -80°C.

4.2.3.3.3 Heat Precipitation

A common method to roughly separate thermophilic proteins expressed in mesophilc organisms like *E. coli* from host proteins is heat precipitation. Taking advantage of the higher thermal stability of proteins from thermophilic bacteria the homologous proteins are denatured and precipitate upon heating while the thermostable fraction remains in the supernatant.

After cell lysis and centrifugation the supernatant was heated at 60°C for 10-30 minutes and then the denatured proteins were removed by centrifugation at 15000 rpm (Sorvall RC-5B, rotor: AK 50-22) for 30 min.

4.2.3.4 Spectroscopic Characterisation

4.2.3.4.1 Oxidised and Reduced P450 Monooxygenase Spectra

UV-visible absorption spectra of enzymes were recorded with a Pharmacia Biotech Ultrospec 3000 spectrophotometer. To observe the characteristic spectra of the oxidised and reduced form different enzyme concentrations of 0.1 to 1 µM were measured. The enzyme delution buffer A was used as negative control. Reduction of the flavin co-factors was initiated by addition of small amounts of sodium dithionite.

4.2.3.4.2 Carbon Monoxide Binding Spectra

Carbon monoxide can bind ferrous P450, inducing a shift of the maximum absorbance of the heme to 450 nm. Differential spectrophotometry can be used to calculate P450 concentration in solution (Omura and Sato 1964).

$$c(P450) = \frac{\Delta A_{450-490}}{\varepsilon \cdot l}$$

c(P450): concentration of P450 (µmol/ml)

$\Delta A_{450-490}$: difference of absorption at 450 and 490 nm

l: pathlength of the cuvette (1 cm)

ε: extinction coefficient of P450 at 450 nm (91 $mM^{-1}cm^{-1}$)

Samples containing P450 enzymes were reduced by addition of a few crystals of sodium dithionite and divided in two cuvettes. One of the aliquots was treated with CO. The absorption of the CO saturated sample was measured in the region between 400 and 500 nm against the reduced sample. Stability of the monooxygenase domain was estimated from changes in corresponding CO-difference spectra after 30 minutes incubation of enzyme samples in a Eppendorf Thermocycler at elevated temperatures with subsequent cooling down to 8°C .

4.2.3.4.3 Substrate Binding Spectra

Ligand free P450s exhibit a Soret absorption maximum at around 420 nm, which is associated with the low spin state of the Fe^{3+}. By interaction with a substrate or an inhibitor the spin state of the heme iron changes accompanied by changes in absorption. According to these changes three categories of ligand binding can be defined: type I, type II and reverse type I. They represent a method for classifying different varieties of P450 active site interactions (Schenkman et al. 1981). Type I binding is connected with substrate binding. It is identified by a reduction of the Soret band at 420 nm and an increase of absorption at 390 nm exhibiting an isobestic point at approximately 407 nm. It is ascribed to a shift in the hemoprotein equilibrium from

low- to high-spin ferric P450. Inhibitors mostly induce type II spectral changes by binding directly to the Fe^{3+} replacing the water molecule. It is characterised by a decrease in absorption at around 390-405 nm accompanied by an increase at 425-435 nm. Reverse type I spectra are typical of oxygen ligands binding to the heme iron they are a mirror image of the type I case.

The substrate induced spectral shifts of the CYP102A enzymes were recorded with a Thermo EvolutionTM100 UV-Vis spectrophotometer at room temperature. For P450 titration 1 µl fatty acid solution in DMSO (5-50 mM) was added with a Hamilton syringe to 1 ml enzyme solution (2-5 µM). Difference spectra were recorded between 370 and 470 nm. P450 solution with the respective volume of DMSO was used as reference. The changes in absorbance (A) were determined by subtracting A_{422} (trough) from A_{388} (peak) and binding constants were calculated by plotting the maximal absorption changes calculated for each difference spectrum against the concentration of fatty acids.

All experiments were performed at least in duplicates in the presence of molecular oxygen.

4.2.3.4.4 Fluorescence Measurements

FAD (flavin adenine dinucleotide) and FMN (riboflavin 5'-monophosphate) show characteristic fluorescence with an excitation wavelength of 470 nm and an emission wavelength of 520 nm. As long as the co-factors stay bound in the enzyme this fluorescence is quenched. Therefore the release of the co-factors upon denaturation of the reductase domains can easily be monitored by increase of fluorescence.

For determination of the melting temperature of the different P450 reductase domains, the enzymes were incubated at different temperatures (25-95°C) for 30 minutes in an Eppendorf thermocycler with subsequent cooling. Aliqouts of 100 µl were measured in black microtiterplates (Nunc maxisorb 96) in triplicates; unheated enzyme solution and also buffer were used as negative controls. The test parameters were 470-12 filter for excitation, 510-10 filter for emmission and one cycle of 30 flashes.

A fluorescent probe normally used for inhibition assays with microsomal P450s like CYP2D6 and 2E1 is 7-ethoxycoumarin. The deethylation to 7-hydroxycoumarin and

acetaldehyde can be monitored by following the increase in fluorescence with excitation at 405 nm and emission at 460 nm. The excitation wavelength of 405 nm is not the maximum for excitation (380 nm) but showed best results in a system also containing NADPH with an excitation maximum of 360 nm and emmision maximum at 480 nm. Substrate concentration in the assay was 12.5-625 µM (max. 2 % in DMSO) while 0.5 µM P450s were used in 180 µl buffer A. Substrate conversion was started by the addition of 300 µM NADPH and monitored over 3-15 minutes every 15 seconds with 12 flashes.

4.2.3.4.5 Circular Dichroism

Circular dichroism (CD) spectroscopy is a form of light absorption spectroscopy that measures the difference in absorbance of right- and left-circularly polarised light by a substance. Circularly polarised light is generated by superposition of two plane polarised waves in perpendicular planes with the same amplitude and wavelength but a phase difference of 90° (-90°)(Figure 4-2). When one wave crosses the zero line the other wave is at its peak. The resulting electric field vector rotates in a circle (right or left) while its length remains constant. To measure CD two circular polarised waves of equal amplitude and wavelength but different orientation (left and right) are superposed resulting in a plane polarised wave (Figure 4-3 a). If this light enters matter with different extinction coefficients for left and right polarized light the amplitude for one component decreases, gets fainter and the superposition of the two circular polarised waves results no longer in a plane polarised wave, they result in a field vector rotating along an ellipsoid path (Figure 4-3 b).

The other effect that could happen is that a sample has different refraction indexes for left and right circularly polarised light. This phenomenon is called circular birefringence, the superposition of the two light components results again in a plane polarised wave but at a different angle than before (Figure 4-3 c).

While in the past the unit of circular dichroism was defined as the tangent of the ratio of the minor to major elliptical axis, ellipticity in degrees or millidegrees, today CD is measured as the difference in absorbance of right- and left-circular polarised light as a function of wavelength.

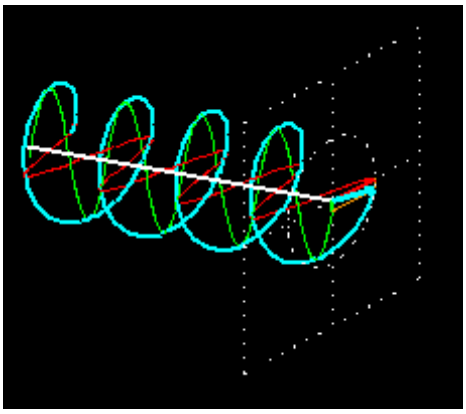

Figure 4-2 Superposition of two plane polarised waves

The superposition of two perpendicular plane polarised waves (green and red) with the same amplitude and frequency results in circular polarised light (light blue)
(Snapshot from András Szilágyi, http://www.enzim.hu/~szia/cddemo/edemo0.htm)

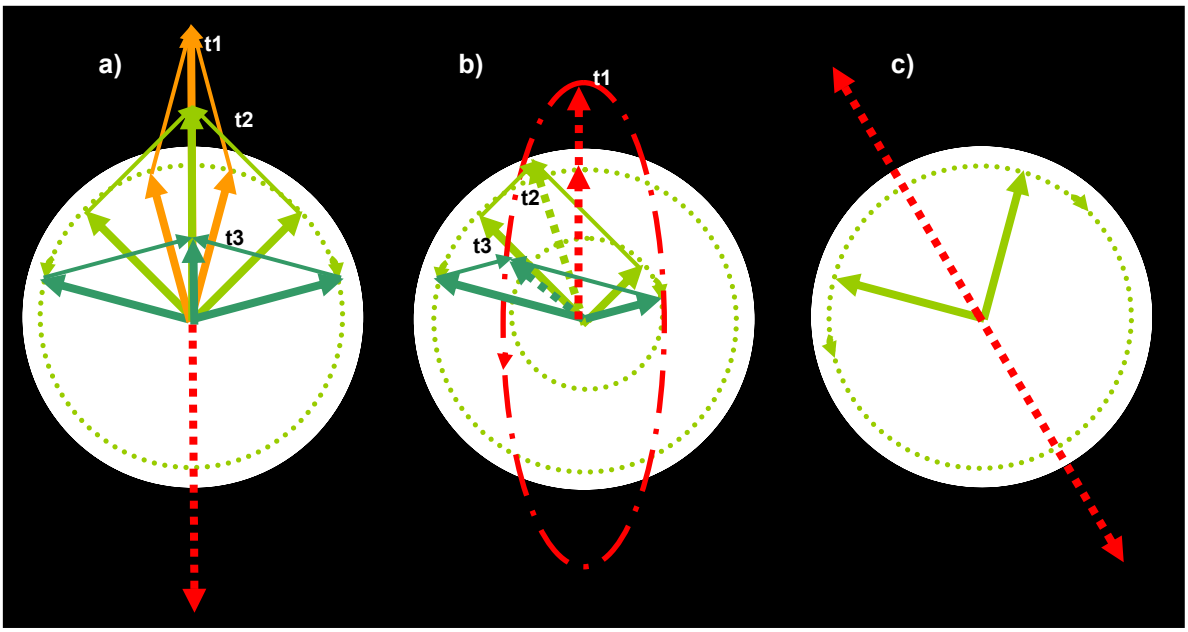

Figure 4-3 The principle of circular dichroism

a) The superposition of two circular polarised waves with opposite orientation results in a plane polarised wave. The picture shows the resulting vector for the addition of the circular polarised waves at three different time points (t1,t2,t3). b) Circular dichroism, if a substance has different extinction coefficients for left and right circular polarised light their amplitudes change to a different extent, therefore the superposition no longer results in a plane polarised wave but in elliptical polarised light. The picture shows the resulting vectors for three different time points (t1,t2,t3). (c) Circular birefringe,

superposition of two circular waves after they entered matter with different refraction indices for left and right circular polarised light (green). The phases are shifted resulting in plane polarised light (red) which is rotated by a specific angle.

CD spectroscopy can be used to analyse chiral substances but also to investigate the secondary structures in peptides and proteins. It has been shown that CD spectra between 260 and approximately 180 nm can be analysed for the different secondary structural types: alpha helix, parallel and antiparallel beta sheet, turn, and other (Johnson 1990)(Figure 4-4).

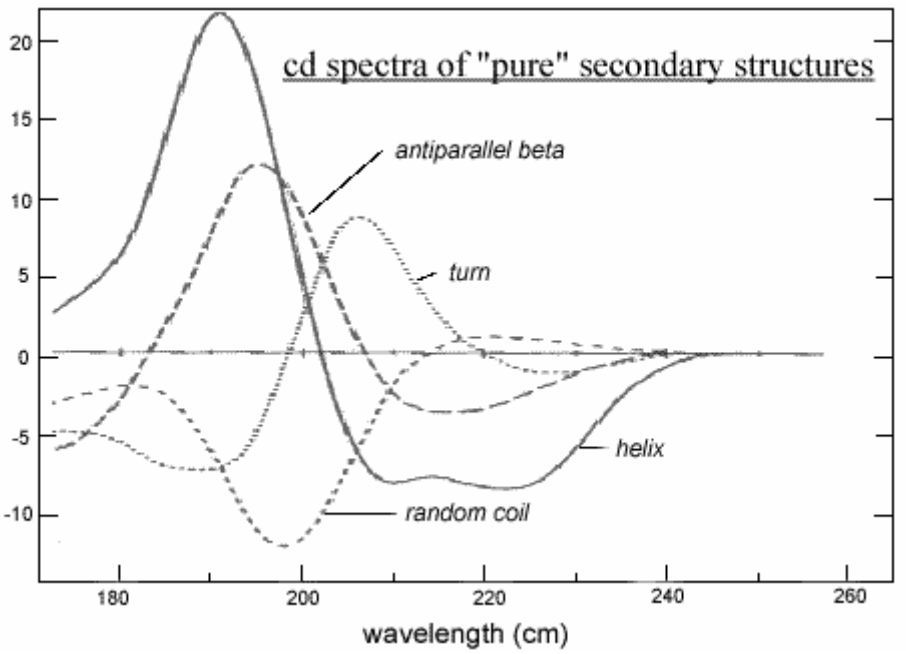

Figure 4-4 CD spectra of pure secondary protein structures

(http://www.huhaha.com/images/cd/cd_pure_secondary_structure.gif)

CD spectra were recorded using the Chirascan circular dichroism spectrometer from Applied Photophysics.

Spectra in the far-UV (190-260 nm) were recorded at ambient temperatures (if not indicated otherwise) at scan rates of 3 seconds per time point (1 nm steps) using 1-1.5 µM enzyme solution in quartz cells of 0.1 cm path length. Spectra in the near-UV-vis region (250-600 nm) were recorded at scan rates of 1 -2s/point (0.5-1 nm steps) using 8-10 µM enzyme solutions in quartz cells of 1 cm path length. To remove

bound substrates, NADPH (10 µM final concentration) was added to the enzyme with subsequent desalting using a PD 10 column. For substrate bound spectra arachidonic acid (55 µM final concentration) was added to the enzyme samples. For each sample 3-5 measurements were done and averaged.

4.2.3.5 Steady State Kinetics and Substrate Conversion

4.2.3.5.1 The Surrogate Substrate 12-pNCA

A fast method to determine P450 activity is the use of the surrogate substrate 12-*para*-nitrophenoxydodecanoic acid (12-*p*NCA). The product of reaction, *para*-nitrophenolate is easily detectable by increase in absorbance at 412 nm under alkaline conditions (pH>8) (Schwaneberg et al. 1999). 20 µl of a 5 mM 12-*p*NCA solution in DMSO were added to buffer B and 0.1 µM enzyme solution. The reaction was started through addition of 150 µM NADPH and activity was determined over 30 seconds using the extinction coefficient of $\Delta\varepsilon_{412}$ 13200 $M^{-1}cm^{-1}$.

Additionally product distribution from 12-*p*NCA was determined by GC/MS analysis. Therefor NADPH was added in 3 steps of 300 µM to a solution containing 300 µM 12-*p*NCA and 0.3 µM P450 enzyme to get a high yield of products. When the reactions were completed, 100 µl of HCl (37 %) were added to 1 ml reaction mixture and incubated for 90 minutes at 95°C to cleave the ether bond between the *para*-nitrophenol and the fatty acid. After cooling on ice for 5 minutes the samples were extracted twice with 0.5 ml diethylether. The organic solvent was allowed to evaporate and the dry samples dissolved in 50 µl derivatisation reagent (N,O-bis(trimethylsilyl)trifluoroacetamide + 0,1 % trimethylsiloxane) and incubated for 30 minutes at 80°C.

4.2.3.5.2 Cytochrome C Reduction by the Reductase Domains

The non-physiological electron acceptor cytochrome c ($\Delta\varepsilon_{550}$ = 22640 $M^{-1}cm^{-1}$) was used for measuring reductase specific activity. The assay was performed in buffer A containing cytochrome c (3-50 µM) at room temperature or for determination of the Gstredu temperature optimum at elevated temperatures (30 - 80°C). After addition of 100 µM NADPH the reaction was followed by monitoring the increase of absorption at 550 nm.

4.2.3.5.3 NADPH Consumption Assays

NADPH consumption during fatty acid hydroxylation was measured spectrophotometrically at 340 nm ($\Delta\varepsilon_{340}$ = 6210 $M^{-1}cm^{-1}$). For standard measurement the following reaction mixture was used: 150-200 µM substrate, 100-150 µM NADPH, 0.02-0.5 µM P450 in buffer A. The reaction velocity was measured in the first minute and the samples left to go to completion for another 15 minutes. Product analysis was done by GC/MS. The reaction mixture was extracted twice with 0.5 ml acidified diethylether (1 % HCl). The organic phases were evaporated to dryness, dissolved in 50 µl derivative (N,O-bis(trimethylsilyl)trifluoroacetamide + 0,1 % trimethylsiloxane) and incubated 30 minutes at 80°C prior to analysis by GC/MS.

4.2.3.6 Determination of Coupling Efficiency

One of the drawbacks of P450 monooxygenases is often the low coupling efficiency especially when using suboptimal substrates. Coupling efficiency is specified as the percentage of product formation to the NAD(P)H consumption. It can be determined by simultaneously measuring the change in absorbance at 340 and 410 nm if 12-*p*NCA is used as a substrate. The assay was performed in a 96 well microtiterplate with 150 µM 12-*p*NCA, 0.09-0.3 µM enzyme solution and 50-200 µM NADPH in buffer B. Eight wells were measured over 5 minutes every 10 seconds in a row per approach. NADPH consumption and *para*-nitrophenolat formation rates were calculated using the specific extinction coefficients (4.2.3.5).

Coupling efficiencies for fatty acids were determined by the use of excess substrate to NADPH, 150 µM versus 100 µM. The reactions were monitored until all NADPH was used up and the samples prepared for GC/MS analysis as before (4.2.3.5). With 100 % coupling efficiency the product formation would be 67 %.

4.2.3.7 Product Distribution and Identification by GC/MS Analysis

GC/MS analysis was performed on Shimadzu GCMS-QP2010 (column: FS-Supreme-5, length: 30 m, internal diameter: 0.25 mm, film thickness: 0.25 µm) using helium as carrier gas. Mass spectra were collected using electron ionisation. The column oven was programmed as follows:

Standard GC parameters:

Injection mode	split
Flow control mode	linear velocity
Purge flow	3 ml/min

Standard MS parameters:

Ion source temperature	200°C
Interface temperature	285°C
Start m/z	50
End m/z	450

Specific programs:

Dodecanoic- and tridecanoic acid

Column oven temperature	165°C
Injection temperature	250°C
Pressure	55.2 kPa
Total flow	9.8 ml/min
Column flow	0.62 ml/min
Linear velocity	30 cm/s
Split ratio	10

Program:	Rate	Final temp	Hold
	-----	165°C	1 min
	6°C/min	215°C	0 min
	30°C/min	275°C	1 min

MS start time	4 minutes

MS end time	12 minutes

Tetradecanoic- and pentadecanoic acid

Column oven temperature	190°C
Injection temperature	250°C
Pressure	32.0 kPa
Total flow	7.5 ml/min
Column flow	0.41 ml/min
Linear velocity	24,6 cm/s
Split ratio	10

Program:	Rate	Final temp	Hold
	-----	190°C	1 min
	7°C/min	245°C	0 min
	30°C/min	275°C	1 min

MS start time	4 minutes
MS end time	10.5 minutes

Hexadecanoic- and heptadecanoic acid

Column oven temperature	190°C
Injection temperature	250°C
Pressure	61.3 kPa
Total flow	9.7 ml/min
Column flow	0.61 ml/min

Linear velocity	30 cm/s
Split ratio	10

Program:	Rate	Final temp	Hold
	-----	190°C	1 min
	6°C/min	255°C	0 min
	30°C/min	285°C	0 min

MS start time	4 minutes
MS end time	13.5 minutes

Oleic-and linoleic acid

Column oven temperature	215°C
Injection temperature	300°C
Pressure	67.3 kPa
Total flow	4.8 ml/min
Column flow	0.60 ml/min
Linear velocity	30 cm/s
Split ratio	2

Program:	Rate	Final temp	Hold
	-----	215°C	1 min
	8°C/min	300°C	1 min

MS start time	4 minutes

MS end time	12.5 minutes

Eicosapentaenoic-, docosahexaenoic- and arachidonic acid

Column oven temperature	215°C
Injection temperature	300°C
Pressure	67.3 kPa
Total flow	9.5 ml/min
Column flow	0.60 ml/min
Linear velocity	30 cm/s
Split ratio	10

Program:	Rate	Final temp	Hold
	-----	215°C	1 min
	8°C/min	300°C	1 min

MS start time	4 minutes
MS end time	16 minutes

The mono hydroxylated fatty acids were identified by their characteristic fragmentation pattern. The reaction rate was calculated on the basis of the integrated peak areas of the product formed and substrate remaining. The stereochemistry of the products was not detected.

4.2.3.8 Temperature Dependant Inactivation Rate

CYP102A1 (3 µM) and A1MA3R (10 µM) were incubated at 50°C. Samples (50 µl) were removed at time intervals 5 min for CYP102A1 and 20 min intervals for A1MA3R. Residual activities were determined using the 12-*p*NCA assay (4.2.3.5). Activities were fit to a first-order exponential decay equation.

4.2.3.9 Storage Stability

For storage stability determination the proteins (3.5-8 µM) were incubated at 30°C for 70 hours. Samples were taken at different time intervals and residual activities for the enzymes were determined using the *p*NCA Assay (4.2.3.5). Additionally stability of the discrete domains was investigated at some time points. All measurements were repeated at least twice with different enzyme charges in triplicates.

4.2.3.10 Determination of Process Stability

A characteristic of an enzyme used for industrial applications is the process stability in contrast to the storage stability. The biggest problem to measure process stability with this family of P450 enzymes is that the natural substrates the fatty acids have such a low solubility in water. Therefore 12-*p*NCA is a good alternative; conversion of this substrate is so low that a sated concentration can be maintained over a long period of time. The second problem is the NADPH supply, because high concentrations of $NADP^+$ inhibit P450 activity and the costs for such an investigation using huge amounts of NADPH would increase dramatically. An elegant solution is the use of a $NADP^+$ dependant formate dehydrogenase to regenerate the co-factor under cleavage of formate to CO_2 and H_2O.

The assay was performed in 50 ml falcons with 5 ml reaction mixture containing 0.2 µM P450 enzyme, 100 µM $NADP^+$, 300 mM formate, 600 U/ml catalase and 1-4 U (depending on P450 activity) fomate dehydrogenase in buffer A. The falcons were incubated either at room temperature or at 30°C under constant smooth mixing. At different time points samples were taken and diluted to measure absorbance at 410 nm. After 3 hours the volume was again filled up to 5 ml with the reaction mixture without new enzyme. This dilution effect was calculated for the following measurements. The assay was performed for 24 hours.

VI. References

Agundez, J. A. (2004). "Cytochrome P450 gene polymorphism and cancer." Curr. Drug. Metab. **5**(3): 211-224.

Appel, D., S. Lutz-Wahl, et al. (2001). "A P450 BM-3 mutant hydroxylates alkanes, cycloalkanes, arenes and heteroarenes." J. Biotechnol. **88**(2): 167-171.

Barnes, H. J. (1996). "Maximizing expression of eukaryotic cytochrome P450s in Escherichia coli." Method Enzymol. **272**: 3-14.

Bayer, E., H. A. O. Hill, et al. (1969). "Interaction between Haem-Iron and Thiols." J. Chem. Soc. Chem. Commun.(3): 109.

Berg, D., M. Plempel, et al. (1988). "Sterol biosynthesis inhibitors. Secondary effects and enhanced in vivo efficacy." Ann. N. Y. Acad. Sci. **544**: 338-347.

Betlach, M. C., J. T. Kealey, et al. (1998). "Characterization of the macrolide P-450 hydroxylase from Streptomyces venezuelae which converts narbomycin to picromycin." Biochemistry **37**(42): 14937-14942.

Birnboim, H. C. and J. Doly (1979). "A rapid alkaline extraction procedure for screening recombinant plasmid DNA." Nucleic Acids Res. **7**(6): 1513-1523.

Bischoff, D., B. Bister, et al. (2005). "The biosynthesis of vancomycin-type glycopeptide antibiotics--a model for oxidative side-chain cross-linking by oxygenases coupled to the action of peptide synthetases." Chembiochem **6**(2): 267-72.

Black, S. D., M. H. Linger, et al. (1994). "Affinity Isolation and Characterization of Cytochrome-P450-102 (Bm-3) from Barbiturate-Induced Bacillus-Megaterium." Arch. Biochem. Biophys. **310**(1): 126-133.

Black, S. D. and S. T. Martin (1994). "Evidence for conformational dynamics and molecular aggregation in cytochrome P450 102 (BM-3)." Biochemistry **33**(40): 12056-12062.

Boddupalli, S. S., R. W. Estabrook, et al. (1990). "Fatty acid monooxygenation by cytochrome P-450BM-3." J. Biol. Chem. **265**(8): 4233-4239.

Boddupalli, S. S., T. Oster, et al. (1992). "Reconstitution of the Fatty-Acid Hydroxylation Function of Cytochrome-P-450bm-3 Utilizing Its Individual Recombinant Hemoprotein and Flavoprotein Domains." J. .Biol. Chem. **267**(15): 10375-10380.

Budde, M., S. C. Maurer, et al. (2004). "Cloning, expression and characterisation of CYP102A2, a self-sufficient P450 monooxygenase from Bacillus subtilis." Appl. Microbiol. Biotechnol. **66**(2): 180-186.

Budde, M., M. Morr, et al. (2006). "Selective hydroxylation of highly branched fatty acids and their derivatives by CYP102A1 from Bacillus megaterium." Chembiochem **7**(5): 789-794.

Carmichael, A. B. and L. L. Wong (2001). "Protein engineering of Bacillus megaterium CYP102.The oxidation of polycyclic aromatic hydrocarbons." Eur J Biochem **268**(10): 3117-25.

Crespi, C. L., V. P. Miller, et al. (2002). "Design and application of fluorometric assays for human cytochrome P450 inhibition." Methods Enzymol **357**: 276-284.

Cryle, M. J., R. D. Espinoza, et al. (2006). "Are branched chain fatty acids the natural substrates for P450(BM3)?" Chem. Commun.(22): 2353-2355.

Cryle, M. J., J. E. Stok, et al. (2003). "Reactions catalyzed by bacterial cytochromes P450." Aust. J. Chem. **56**(8): 749-762.

Delgado, M. J., E. J. Bedmar, et al. (1998). "Genes involved in the formation and assembly of rhizobial cytochromes and their role in symbiotic nitrogen fixation." Adv. Microb. Physiol **40**: 191-231.

Denisov, I. G., T. M. Makris, et al. (2005). "Structure and chemistry of cytochrome P450." Chem. Rev. **105**(6): 2253-2277.

Du, J., B. H. Knowles, et al. (1999). "Biochemical characterization of Bacillus thuringiensis cytolytic toxins in association with a phospholipid bilayer." Biochem. J. **338 (Pt 1)**: 185-193.

Eiben, S., L. Kaysser, et al. (2006). "Preparative use of isolated CYP102 monooxygenases -- a critical appraisal." J Biotechnol **124**(4): 662-9.

English, N., V. Hughes, et al. (1994). "Common pathways of cytochrome P450 gene regulation by peroxisome proliferators and barbiturates in Bacillus megaterium ATCC14581." J. Biol. Chem. **269**(43): 26836-26841.

English, N., C. N. Palmer, et al. (1997). "Fatty acid signals in Bacillus megaterium are attenuated by cytochrome P-450-mediated hydroxylation." Biochem. J. **327 (Pt 2)**: 363-368.

Estabrook, R. W. (1968). "Hepatic microsomes and drug oxidation." Science **160**(834): 1368-1377.

Feyereisen, R. (1999). "Insect P450 enzymes." Annu. Rev. Entomol. **44**: 507-533.

Fuziwara, S., I. Sagami, et al. (2002). "Catalytically functional flavocytochrome chimeras of P450BM3 and nitric oxide synthase." J. of Inorg. Biochem. **91**(4): 515-526.

Garfinkel, D. (1958). "Studies on pig liver microsomes. I. Enzymic and pigment composition of different microsomal fractions." Arch. Biochem. Biophys. **77**(2): 493-509.

Glieder, A., E. T. Farinas, et al. (2002). "Laboratory evolution of a soluble, self-sufficient, highly active alkane hydroxylase." Nat. Biotechnol. **20**(11): 1135-1139.

Goldstein, J. A. and M. B. Faletto (1993). "Advances in mechanisms of activation and deactivation of environmental chemicals." Environ. Health Perspect. **100**: 169-176.

Graham-Lorence, S. and J. A. Peterson (1996). "P450s: structural similarities and functional differences." Faseb J. **10**(2): 206-214.

Graham, S. E. and J. A. Peterson (1999). "How similar are P450s and what can their differences teach us?" Arch Biochem Biophys **369**(1): 24-9.

Gunsalus, I. C., J. D. Lipscomb, et al. (1971). "Structure and reactions of oxygenase active centres: cytochrome P-450 and iron-sulphur proteins." Biochem. J. **125**(2): 5P-6P.

Gustafsson, M. C., C. N. Palmer, et al. (2001). "Fatty-acid-displaced transcriptional repressor, a conserved regulator of cytochrome P450 102 transcription in Bacillus species." Arch. Microbiol. **176**(6): 459-464.

Gustafsson, M. C., O. Roitel, et al. (2004). "Expression, purification, and characterization of Bacillus subtilis cytochromes P450 CYP102A2 and CYP102A3: flavocytochrome homologues of P450 BM3 from Bacillus megaterium." Biochemistry **43**(18): 5474-5487.

Haines, D. C., D. R. Tomchick, et al. (2001). "Pivotal role of water in the mechanism of P450BM-3." Biochemistry **40**(45): 13456-13465.

Han, C. S., G. Xie, et al. (2006). "Pathogenomic sequence analysis of Bacillus cereus and Bacillus thuringiensis isolates closely related to Bacillus anthracis." J. Bacteriol. **188**(9): 3382-3390.

Hasemann, C. A., R. G. Kurumbail, et al. (1995). "Structure and function of cytochromes P450: a comparative analysis of three crystal structures." Structure **3**(1): 41-62.

Hezari, M. and R. Croteau (1997). "Taxol biosynthesis: an update." Planta Med. **63**(4): 291-295.

Hill, H. A. O., A. Roder, et al. (1969). "Haem-Protein Interaction in Cytochrome P-450." Biochem. J. **115**(5): 59P-60P.

Hill, H. A. O., A. Roder, et al. (1970). "Cytochrome P-450 - Suggestions as to Structure and Mechanism of Action." Naturwissenschaften **57**(2): 69-72.

Hogg, J. A. (1992). "Steroids, the steroid community, and Upjohn in perspective: a profile of innovation." Steroids **57**(12): 593-616.

Ioannides, C. and D. F. Lewis (2004). "Cytochromes P450 in the bioactivation of chemicals." Curr. Top. Med. Chem. **4**(16): 1767-1788.

Ivanova, N., A. Sorokin, et al. (2003). "Genome sequence of Bacillus cereus and comparative analysis with Bacillus anthracis." Nature **423**(6935): 87-91.

Johnson, W. C., Jr. (1990). "Protein secondary structure and circular dichroism: a practical guide." Proteins **7**(3): 205-214.

Joyce, M. G., H. M. Girvan, et al. (2004). "A single mutation in cytochrome P450 BM3 induces the conformational rearrangement seen upon substrate binding in the wild-type enzyme." J. Biol. Chem. **279**(22): 23287-23293.

Kaneda, T. (1977). "Fatty-Acids of Genus Bacillus - Example of Branched-Chain Preference." Bacteriol. Rev. **41**(2): 391-418.

Kaneda, T. (1991). "Iso- and anteiso-fatty acids in bacteria: biosynthesis, function, and taxonomic significance." Microbiol. Rev. **55**(2): 288-302.

Kaneko, T., Y. Nakamura, et al. (2002). "Complete genomic sequence of nitrogen-fixing symbiotic bacterium Bradyrhizobium japonicum USDA110." DNA Res. **9**(6): 189-197.

Karuzina, I. I. and A. I. Archakov (1994). "The Oxidative Inactivation of Cytochrome-P450 in Monooxygenase Reactions." Free Radical Biol. Med. **16**(1): 73-97.

Katz, E. and A. L. Demain (1977). "The peptide antibiotics of Bacillus: chemistry, biogenesis, and possible functions." Bacteriol. Rev. **41**(2): 449-474.

Klingenberg, M. (1958). "Pigments of rat liver microsomes." Arch. Biochem. Biophys. **75**(2): 376-386.

Konz, D., A. Klens, et al. (1997). "The bacitracin biosynthesis operon of Bacillus licheniformis ATCC 10716: molecular characterization of three multi-modular peptide synthetases." Chem. Biol. **4**(12): 927-937.

Laemmli, U. K. (1970). "Cleavage of structural proteins during the assembly of the head of bacteriophage T4." Nature **227**(5259): 680-685.

Lentz, O., A. Feenstra, et al. (2006). "Altering the regioselectivity of cytochrome P450CYP102A3 of Bacillus subtilis by using a new versatile assay system." Chembiochem **7**(2): 345-350.

Lentz, O., V. Urlacher, et al. (2004). "Substrate specificity of native and mutated cytochrome P450 (CYP102A3) from Bacillus subtilis." J. Biotechnol. **108**(1): 41-49.

Lewis, D. F., P. J. Eddershaw, et al. (1996). "Molecular modelling of CYP3A4 from an alignment with CYP102: identification of key interactions between putative active site residues and CYP3A-specific chemicals." Xenobiotica **26**(10): 1067-1086.

Lewis, D. F., B. G. Lake, et al. (1999). "Molecular modelling of CYP2B6, the human CYP2B isoform, by homology with the substrate-bound CYP102 crystal structure: evaluation of CYP2B6 substrate characteristics, the cytochrome b5 binding site and comparisons with CYP2B1 and CYP2B4." Xenobiotica **29**(4): 361-393.

Lewis, D. F., B. G. Lake, et al. (1999). "Molecular modelling of CYP1 family enzymes CYP1A1, CYP1A2, CYP1A6 and CYP1B1 based on sequence homology with CYP102." Toxicology **139**(1-2): 53-79.

Li, H. and T. L. Poulos (2004). "Crystallization of cytochromes P450 and substrate-enzyme interactions." Curr. Top. Med. Chem. **4**(16): 1789-1802.

Li, H. Y., K. Darwish, et al. (1991). "Characterization of Recombinant Bacillus-Megaterium Cytochrome-P-450bm-3 and Its 2 Functional Domains." J. Biol. Chem. **266**(18): 11909-11914.

Li, Q. S., J. Ogawa, et al. (2001). "Engineering cytochrome P450BM-3 for oxidation of polycyclic aromatic hydrocarbons." Appl. Environ. Microbiol. **67**(12): 5735-5739.

Li, Q. S., J. Ogawa, et al. (2001). "Residue size at position 87 of cytochrome P450BM-3 determines its stereoselectivity in propylbenzene and 3-chlorostyrene oxidation." Febs Letters **508**(2): 249-252.

Li, Q. S., U. Schwaneberg, et al. (2000). "Directed evolution of the fatty-acid hydyoxylase P450BM-3 into an indole-hydroxylating catalyst." Chem.-Euro. J. **6**(9): 1531-1536.

Liang, Q., J. S. He, et al. (1995). "The role of Barbie box sequences as cis-acting elements involved in the barbiturate-mediated induction of cytochromes P450BM-1 and P450BM-3 in Bacillus megaterium." J. Biol. Chem. **270**(9): 4438-4450.

Liu, M., P. D. Hurn, et al. (2004). "Cytochrome P450 in neurological disease." Curr. Drug Metab. **5**(3): 225-234.

Macdonald, I. D. G., W. E. Smith, et al. (1996). "Inhibitor fatty acid interactions with cytochrome P-450 BM3." FEBS Lett. **396**(2-3): 196-200.

Mason, H. S., J. C. North, et al. (1965). "Microsomal mixed-function oxidations: the metabolism of xenobiotics." Fed. Proc. **24**(5): 1172-1180.

McLean, K. J., M. Sabri, et al. (2005). "Biodiversity of cytochrome P450 redox systems." Biochem. Soc. Trans. **33**(Pt 4): 796-801.

Meinhold, P., M. W. Peters, et al. (2005). "Direct conversion of ethane to ethanol by engineered cytochrome P450BM3." Chembiochem **6**(10): 1765-1768.

Mestres, J. (2005). "Structure conservation in cytochromes P450." Proteins **58**(3): 596-609.

Meyer, U. A. (1996). "Overview of enzymes of drug metabolism." J. Pharmacokinet. Biopharm. **24**(5): 449-459.

Miura, Y. and A. J. Fulco (1974). "(Omega - 2) Hydroxylation of Fatty-Acids by a Soluble System from Bacillus-Megaterium." J. Biol. Chem. **249**(6): 1880-1888.

Miura, Y. and A. J. Fulco (1975). "Omega-1, Omega-2 and Omega-3 Hydroxylation of Long-Chain Fatty-Acids, Amides and Alcohols by a Soluble Enzyme-System from Bacillus-Megaterium." Biochim. Biophy. Acta **388**(3): 305-317.

Morant, M., S. Bak, et al. (2003). "Plant cytochromes P450: tools for pharmacology, plant protection and phytoremediation." Curr. Opin. Biotechnol. **14**(2): 151-162.

Munro, A. W., S. N. Daff, et al. (1997). "Probing inter-domain electron transfer in a model flavocytochrome P-450." Biochem. Soc. Trans. **25**(4): S629.

Munro, A. W., J. G. Lindsay, et al. (1994). "Structural and Enzymological Analysis of the Interaction of Isolated Domains of Cytochrome-P-450 Bm3." FEBS Lett. **343**(1): 70-74.

Murataliev, M. B., R. Feyereisen, et al. (2004). "Electron transfer by diflavin reductases." Biochim. Biophys. Acta **1698**(1): 1-26.

Murataliev, M. B., M. Klein, et al. (1997). "Functional interactions in cytochrome P450BM3: flavin semiquinone intermediates, role of NADP(H), and mechanism of electron transfer by the flavoprotein domain." Biochemistry **36**(27): 8401-8412.

Narhi, L. O. and A. J. Fulco (1982). "Phenobarbital Induction of a Soluble Cytochrome P-450-Dependent Fatty-Acid Mono-Oxygenase in Bacillus-Megaterium." J. Biol.Chem. **257**(5): 2147-2150.

Narhi, L. O. and A. J. Fulco (1986). "Characterization of a catalytically self-sufficient 119,000-dalton cytochrome P-450 monooxygenase induced by barbiturates in Bacillus megaterium." J. Biol. Chem. **261**(16): 7160-7169.

Narhi, L. O. and A. J. Fulco (1987). "Identification and Characterization of 2 Functional Domains in Cytochrome-P-450bm-3, a Catalytically Self-Sufficient Monooxygenase Induced by Barbiturates in Bacillus-Megaterium." J. Biol. Chem. **262**(14): 6683-6690.

Narhi, L. O., B. H. Kim, et al. (1983). "Partial Characterization of a Barbiturate-Induced Cytochrome-P-450-Dependent Fatty-Acid Monooxygenase from Bacillus-Megaterium." Biochem. Bioph. Res. Co. **116**(3): 851-858.

Nebert, D. W., M. Adesnik, et al. (1987). "The P450 gene superfamily: recommended nomenclature." DNA **6**(1): 1-11.

Neeli, R., H. M. Girvan, et al. (2005). "The dimeric form of flavocytochrome P450 BM3 is catalytically functional as a fatty acid hydroxylase." FEBS Lett. **579**(25): 5582-5588.

Nelson, D. R., T. Kamataki, et al. (1993). "The P450 superfamily: update on new sequences, gene mapping, accession numbers, early trivial names of enzymes, and nomenclature." DNA Cell Biol. **12**(1): 1-51.

Nelson, D. R., L. Koymans, et al. (1996). "P450 superfamily: update on new sequences, gene mapping, accession numbers and nomenclature." Pharmacogenetics **6**(1): 1-42.

Nicosia, S. and C. Patrono (1989). "Eicosanoid biosynthesis and action: novel opportunities for pharmacological intervention." Faseb J. **3**(8): 1941-1948.

Noble, M. A., C. S. Miles, et al. (1999). "Roles of key active-site residues in flavocytochrome P450 BM3." Biochem. J. **339**: 371-379.

Ohta, D. and M. Mizutani (2004). "Redundancy or flexibility: Molecular diversity of the electron transfer components for P450 monooxygenases in higher plants." Front Biosci. **9**: 1587-1597.

Omura, T. (2005). "Heme-thiolate proteins." Biochem Biophys Res Commun **338**(1): 404-409.

Omura, T. and R. Sato (1964). "Carbon Monoxide-Binding Pigment of Liver Microsomes .I. Evidence for Its Hemoprotein Nature." J. Biol. Chem. **239**(7): 2370-2378.

Ost, T. W., C. S. Miles, et al. (2000). "Rational re-design of the substrate binding site of flavocytochrome P450 BM3." FEBS Lett. **486**(2): 173-177.

Ost, T. W., A. W. Munro, et al. (2001). "Structural and spectroscopic analysis of the F393H mutant of flavocytochrome P450 BM3." Biochemistry **40**(45): 13430-13438.

Palmer, C. N., E. Axen, et al. (1998). "The repressor protein, Bm3R1, mediates an adaptive response to toxic fatty acids in Bacillus megaterium." J. Biol. Chem. **273**(29): 18109-18116.

Palmer, C. N., M. Causevic, et al. (1997). "Modulation of fatty acid signalling by cytochrome P-450-mediated hydroxylation." Biochem. Soc. Trans. **25**(4): 1160-1165.

Palmer, C. N., M. C. Gustafsson, et al. (1999). "Adaptive responses to fatty acids are mediated by the regulated expression of cytochromes P450." Biochem. Soc. Trans. **27**(4): 374-378.

Park, J. W., J. K. Lee, et al. (2003). "Bioconversion of compactin into pravastatin by Streptomyces sp." Biotechnol. Lett. **25**(21): 1827-1831.

Payne, A. H. and D. B. Hales (2004). "Overview of steroidogenic enzymes in the pathway from cholesterol to active steroid hormones." Endocr. Rev. **25**(6): 947-970.

Peters, M. W., P. Meinhold, et al. (2003). "Regio- and enantioselective alkane hydroxylation with engineered cytochromes P450 BM-3." J.Am. Chem. Soc. **125**(44): 13442-13450.

Peterson, D. H., H. C. Murray, et al. (1952). "Microbiological Transformations of Steroids .1. Introduction of Oxygen at Carbon-11 of Progesterone." J.Am. Chem. Soc. **74**(23): 5933-5936.

Petzoldt, K. A., K. Laurent, H. Wiechert, R. (1982). Process for the preparation of 11-beta-hydroxy steroids. Germany, Schering Aktiengesellschaft (Berlin, Germany).

Poulos, T. L., B. C. Finzel, et al. (1985). "The 2.6-A crystal structure of Pseudomonas putida cytochrome P-450." J. Biol. Chem. **260**(30): 16122-16130.

Ravichandran, K. G., S. S. Boddupalli, et al. (1993). "Crystal structure of hemoprotein domain of P450BM-3, a prototype for microsomal P450's." Science **261**(5122): 731-6.

Read, T. D., S. N. Peterson, et al. (2003). "The genome sequence of Bacillus anthracis Ames and comparison to closely related bacteria." Nature **423**(6935): 81-86.

Rey, M. W., P. Ramaiya, et al. (2004). "Complete genome sequence of the industrial bacterium Bacillus licheniformis and comparisons with closely related Bacillus species." Genome Biol. **5**(10): R77.

Sambrook, R. (2000). Molecular Cloning: A Laboratory Manual. New York, Cold Spring Harbor Laboratory Press.

Sato, H. and F. P. Guengerich (2000). "Oxidation of 1,2,4,5-tetramethoxybenzene to a cation radical by cytochrome P450." J. Am. Chem. Soc. **122**(33): 8099-8100.

Schenkman, J. B., S. G. Sligar, et al. (1981). "Substrate Interaction with Cytochrome-P-450." Pharmacol. Therapeut. **12**(1): 43-71.

Schuler, M. A. and D. Werck-Reichhart (2003). "Functional genomics of P450s." Annu. Rev. Plant Biol. **54**: 629-667.

Schwaneberg, U., C. Schmidt-Dannert, et al. (1999). "A continuous spectrophotometric assay for P450 BM-3, a fatty acid hydroxylating enzyme, and its mutant F87A." Anal. Biochem. **269**(2): 359-366.

Seelbach, K., B. Riebel, et al. (1996). "A novel, efficient regenerating method of NADPH using a new formate dehydrogenase." Tetrahedron Lett. **37**(9): 1377-1380.

Sevrioukova, I. F., H. Li, et al. (1999). "Structure of a cytochrome P450-redox partner electron-transfer complex." Proc. Natl. Acad. Sci **96**(5): 1863-1868.

Shaw, G. C. and A. J. Fulco (1992). "Barbiturate-mediated regulation of expression of the cytochrome P450BM-3 gene of Bacillus megaterium by Bm3R1 protein." J. Biol. Chem. **267**(8): 5515-5526.

Shaw, G. C. and A. J. Fulco (1993). "Inhibition by barbiturates of the binding of Bm3R1 repressor to its operator site on the barbiturate-inducible cytochrome P450BM-3 gene of Bacillus megaterium." J. Biol. Chem. **268**(4): 2997-3004.

Shyadehi, A. Z., D. C. Lamb, et al. (1996). "The mechanism of the acyl-carbon bond cleavage reaction catalyzed by recombinant sterol 14 alpha-demethylase of Candida albicans (other names are: lanosterol 14 alpha-demethylase, P-45014DM, and CYP51)." J. Biol. Chem. **271**(21): 12445-50.

Sih, C. J. (1969). "Enzymatic mechanism of steroid hydroxylation." Science **163**(873): 1297-1300.

Sorokin, A., A. Bolotin, et al. (1997). "Sequence of the Bacillus subtilis genome region in the vicinity of the lev operon reveals two new extracytoplasmic function RNA polymerase sigma factors SigV and SigZ." Microbiology **143 (Pt 9)**: 2939-2943.

Sowden, R. J., S. Yasmin, et al. (2005). "Biotransformation of the sesquiterpene (+)-valencene by cytochrome P450cam and P450BM-3." Org. Biomol. Chem. **3**(1): 57-64.

Strauch, M. A., D. de Mendoza, et al. (1992). "cis-unsaturated fatty acids specifically inhibit a signal-transducing protein kinase required for initiation of sporulation in Bacillus subtilis." Mol. Microbiol. **6**(20): 2909-2917.

Stresser, D. M., S. D. Turner, et al. (2002). "Cytochrome P450 fluorometric substrates: identification of isoform-selective probes for rat CYP2D2 and human CYP3A4." Drug. Metab. Dispos. **30**(7): 845-852.

Strittmatter, P. (1965). "Protein and coenzyme interactions in the NADH-cytochrome b5 reductase system." Fed. Proc. **24**(5): 1156-1163.

Suutari, M. and S. Laakso (1992). "Unsaturated and Branched-Chain Fatty-Acids in Temperature Adaptation of Bacillus-Subtilis and Bacillus-Megaterium." Biochimi. Biophys. Acta **1126**(2): 119-124.

Tishkov, V. I., A. G. Galkin, et al. (1999). "Pilot scale production and isolation of recombinant NAD+- and NADP+-specific formate dehydrogenases." Biotechnol. Bioeng. **64**(2): 187-193.

Tishkov, V. I., A. G. Galkin, et al. (1991). "Nad-Dependent Formate Dehydrogenase from Methylotrophic Bacterium Pseudomonas Sp 101 - Cloning, Expression and Study of Gene Structure." Dokl. Akad Nauk. Sssr+ **317**(3): 745-748.

Tsigelny, I. F., V. Kotlovyi, et al. (2004). "SNP analysis combined with protein structure prediction defines structure-functional relationships in cancer related cytochrome P450 estrogen metabolism." Curr. Med. Chem. **11**(5): 525-538.

Ulrich, C. M., C. S. Carlson, et al. (2005). "Thromboxane synthase (TBXAS1) polymorphisms in African-American and Caucasian populations: evidence for selective pressure." Hum. Mutat. **26**(4): 394-395.

Urlacher, V. B., A. Makhsumkhanov, et al. (2006). "Biotransformation of beta-ionone by engineered cytochrome P450 BM-3." Appl. Microbiol. Biotechnol. **70**(1): 53-59.

van Beilen, J. B., W. A. Duetz, et al. (2003). "Practical issues in the application of oxygenases." Trends Biotechnol. **21**(4): 170-177.

Villeneuve, J. P. and V. Pichette (2004). "Cytochrome P450 and liver diseases." Curr. Drug Metab. **5**(3): 273-282.

Warman, A. J., O. Roitel, et al. (2005). "Flavocytochrome P450 BM3: an update on structure and mechanism of a biotechnologically important enzyme." Biochem. Soc. Trans. **33**(Pt 4): 747-753.

Wen, L. P. and A. J. Fulco (1987). "Cloning of the gene encoding a catalytically self-sufficient cytochrome P-450 fatty acid monooxygenase induced by barbiturates in Bacillus megaterium and its functional expression and regulation in heterologous (Escherichia coli) and homologous (Bacillus megaterium) hosts." J. Biol. Chem. **262**(14): 6676-6682.

Werck-Reichhart, D. and R. Feyereisen (2000). "Cytochromes P450: a success story." Genome Biol. **1**(6): 3003.1-3003.9.

Wichmann, R. and D. Vasic-Racki (2005). "Cofactor regeneration at the lab scale." Adv. Biochem. Eng. Biotechnol. **92**: 225-260.

Yamamoto, H., S. Uchiyama, et al. (1997). "A 23.4 kb segment at the 69 degrees-70 degrees region of the Bacillus subtilis genome." Microbiology **143 (Pt 4)**: 1317-1320.

Zerbe, K., K. Woithe, et al. (2004). "An oxidative phenol coupling reaction catalyzed by oxyB, a cytochrome P450 from the vancomycin-producing microorganism." Angew. Chem. Int. Ed. **43**(48): 6709-6713.